Spring 2010

Adsorption and segmental dynamics of acrylate and methacrylate polymers adsorbed on a silica surface

Piyawan Krisanangkura

Department: Chemistry

ADSORPTION AND SEGMENTAL DYNAMICS OF ACRYLATE AND METHACRYLATE POLYMERS ADSORBED ON A SILICA SURFACE

by

PIYAWAN KRISANANGKURA

A DISSERTATION

Presented to the Faculty of the Graduate School of the

MISSOURI UNIVERSITY OF SCIENCE AND TECHNOLOGY

In Partial Fulfillment of the Requirements for the Degree

DOCTOR OF PHILOSOPHY

in

CHEMISTRY

2010

Approved by

Frank D. Blum, Advisor
Thomas Schuman
Jeffrey Winiarz
Nuran Ercal
Douglas Ludlow

PUBLICATION DISSERTATION OPTION

This dissertation has been prepared in the style utilized by the Journal of Polymer Science Part B: Polymer Physics. Paper-1 (pages 41-78), Paper-2 (pages 79-98) and Paper-3 (pages 99-124) will be submitted for publication in that journal. Appendices A, B, and C have been added for purposed normal to dissertation writing.

ABSTRACT

Poly(isopropyl acrylate)-d_7 (PIPA- d_7) was studied using ^{2}H solid-state NMR and modulated differential scanning calorimetry (MDSC). The polymer was deuterated on the methyl groups and side-chain methine. The PIPA- d_7 was adsorbed onto Cab-O-Sil silica. These two types of deuterons each showed their own characteristic deuterium nuclear magnetic resonance (NMR) spectra for bulk PIPA- d_7. The ^{2}H NMR spectra of adsorbed PIPA- d_7 samples showed the presence of heterogeneity of the segmental dynamics. A residual powder pattern was found in the spectra of the surface samples at higher temperatures, indicating that the segments were tightly attached to the silica. The tightly bound segments were due to the hydrogen bonding between carbonyl groups on the side chains and silanol groups on the silica surface. This resulted in a higher glass transition temperature (T_g) of the PIPA-d_7-silica composite, which was also observed from MDSC experiments. Simulated ^{2}H NMR lineshapes (with different jump rates) were generated based upon two different jump models--a soccer ball model (60-site jump) based on vertices of a truncated icosahedron, and a tetrahedral angle model (2-site hop).

The hydrogen bonding interaction at the interface between polymers-containing carbonyl groups and the silica surface was monitored by using FTIR. Methacrylate polymers with different side chain lengths, including poly(ethyl methacrylate) (PEMA), poly(n-butyl methacrylate) (PnBMA), poly(benzyl methacrylate) (PBenzylMA), and poly(lauryl methacrylate) (PLMA), were studied. Two different surface areas of silica were used as the substrates for PEMA for comparison of the effect surface area sizes. Ratios of the absorption coefficients of bound to free carbonyls, and bound fractions of each system were estimated.

ACKNOWLEDGMENTS

This dissertation would be incomplete without the invaluable contribution of many people, so I would like to use this opportunity to mention these individuals. First, I would like to express my gratitude to the dissertation committee members -- Dr. Frank D. Blum, Dr. Thomas Schuman, Dr. Jeffrey Winiarz, Dr. Nuran Ercal, and Dr. Douglas Ludlow-- for their time, valuable comments, patience and suggestions. In particular, I would like to thank my advisor, Dr. Blum, for his guidance on this dissertation. My successful completion of the Ph.D. program would not have been possible without his practical advice, and support. He always shared insights and his stories lightened the research environment. I am very fortunate to have him as my advisor. Several friends and colleagues also deserve special recognition for their contributions to this thesis. This work could not be completed without their efforts. In particular, I would like to express my gratitude to Dr. Burak Metin for assisting me with the MXQET program. My sincere gratitude also goes to all my former and current lab colleagues for their support and patience in handling a significant amount of complaining by someone who shares a similar fate. Another person who contributed greatly to the thesis is Barbara Harris, who patiently read and corrected this dissertation. In addition, I truly appreciate the efforts of Joe Counsil, Mike Myers, Dean Lenz, and Dave Satterfield, who very kindly assisted me when I was in trouble with the instruments.

I would like to thank my family for understanding my stubbornness and supporting me throughout several years in the United States. I am forever indebted for their love, encouragement, understanding and support. I am also extremely grateful to my bosses and colleagues in the Office of Atomic Energy for Peace, Ministry of Science and

Technology for giving me an opportunity to be here to develop my expertise. Finally, I would like to thank anyone that I have failed to mention in this limited space. I admire and appreciate all of your kindness and goodwill.

TABLE OF CONTENTS

Page

Page

Page

LIST OF ILLUSTRATIONS

Page

Page

LIST OF TABLES

1. INTRODUCTION

1.1 PROLOGUE

Polymer composites, which have been widely used in a variety of applications, commonly use inorganic components such as glass fibers or silica particles as fillers to enhance performance. Certain combinations of fillers and a polymer matrix can give rise to new modified materials with different properties. For example, when mineral fillers are added to a polymer matrix, the moduli and heat deflection temperatures increase. Because inorganic fillers have greater strength and moduli, as compared to an organic material like a polymer, the load is transferred to those fillers. Hence, reinforcement can be achieved.

The key to developing new polymer composites lies in determining their molecular structure, physical properties, and interactions. One of the properties of interest in polymer science is the glass transition temperature (T_g), which is a range of temperatures through which a polymer in the glassy state transitions to a rubbery state. A good understanding of the behavior of polymers at an interface around the glass transition region could also give crucial information about the interaction between polymers and substrates.[1-3] Good adhesion and interfacial bonding play an important role in the transverse strength of polymer composites, as well as providing resistance to environmental factors. At the surface, the microstructure and the mobility of polymers obviously differ from those of the bulk materials. Studies of these influences would undoubtedly reveal notable differences in segmental dynamics near the surface, and promote understanding of behaviors that could possibly lead to the discovery of new composites.

Several theoretical approaches and experimental techniques can be used to study a polymer on a surface. Ellipsometry,[2, 4, 5] X-ray and neutron reflectometry,[6-8] modulated differential scanning calorimetry (MDSC),[9, 10] dielectric spectroscopy,[11, 12] and Brillouin light scattering[13-15] are the techniques that have been extensively used to study the T_g of polymer thin films. Other techniques have included secondary ion mass spectroscopy (DSIMS),[16] X-ray photoelectron spectroscopy,[17] positron annihilation,[18] and thermal probe measurement.[19] Common techniques, such as fluorescence spectroscopy[20, 21] and Fourier transform infrared spectroscopy (FTIR),[22-25] have been developed for use in polymer thin film systems. Solid-state nuclear magnetic resonance spectroscopy (NMR)[26, 27] is another technique used to observe polymers at interfaces.

Among the techniques mentioned above, FTIR is one of the simplest methods for studying polymer materials. It can be used to characterize various aspects, including chain conformation,[28-30] as well as determining T_g.[31] Observing changes in the locations of resonances and/or intensities is very useful in identifying and understanding the molecular structures of polymer composites and polymer-interface interactions. In addition, with appropriate parameters like absorption coefficients and calibration curves, FTIR can also provide quantitative information on species. However, in many cases, the IR radiation does not probe the entire sample, which limits usefulness of this technique.

Solid-state deuterium (^{2}H) NMR has been shown to be successful for probing polymer chain re-orientation.[32-36] Due to a low natural abundance of deuterium, there is minimal background interference from the naturally occurring deuterium in specially labeled compounds, in which case labeling can be very effective. The analysis can be done on solid samples, and the shape of a spectrum will correspond only to the labeled

segments of the material studied. The interpretation of solid-state ^{2}H NMR spectra of a deuterium-labeled polymer can provide valuable information on the molecular motion and the physical properties of the polymer.

This study involves research on acrylate- and methacrylate- polymers adsorbed on a substrate. Amorphous fumed silica, Cab-O-Sil M5-P, which was usually used as the substrate, has a large specific surface area of 200 m^2/g. The first part of this thesis involves the study of the segmental dynamics of poly(isopropyl acrylate)-d_7 (PIPA-d_7), using deuterium solid-state NMR. Monomer and polymer synthesis were performed in order to obtain deuterated polymers. Atom transfer radical polymerization (ATRP) was selected as the preferred technique for making the polymers because it is a fast and simple technique, which can be used to target molecular masses of polymers with rather small polydispersities. The characterization of bulk and determination of adsorbed PIPA-d_7 molecular motion mechanisms were established using solid-state ^{2}H NMR. Simulated spectra were generated by using the MXQET program[37] with several trial jump models to get the best fit of the experimental spectra.

The second part of this study involves using Fourier transform infrared (FTIR) spectroscopy to determine the behavior of some polymers of interest on a surface. Methacrylate polymers, with various side-chain lengths adsorbed on a surface (typically silica), were studied. The interaction between the polymer and the surface was observed via the carbonyl group resonances. The ratios of molar extinction coefficients of free carbonyls to bound carbonyls for each system were calculated by using the integrated resonance intensities. Then, the fractions of the carbonyl groups of methacrylate polymers that were bound to the surface were estimated.

1.2 POLYMER SYSTHESIS BY ATOM TRANSFER RADICAL POLYMERIZATION (ATRP)

Conventional free-radical polymerization (RP) is a very important commercial process used for the preparation of generally high molecular mass polymers. Many vinyl monomers can be employed for polymerization, with the reactions taking place over a wide temperature ranges (-80 to 250 °C),[38] and even under mild conditions. The absence of oxygen is required, but water is tolerated. Thus, polymerization can be performed in water as an emulsion or suspension.[39] RP is limited because of its poor control of macromolecular structure, such as molecular mass, polydispersity, end functionality, chain architecture, and composition.

In order to make a polymer with a targeted molecular mass, ionic living polymerization is often a better option than RP. This synthesis method can be used to produce well-defined polymers with precisely controlled structural parameters and to enable the synthesis of block copolymers by sequential monomer addition.[40-43] However, the ionic reactions are quite sensitive to moisture, as well as only being useful for a relatively small number of monomers.

Controlled/living radical polymerization (CRP or LRP) is a newly developed methodology for overcoming those limitations, as well as for providing well-defined polymers with controlled molecular masses. The method is based on the existence of dynamic equilibrium between active and dormant species. Even though the exchange process is slow, this mechanism simultaneously produces growth of all chains while keeping the radical concentration low enough to minimize termination. In principle, the degree of polymerization from CRPs can be determined by the ratio of the concentration of the consumed monomer to the initial concentration of the initiator, $DP_n = \Delta[M]/[I]_{0,}$

with polydispersities close to those given by the Poisson ratio, ($DP_w/DP_n \approx 1+1/DP_n$),[44] and complete end-group functionalization. Because, under CRP conditions, the long lifetime of a growing chain requires not only sufficiently low concentrations of macroradicals, but also a sufficiently high concentration of propagating chains; the exchange between active free radicals and dormant chains should occur rapidly. The proportion of terminated chains must be kept low (usually less than 5%).[45] Generally, the basic requirement for CRP is a slow exchange between the dormant and the growing radicals. This technique has been widely used because it can yield relatively monodisperse polymers with well-defined compositions.

Many types of CRP, including atom transfer radical polymerization (ATRP), nitroxide mediated polymerization (NMP), and reversible addition-fragmentation transfer/degenerative (RAFT),[46, 47] have been developed by Matyjaszewski and coworkers. A number of monomers can be employed to yield a targeted molecular mass with low polydispersity. Atom transfer radical polymerization (ATRP) is one CRP method that is extensively used for polymer synthesis. The process can be used to achieve a polydispersity (M_w/M_n) of less than 1.5,[45] which is inaccessible by conventional radical polymerization. This technique provides the ability to control the chain topology, molecular composition, and the end functionality for a large range of monomers.

ATRP, based on the use of free-radical polymerization, can be initiated by a conventional radical initiator with a transferable halogen or pseudo-halogen with a catalyst (a transition metal with any suitable ligands), to propagate the monomer to polymer with the targeted molecular mass. The key step is an atom transfer to produce

uniformly growing polymer chains; therefore, the process is named "*atom transfer radical polymerization*" (ATRP). ATRP, which originates from atom transfer radical addition, with 1:1 adducts of alkyl halides and alkenes, is then catalyzed by complex catalyst. ATRP occurs with activation and deactivation processes due to a redox reaction via the transition metal. Typically, monomers with an appropriate substituent can stabilize propagating radicals, such as those of styrene, acrylate, methacrylate, acrylamides, and acrylonitrile.[44, 48] Each monomer has its own polymerization conditions, as shown in Table 1.1.

Table 1.1. The conditions, range and polydispersity of each monomer in ATRP[38, 43, 49-71]

Monomer	**Catalyst**	**Initiator**	**T, ^{o}C**	**MW range (M_n), g/mol**	**M_w/M_n**
Methacrylate	Ru, Cu, Ni, Fe, Pd, Rh	Sulfonyl chloride, 2-halopropionitrile	70 - 90	100 – 200,000	< 1.2
Acrylonitrile	CuBr-$(bpy)_2$	α-bromopropionitrile	40 - 64	1,000-15,000	< 1.05
Styrenes	Cu, Fe, Ru, Re	1-phenylethyl halide and benzylic halide, allylic chloride and functional α haloes-ters, polyhalogenated alkanes and arene sulfonyl chloride	80-90 ^{o}C for CuBr/PMDETA 110^{o}C for CuBr(dNby)$_2$ 130 ^{o}C for Cl mediated	1,000-100,000	< 1.1
Acrylates	Ru, Fe, Cu	Alkyl-2-bromopropionate	Ambient	< 100,000	< 1.1
(Meth) Acrylamides	CuCl/Me_4Cy-clam	Alkyl chloride	20	8,400	~ 1.12
(Meth) acrylic Acids	CuBr-$(bpy)_3$	Poly(ethyleneoxide)-based macroinitiator		>10,000	~ 1.3

In the ATRP method, the molecular mass range of the polymers normally varies from 1,000 to 100,000 g/mol, and the molecular mass distribution or polydispersity narrows in a range of $1.0 < M_w/M_n < 1.5$. The polydispersity can be estimated from equation (1.1),[46] where $[RX]_0$ is the initial concentration of an initiator with halogen (RX), and $[RX]_t$ is the concentration of RX at the time t, [D] is the concentration of deactivator, p is monomer conversion, and k_p and k_d are the rate constants of propagation and deactivation, respectively.

$$\frac{M_w}{M_n} = 1 + \left(\frac{([RX]_0 - [RX]_t)k_p}{k_d[D]} \right) \left(\frac{2}{p} - 1 \right) \qquad (1.1)$$

Equation (1.1) is valid for constant concentrations of the radical and deactivator. Thus, faster deactivation will result in a lower polydispersity (small value of k_p/k_d). This equation also indicates that the polydispersity decreases when monomer conversion increases, but increases with a higher value of $[RX]_0$. The general ATRP mechanism is shown in Figures 1.1 and 1.2.[46]

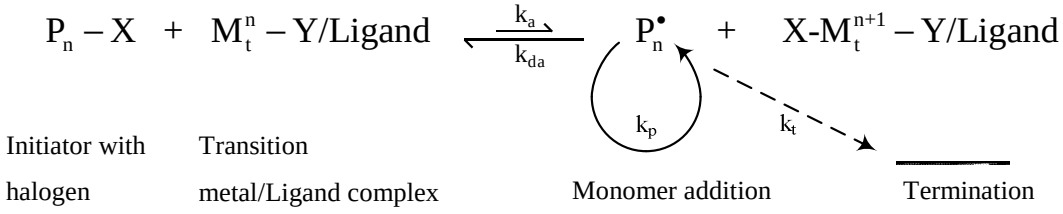

Figure 1.1. The transition-metal-catalyzed ATRP mechanism.

Initiation

$$R\text{-}X + M_t^n\text{-}Y/Ligand \underset{k_{da}^{\circ}}{\overset{k_a^{\circ}}{\rightleftharpoons}} R^{\bullet} + X\text{-}M_t^{n+1}\text{-}Y/Ligand$$

$$R^{\bullet} + M \xrightarrow{k_i} P_1^{\bullet}$$

Propagation

$$P_n\text{-}X + M_t^n\text{-}Y/Ligand \underset{k_{da}}{\overset{k_a}{\rightleftharpoons}} P_n^{\bullet} + X\text{-}M_t^{n+1}\text{-}Y/Ligand$$

$$P_n^{\bullet} + M \xrightarrow{k_p} P_{n+1}^{\bullet}$$

Termination

$$P_n^{\bullet} + P_m^{\bullet} \xrightarrow{k_t} P_{n+m} \text{ or } P_n^{=} + P_m^{H}$$

Figure 1.2. Elementary reaction in ATRP.

The active radicals or propagating species, P_n^*, are generated via the one-electron oxidation redox reaction of the activator. The transition metal forms a complex with a suitable ligand, M_t^n-Y/ligand (where Y may be another ligand or counterion), then abstracts a halogen, X, from the initiator or dormant species, P_n-X. In reverse, the radical can be deactivated by reforming the dormant species via reacting with the oxidized metal species, X-M_t^{n+1}-Y/Ligand (called deactivator). These radicals undergo propagation with the monomer to grow polymer chains. The termination mainly occurs through radical coupling ($P_n^=$) or disproportionation (P_m^H).

Cu (I) preferably forms a complex with tetradentate or two bidentate ligands to give a tetrahedral or square planar configuration. After undergoing one electron oxidation to generate an active radical, this radical propagates with the monomer and is stabilized

by a Cu(II) complex (Figure 1.3), usually forming a cationic trigonal bipyramidal configuration.

Figure 1.3. Catalyst Reaction.

By assuming that the termination is insignificant and using a fast equilibrium approximation, the rate law for ATPR can be given as

$$R_p = k_p[M][P^\bullet] = k_p K_{eq}[M][I]_0 \frac{M_t^n}{X - M_t^{n+1}} \tag{1.2}$$

where k_p is the rate constant of propagation, K_{eq} is the equilibrium constant, which is equal to k_a/k_d; [M] is the monomer concentration; [$P^\bullet$] is the active radical concentration; $[I]_0$ is the original concentration of the initiator; [M_t^n] is the catalyst concentration and [$X\text{-}M_t^{n+1}$] is the oxidized metal concentration. Equation (1.2) indicates that the kinetics of polymerization are first order in both initiator and activator, and inverse first order for the deactivator. The kinetics of polymerization is first order with respect to the monomer concentration.

$$\ln\left(\frac{[M]_0}{[M]}\right) = k_p \frac{k_a}{k_d} \frac{[RX][M_t^n]}{[XM_t^{n+1}]} t \tag{1.3}$$

$$\ln\left(\frac{[M]_0}{[M]}\right) = \frac{3}{2} k_p ([RX]_0[M_t^n]_0)^{1/3} \left(\frac{k_a}{3k_d 2k_t}\right)^{1/3} t^{2/3} \tag{1.4}$$

$$[P^{\bullet}] = ([RX]_0[M_t^n]_0)^{1/3}\left(\frac{k_a}{3k_d 2k_t}\right)^{1/3} t^{-1/3} \quad (1.5)$$

$$[XM_t^{n+1}] = ([RX]_0[M_t^n]_0)^{2/3}\left(\frac{3k_a{}^2 2k_t}{k_d{}^2}\right)^{1/3} t^{1/3} \quad (1.6)$$

Equations (1.3) – (1.6) are the kinetic equations which account for the persistent radical effect (PRE) described for the monomer, radical, and deactivator concentrations. The precise kinetic law for the deactivator, however, is more complex due to the spontaneous generation of oxidized metal via PRE. The equilibrium constant decreases in order of the α-substituents on the alkenes: CN > Ph > C(CO)OR > $C(O)NR_2$ > COC(O)R.[20] K_{eq} must be very small because ATRP propagates very slowly. In contrast, a very large K_{eq} leads to rapid termination because of the higher radical concentration.

In the case of polymerization of poly(isopropyl acrylate), the mechanism of the initiation step by ATRP is described in Figure 1.4. ATRP usually takes place in the presence of a monomer, isopropyl acrylate, a conventional radical initiator with a transferable halogen (ethyl 2-bromopropionate) or pseudo-halogen, and a catalyst (a transition metal with any suitable ligand). The free radical of the initiator is generated by Br abstraction by Cu(I)Br (chelated with PMDETA) from 2-EBP. This very active radical rapidly attacks the vinyl methylene of the acrylate and forms the initial step of polymerization.

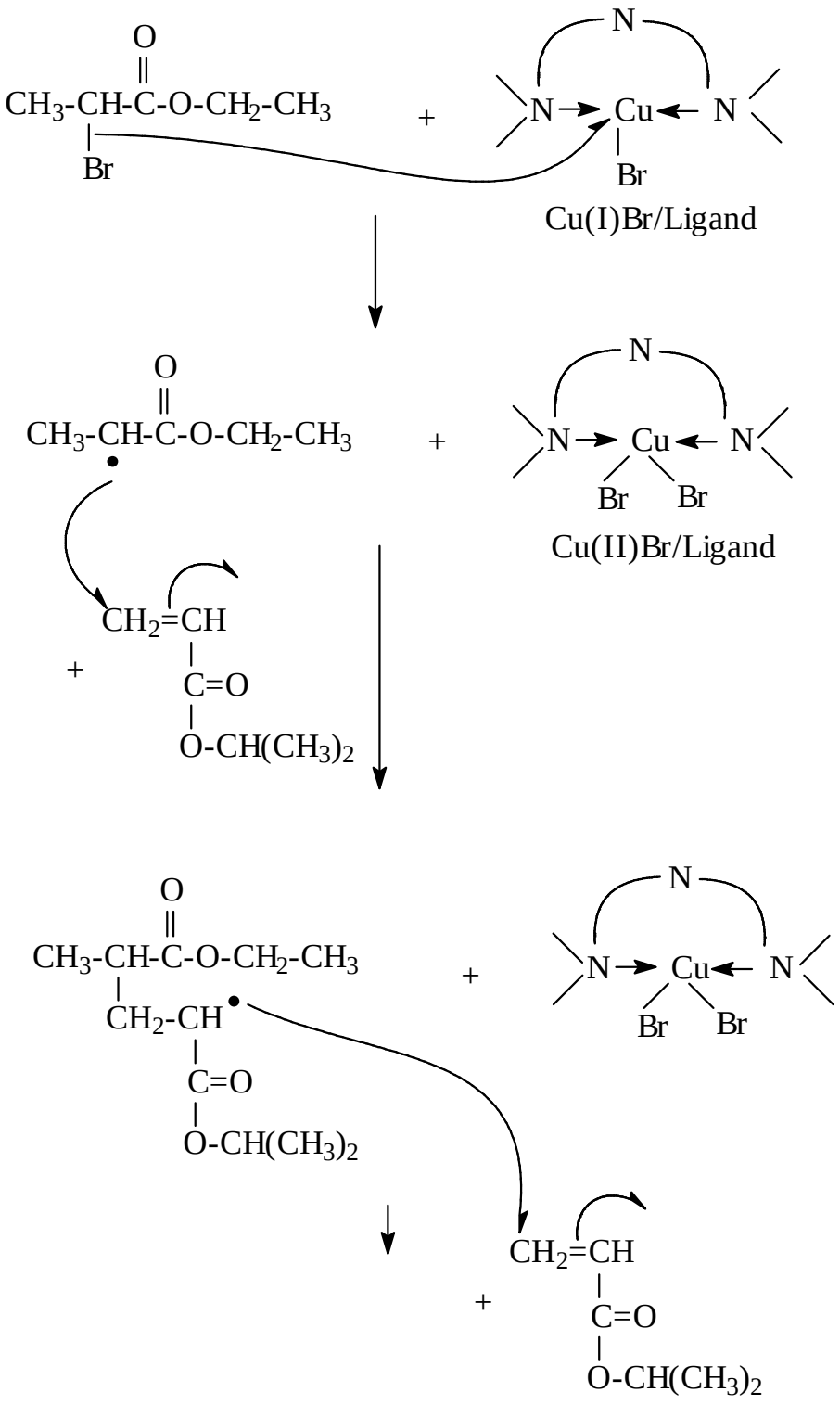

Figure 1.4. Polymerization reaction of PIPA.

The propagation step proceeds with a reversible transfer of the Br atom back and forth between Cu(II)Br and the organic radical, as shown in Figure 1.5.

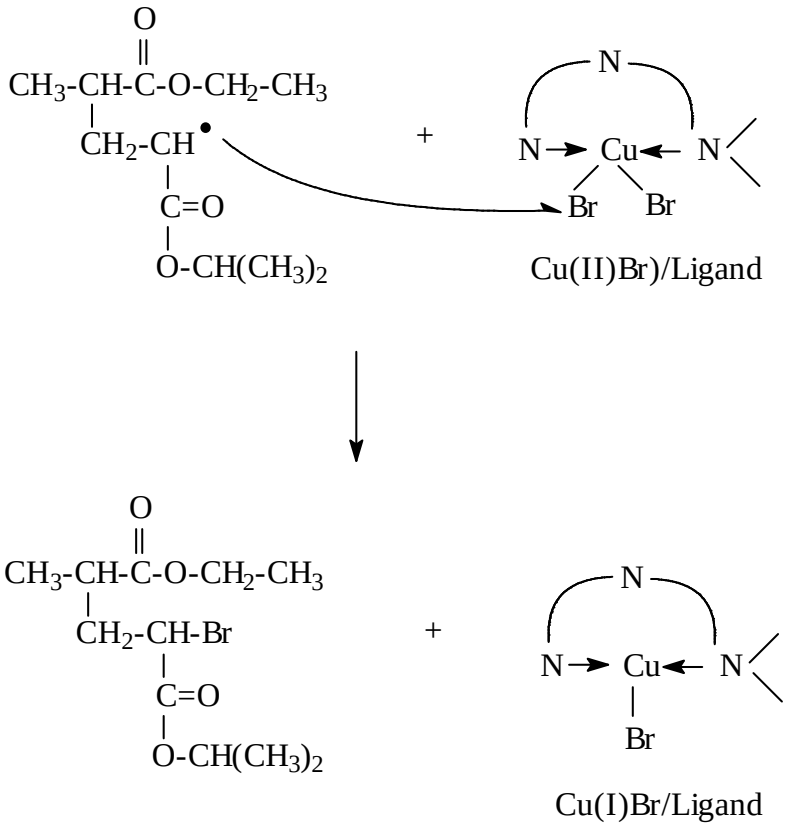

Figure 1.5. The reversible transfer reaction in the propagation step.

1.3 POLYMER ADSORPTION

Polymers adsorbed on surfaces have been studied for decades,[72-75] and several models have been proposed to describe them. One particularly successful model used to explain the structure of a polymer adsorbed on a surface is the self-consistent field lattice model of Scheutjens and Fleer.[76, 77] This model is based on a "Mean-field lattice model of polymers at interfaces".[78] Figure 1.6 illustrates an adsorbed homopolymer at low, normal, and very high surface coverage. At a low coverage level, the polymer would be expected

to have a relatively flat conformation, as shown in Figure 1.6a. At higher adsorbed amounts, only portions of the polymer (called trains) are directly bound to the surface, whereas the parts that are not bound are referred to as loops or tails (Figure 1.6b). Loops end in trains at both ends, whereas tails have only one end attached, and the other end is free. The formation of loops and tails is due to the fact that parts of the polymer chain are not attached on the surface. When the adsorbed amounts are very high (as shown in Figure 1.6c), the loops and tails become longer and/or thicker with a relatively smaller number in trains. The segmental dynamics of the polymer can be probed by a multitude of techniques, including MDSC,[3, 10, 79, 80] and NMR,[81-83] and the interaction between polymers and surfaces can also be easily observed by FTIR.[22]

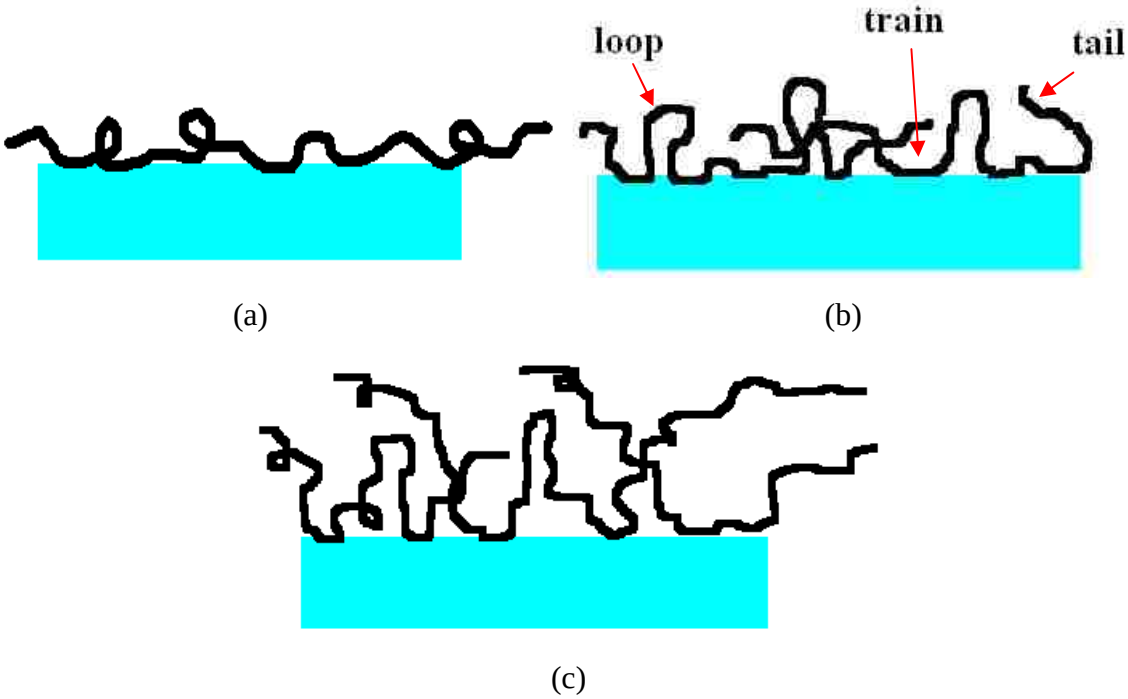

Figure 1.6. Conformation of adsorbed polymer at (a) low, (b) normal, and (c) very high surface coverage.

1.4 ADSORPTION ISOTHERM

Adsorption is a process of binding molecules or particles to a surface. Generally, adsorption can be classified into two types, depending upon the interaction between the molecules and a surface. If the process only involves weak interaction (e.g. Van der Waals, hydrogen bonding), and there is no significant redistribution of electron density between the adsorbate and the adsorbent, it is defined as physical adsorption or physisorption. However, when binding occurs via the rearrangement of electron density, and chemical bond (e.g. covalent bond) formed between the adsorbate and the substrate, it is known as chemical adsorption or chemisorption. The mole fraction of adsorbate on a surface is a function of the equilibrium concentration and temperature, which can be described through an adsorption isotherm. The Langmuir isotherm is the most frequently used isotherm for polymer systems and others.

The Langmuir isotherm is generally used to describe the adsorption phenomena for an ideal gas on a non-porous solid substrate. However, the model can be plausibly applied to other adsorption systems, such as adsorption from solution onto a surface. Based on Langmuir's assumptions, a surface consists of adsorption sites, each with a specific area; each of these sites can only interact with an adsorbate. When S is the total number of adsorption sites, S_0 is the unoccupied sites, and S_1 is the number of occupied sites on a surface, then

$$S_0 = S - S_1 \tag{1.7}$$

The rate of adsorption is taken to be proportional to the number of unoccupied sites multiplied by the concentration of the adsorbate (C). Similarly, the rate of desorption is proportional to the number of filled sites. At equilibrium, the equation becomes:

$$k_1 S_1 = k_2 C S_0 \quad (1.8)$$

where k_1 and k_2 are the rates of adsorption and desorption, respectively.

The fraction of the covered surface sites, θ, can be set equal to S_1/S, and b set equal to k_2/k_1; Equation (1.8) can then be rearranged to Equation (1.9), which is known as the Langmuir Equation,[84]

$$\theta = \frac{bC}{1+bC} \quad (1.9)$$

For a dilute solution, the adsorbed amount would be proportional to the solution concentration. At some concentration, the surface would be saturated with the adsorbed species, and then the adsorption would be independent of the concentration. Figure 1.7 is a general picture of the Langmuir adsorption isotherm.[85] The curve is plotted to show the adsorbed amount as a function of the equilibrium adsorbate concentration at a given temperature.

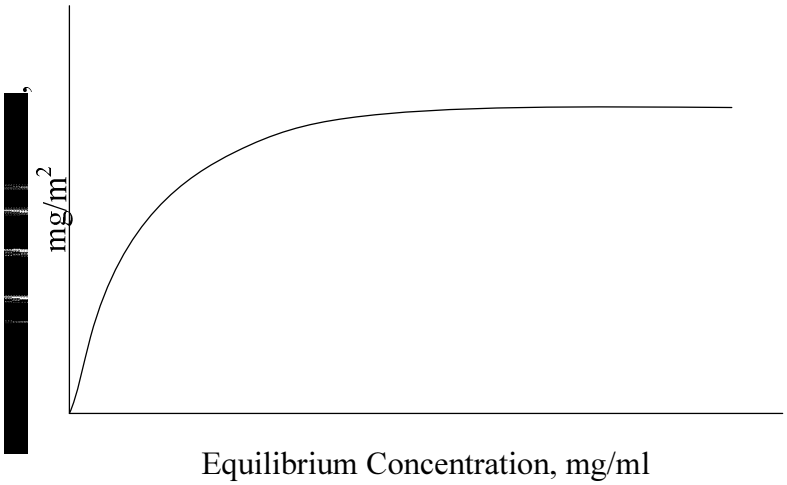

Figure 1.7. Plot of adsorbed amount as a function of concentration for a Langmuir equation.

The adsorbed amount for a polymer on a surface, Γ, can easily be determined using thermogravimetric analysis (TGA). The analysis is typically carried out by monitoring the mass of a sample which is loaded on a high precision balance, as a function of temperature. The adsorbed samples can be heated up to 700 °C. Most organic compounds, including polymers, usually degrade in the range of 350 – 500 °C, and the solid substrate (which is an inorganic oxide) will not vaporize but will be left as a residue. If there is no contamination, the mass difference between the final and the initial masses would be the mass of the polymer, and the final mass would be the mass of the substrate. The amounts of the adsorbed (in mass polymer/surface area) polymer can be calculated by Equation (1.10).

$$\Gamma = \frac{\Delta W}{R \times A} \tag{1.10}$$

where ΔW is the mass change, R is the residue mass, and A is the specific surface area of solid substrate. In this case, the adsorbed amount would be expressed as the mass of polymer per unit surface area.

1.5 METHODOLOGIES FOR DYNAMICS STUDY

1.5.1. NMR Spectroscopy. Nuclei with non-zero spin quantum numbers (I) have a magnetic moment, and this magnetic moment can be considered as analogous to that resulting from the spinning of a charged particle. When an atom, whose nucleus has a spin, is placed in an external magnetic field, the spin aligns in discrete orientations with respect to the magnetic field. Different orientations have different energy levels. The energy of the transition, E, related to its frequency, ν, is described as

$$E = h\nu \tag{1.11}$$

where h is Planck's constant. Since the spin orientations are not linear with the applied magnetic field, a torque causes the spin to precess about the applied field. The precessional or resonance frequency is given by the Lamor equation

$$\nu_0 = -\gamma B_0/2\pi \tag{1.12}$$

where ν_0 (Hz) is the precessional frequency, γ is the magnetogyric ratio, and B_0 (T) is the magnetic field strength taken along z of the laboratory frame of reference. The precession, which is also related to the energy of the transition between the adjacent energy levels, depends on the strength of the external magnetic field and the magnetogyric ratio, so that the energy difference between the transitions of spin state is given by

$$\Delta E = -\gamma h B_0/2\pi \tag{1.13}$$

where h is Planck's constant.

For magnetic field strengths that are commonly used in NMR experiments, ν_0 is in the radio-frequency range. Within a given molecule, the nuclei of the same isotope experience minute differences in magnetic field strength, due to variations in electron density and the magnetic fields of adjacent nuclei. These differences give a molecule a spectrum of precessional frequencies for a given applied magnetic field. NMR is the powerful technique for probing the molecular structure of materials, especially solid-state NMR. For certain nuclei of low isotopic abundance, the NMR technique, coupled with isotopic enrichment gives specific information for labeled nuclei observed on a chain segment or a repeating unit of the polymer of interest. Information on the molecular

motions, isotropic or anisotropic rotation, can be obtained from the spectra lineshapes in favorable circumstances.

1.5.1.1 Solid-State NMR. Unlike liquid-state NMR, solid-state NMR is required in environments with much slower molecular motion. There are several interactions that need to be considered in the NMR spectra of solids. The Hamiltonian for all of the important interactions can be written as

$$\hat{H} = \hat{H}_z + \hat{H}_D + \hat{H}_{SC} + \hat{H}_{CS} + \hat{H}_Q \tag{1.14}$$

Each of these will be defined below.

For a spin, the magnetic moment, μ, and spin, I, operators are defined as:

$$\boldsymbol{\mu} = \gamma\hbar\boldsymbol{I} \tag{1.15}$$

where ħ is Planck's constant divided by 2π. In a static magnetic field, B_0, a spin with spin quantum number, I, will have 2I+1 energy levels associated with it. This interaction is called the Zeeman interaction and its Hamiltonian is given as:

$$\hat{H}_z = -\gamma\hbar IB_0 = \omega_0\hbar I_z \tag{1.16}$$

The dipole-dipole coupling is the interaction between the local magnetic fields from two nuclei, which are either similar or dissimilar. The interaction between two nuclei depends on the internuclear distance between the nuclei and the magnitudes of their magnetic moments. The dipolar Hamiltonian of spin S acting on spin I is:

$$\hat{H}_D = -\frac{h^2\gamma_I\gamma_S}{4\pi^2 r^3}\mathbf{I}\cdot\mathbf{D}\cdot\mathbf{S} \tag{1.17}$$

where **D** is the dipolar coupling tensor, describing the strength and orientation dependence of the interaction between the two nuclei, and r is the internuclear distance between the two.

Scalar coupling (or J) is sometimes called spin-spin coupling. It is the interaction between the spins of two active NMR nuclei. For scalar coupling, the Hamiltonian interaction between spin I and S is:

$$\hat{H}_{SC} = \sum \mathbf{I} \cdot \mathbf{J} \cdot \mathbf{S} \qquad (1.18)$$

where **J** is scalar coupling tensor.

The source of chemical shift anisotropy is chemical shielding, which arises from the electrons around the nuclear spin, producing a secondary field. The perturbation of the secondary field results in a change in the resonance frequency, thereby causing a change in the NMR spectrum. The chemical shielding Hamiltonian acts on I, as shown in Equation (1.19):

$$\hat{H}_{CS} = \gamma \mathbf{I} \ddot{\sigma} \mathbf{B_0} \qquad (1.19)$$

where $\ddot{\sigma}$ is called the chemical shielding tensor.

One interaction of particular interest to the thesis is quadrupolar coupling. The quadrupole interaction is not a magnetic interaction in the same sense as the other interactions described above. A quadrupolar coupling is the interaction between a nuclear electric quadrupole and an electric field gradient that occurs only with nuclei that have a spin quantum number (I) greater than ½. The quadrupolar Hamiltonian for spin I is given by:

$$\hat{H}_Q = \frac{eQ}{2I(2I-1)\hbar}\mathbf{I}\cdot\mathbf{V}\cdot\mathbf{I} \tag{1.20}$$

where Q is the nuclear quadruple moment, **V** is the electric field gradient operator, and eQ is the constant for each given nucleus. The strength of the quadrupole moment depends upon the molecular orientation with respect to the applied magnetic field B_0 and the electric field gradient at the nucleus.

1.5.1.2 Deuterium NMR and Motion Theory. In deuterium solid-state NMR (I=1), when a nuclei is placed in a magnetic field, the electric field gradient (EFG) produced by the electrons surrounding the deuterium nucleus, yielding a non-zero quadrupole moment, which dominates the NMR spectra of most deuterated species. Figure 1.8 illustrates the geometry of the EFG with the magnetic field within a co-ordination system for a C-D bond. Here, θ and Φ are the polar angles of the coordinates of the C-D bond in the magnetic field.

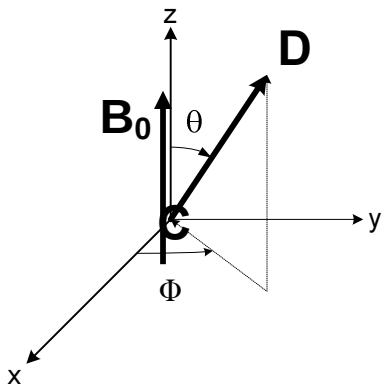

Figure 1.8. The orientation of the magnetic field within the principal axis system of an electric field gradient (EFG) tensor.

A list of the magnitudes of all interactions is shown in Table 1.2. In Table 1.2, other interactions, excluding the Zeeman interaction, are relatively small compared to quadrupolar interaction (at least for the species of interest to the thesis); therefore, other interactions (excluding the Zeeman Effect) can be taken as negligible. In that case, Equation (1.14) becomes:

$$\hat{H} = \hat{H}_z + \hat{H}_Q \tag{1.20}$$

In general, the deuterium spectrum is dominated by the Zeeman and quadrupolar interactions, to yield a specific lineshape. In the presence of a magnetic field, the deuterium nucleus, which has a spin I = 1, would have three spin states (-1, 0, and +1). Two transitions between those states are allowed: -1 ↔ 0 and 0 ↔ +1, as illustrated in Figure 1.9. The transition frequency between those energy states is given by Equation (1.21). The term e^2qQ/h is called the quadrupole coupling constant (QCC), which is the product of a deuterium quadrupole moment (eQ) and the electric-field gradient (eq).[86]

$$\omega_{0\to-1} = \frac{E(-1)-E(0)}{h} = \omega_0 + \frac{3}{4}\left[\frac{e^2Qq}{h}\right](3\cos^2\theta - 1) \tag{1.21a}$$

$$\omega_{1\to0} = \frac{E(0)-E(1)}{h} = \omega_0 - \frac{3}{4}\left[\frac{e^2Qq}{h}\right](3\cos^2\theta - 1) \tag{1.21b}$$

Table 1.2. Typical orders of magnitude of interactions in NMR

Interaction	**Magnitude, Hz**
Zeeman	10^8
Chemical Shift	10^3
Scalar (Spin-Spin Coupling)	1-100
Dipole-Dipole	10^3
Quadrupole	10^6

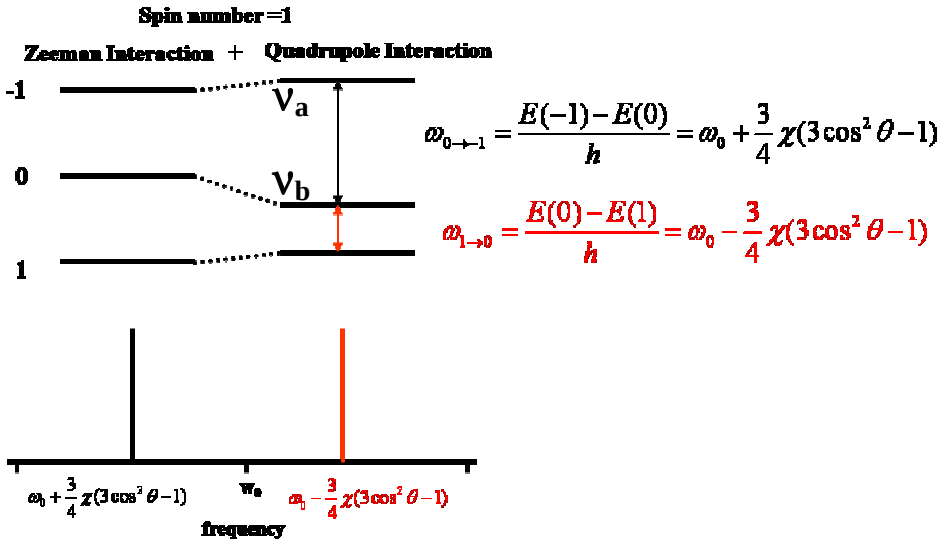

Figure 1.9. Quadrupolar splitting for nuclei with I = 1. The χ is set equal to e^2Qq/h.

Generally, the frequency of the quadrupole splitting ($\Delta\nu_Q$) in the NMR transition is given by Equation (1.22):[86]

$$\Delta\nu_Q = \frac{3}{2}\left(\frac{e^2Qq}{h}\right)\left[\frac{1}{2}(3\cos^2\theta(t)-1)+\frac{1}{2}(\eta\sin^2\theta(t)\cos 2\Phi(t))\right] \qquad (1.22)$$

where η is defined as the asymmetry parameter, and θ and Φ are the Euler angles for the C-D bond that are relative to orientations of the principle axis system of the EFG with respect to the external magnetic field. The quadrupole coupling constant is dependent upon the quadrupole moment of the nuclei and the EFG. The quadrupole moment, *Q*, of the deuterium nuclei is 2.73×10^{-31} m^2, which is a relatively small value.[86] If the EFG is axially symmetric, or nearly so, it would lead to a zero value of η, and Equation (1.22) would be reduced to Equation (1.23). For aliphatic C-D bonds, η is usually very small, almost zero. The quadrupole splitting varies with θ, as shown in Figure 1.10.

$$\Delta\nu = \frac{3}{4}\frac{e^2qQ}{h}(3\cos^2\theta - 1) \qquad (1.23)$$

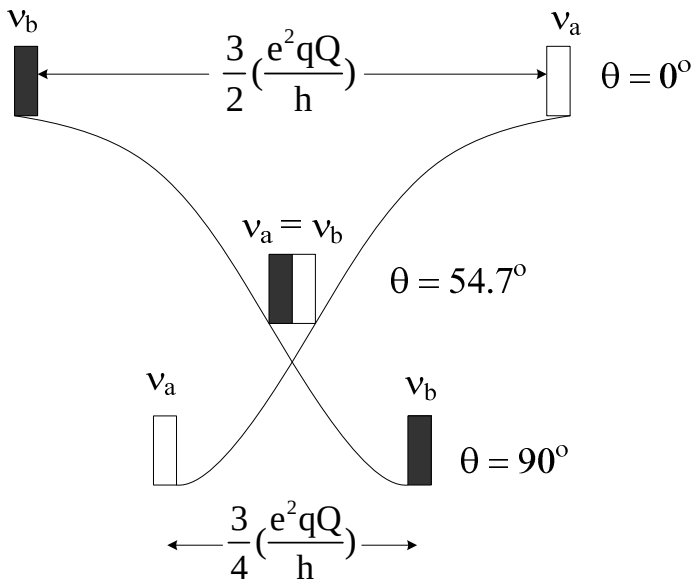

Figure 1.10. Peak splitting for the two I = 1 transitions as a function of θ.

For one transition of a single polycrystalline solid, the contribution of randomly oriented bond vectors, (e.g., random θ's) is proportional to the surface area on a sphere at a given θ. This situation is described in Figure 1.11. When the two transitions, -1 $\leftrightarrow$ 0 and 0 $\leftrightarrow$ +1, are combined, the deuterium solid-state NMR spectrum will be obtained. The overall quadrupolar lineshape of a deuterium spectrum is shown in Figure 1.12. The NMR powder spectra of deuterated species would consist of a series of doublets, called a *Pake Pattern*.

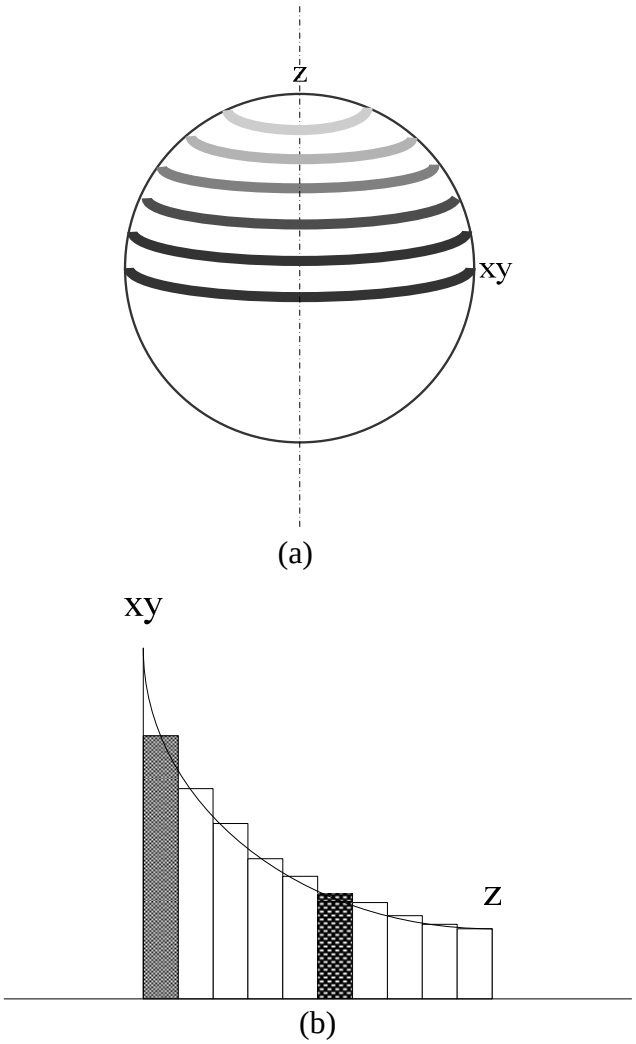

Figure 1.11. The origin of a powder pattern lineshape for one of the transitions of an I = 1 axially symmetric nucleus: (a) the bond vector at a different angle with equal frequencies; (b) a histogram of the surface areas related to the angle.

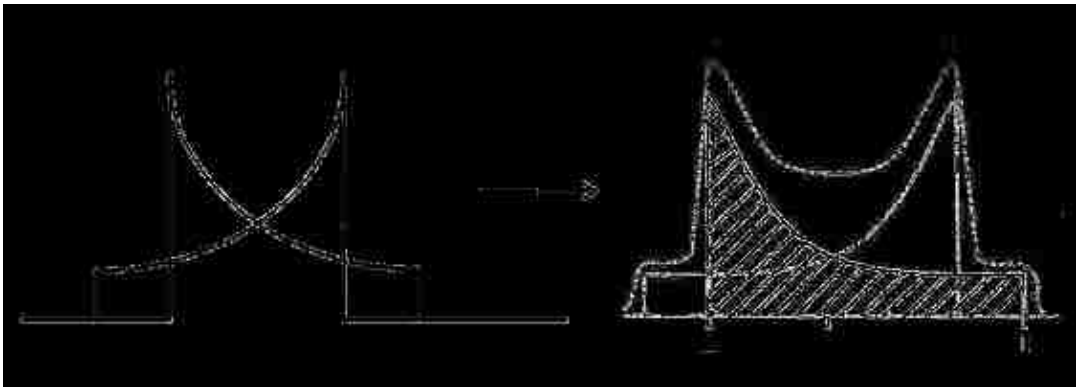

Figure 1.12. Spectral lineshapes based on two deuterium transitions.

The details of a deuterium lineshape can provide information concerning molecular motion in polymers. Each type of molecular motion gives a specific lineshape. Table 1.3 illustrates examples of the types of molecular motions and their lineshapes. Static C-D bonds are often observed in the glassy regions of polymers (Table 1.3(a)). The splitting between the doublets, d, is generally three-fourths of the QCC. For a methyl group, the $(3\cos^2\theta(t) -1)$ term can become Equation (1.24) due to rapid rotation of the methyl group around its symmetry axis.[87]

$$3\cos^2\theta(t) - 1 = \frac{1}{2}(3\cos^2\beta(t) - 1)(3\cos^2\varphi - 1) \qquad (1.24)$$

where the first term on the right hand side represents the orientation, $\beta(t)$, that the symmetry axis of the methyl group makes with the magnetic field axis. φ is the angle between C-D bonds and the symmetry axis, which is 70.5° for the methyl group; therefore, the $(3\cos^2\theta(t) -1)$ is equal to one-third and the quadrupolar splitting is reduced to one-third of its original (Table 1.3(b)). The QCC of the methyl group is typically on the order of 150 to 170 kHz. Equation (1.23) becomes:

$$\Delta\nu = \frac{1}{3}[\frac{3}{4}\frac{e^2qQ}{h}(3\cos^2\theta - 1)] \quad (1.24)$$

The two-site hop model has been used to describe the motion of the deuterons which undergo jumps between two positions through a dihedral angle of 54.7°, the magic angle. The term ($3\cos^2\theta$ - 1) equals zero at the magic angle; hence, the average EFG tensor is zero for this case, as shown in Table 1.3(c). Molecules that have this type of motion would be those with gauche-trans-conformational transitions; for example, poly(butylene terephthalate), with the correlation for the motion being 7×10^{-6} s at 20 °C.[65]

Some possible modes of motions for a deuterated aromatic ring are a phenyl ring flip of about 180°, and free rotation of the phenyl ring around the 1,4-phenylene axis. The ring-flip motion is represented by the 180° jump of the deuteron attached to a phenyl ring at about 1,4-phenylene axis. The situation is described in Table 1.3(d). Since there was no effect from the motion of the EFG tensor that was perpendicular to the flip axis, the horns remained at –d/2. The deuterons in the phenyl ring, however, changed positions by 120° in the flip process. The EFG tensor occurred at –d/8, and remains traceless, so another component took its place at -5d/8. If the phenyl ring undergoes a free rotation of about 1,4-phenylene axis, sweeping out a cylinder, the entire spectrum would be averaged by a factor of one-eighth (Table 1.3(e)).

Anisotropic rotation is a situation where a molecule undergoes molecular motion at an intermediate range on the deuterium NMR time scale (when the correlation time is less than 10^{-5} s, but greater than 10^{-7} s).[88] The anisotropic rotation of the methyl group through a tetrahedral bond angle, 109.5°, is shown in Table 1.3(f). A particularly

interesting situation in the study of the dynamics of polymers arises when the molecular motion is in this range. If the rate of the molecular motion is greater than 10^{-7} s, that mode is defined as an isotropic rotation, which gives rise to a liquid-like spectrum because of the very fast motion, as illustrated in Table 1.3(g).

Table 1.3. Types of molecular motions and lineshapes for various deuterons

(a) Static C-D

C-D

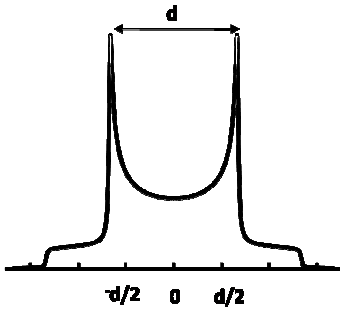

(b) Rotating Methyl Group

(fast)

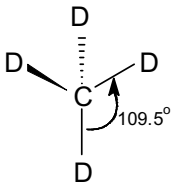

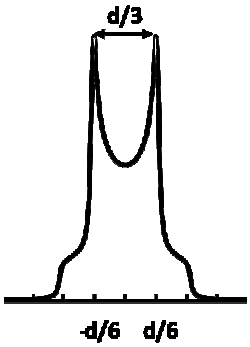

(c) Two-Site Hop (fast)

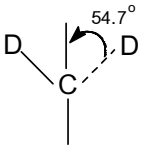

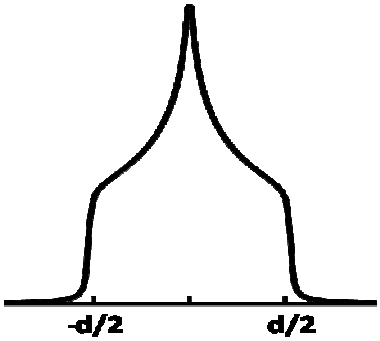

(d) 180° Phenyl Ring Flip

(fast)

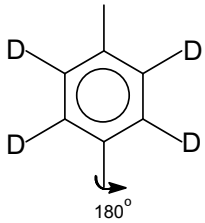

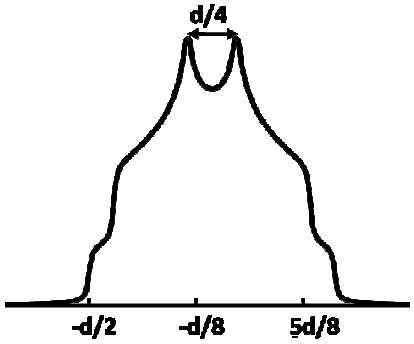

Table1.3. Types of molecular motions and lineshapes for various deuterons (Continued)

(e) Free Diffusion of Phenyl Ring (fast)

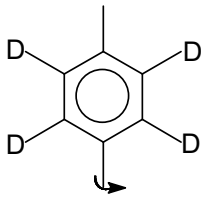

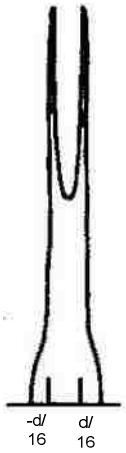

(f) Anisotropic Rotation ($10^{-7} < \tau_c^* < 10^{-5}$ s)[88]

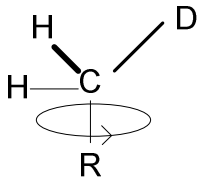

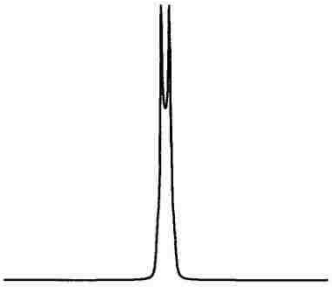

(g) Isotropic Fast Rotation ($\tau_c \leq 10^{-7}$ s)[88]

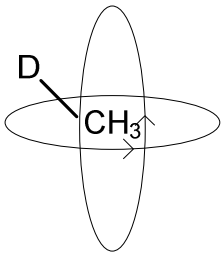

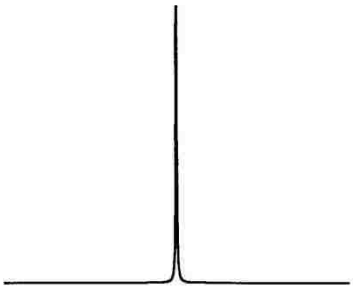

∗ τ_c is correlation time

The quadrupole echo pulse sequence is commonly used in solid-state deuterium NMR to study molecular motion. Because the effect of the quadrupole interaction can lead to a very broad spectrum, a short and high-powered pulse is required in order to

increase the spectral coverage. Also, since the magnetization decays quite rapidly, some signal will be lost during the dead time (time in which the receiver is recovering from the pulse). Some of this problem can be circumvented by a pulse used for refocusing. A quadrupole echo pulse sequence, $90^{o}_{x} - \tau_1 - 90^{o}_{y} - \tau_2 -$ acquisition, is composed of two 90° pulses, 90° out of phase. When the first 90° pulse is applied, the spins dephase in the rotating frame. After some time (τ), the other 90° pulse was is applied to refocus the spins. An echo is generated at the time τ after the second pulse, so that an FID signal would be acquired with little interference. In some cases there can be distortions of the lineshape, especially when the molecular motion is on the order of the time between the two pulses. The quadrupole echo pulse sequence is described in Figure 1.13.

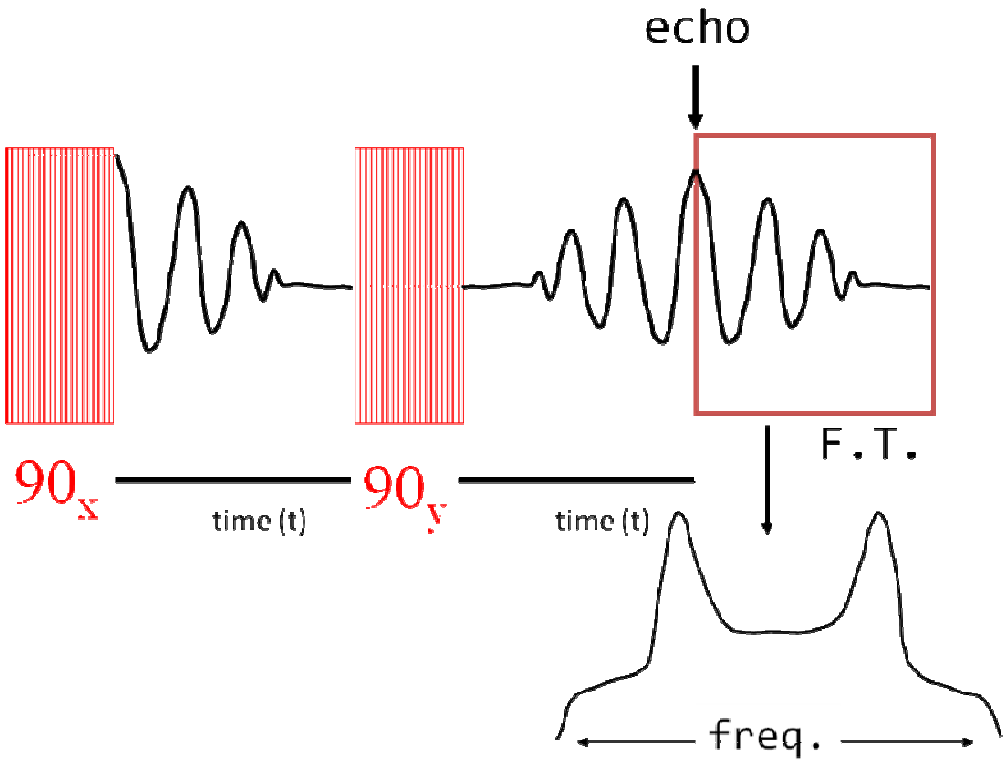

Figure 1.13. Schematic diagram of the quadrupole echo pulse sequence experiment.

1.5.2. FTIR Spectroscopy. FTIR spectroscopy is a type of absorption spectroscopy that uses electromagnetic radiation with wavelengths that approximately range from 1 to 100 μm. In FTIR, wavenumbers (the reciprocal of the wavelength expressed in centimeters) are generally used instead of wavelengths. The infrared spectrum can be divided into three regions, far-IR (10 to 400 cm^{-1}), mid-IR (MIR) (400 to 4,000 cm^{-1}), and near-IR (4,000 to 14,000 cm^{-1}). The most used region in IR spectroscopy is the mid-IR, where structural information can be obtained. This region is often used to determine the molecular structure of compounds.

IR absorption intensities are proportional to the distance that the radiation passes through a medium, b, and also to the concentration of absorbent species, c. Therefore, the linear range of absorbance, A, can be written:

$$A = \alpha bc \qquad (1.25)$$

where α is the molar absorption coefficient, sometimes called the specific absorptivity. Equation (1.25) is also known as the Beer-Lambert law, which is generally applied in all absorption spectroscopy as long as the system is in the linear range. From Equation (1.25), a concentration of an unknown can be determined if α and b are known.

FTIR is a simple and effective technique that has been widely used in polymer science for characterization of structure, stereochemistry or tacticity,[89] and glass transition temperature (T_g).[90] The technique has also been applied to investigate polymer composites.[22, 91] When a polymer is adsorbed onto a surface, the interaction at or near the interface can simply be observed using FTIR. FTIR spectra give information concerning the interaction between the polymers studied and the surface via the shifts of resonances. For example, the frequency of carbonyl groups in poly(alkyl methacrylate) that formed

hydrogen bonding with a silica surface, was found to be approximately 20 cm^{-1} lower than that of the bulk polymer.[91-93] The FTIR, moreover, can also be used to quantitatively determine the number of segments or carbonyls in poly(alkyl methacrylates) attached to the surface. [94, 95]

Quantitative analysis for a system like a polymer adsorbed on a surface, however, is quite complicated, due to the several parameters required. The absorption coefficients for bulk and adsorbed polymers were determined first. An external calibration was required to accurately determine the concentration of a component, which directly correlated to the number of molecules of the species of interest. This calibration can be used to determine the molar absorption coefficient, α. Not only are several different experiments required to obtain a final result, but numerous errors can occur during the process. Koenig et al. suggested a quantitative IR method, without external calibration, by using the ratio of the intensities of two resonances.[96] This concept was very useful for quantitative analysis.

The number adsorbed of polymer segments can be calculated in terms of a fraction by using the ratio of the intensities of two resonances.[22] With this method, the experiment is more practical and results can be easily achieved. A bound fraction is typically equal to the number of segments or groups that are attached to a surface, as compared to the total number of carbonyl groups contained in a polymer. If M_t is defined as the total adsorbed amount (in mg polymer/m^2 surface), M_b is equal to the adsorbed amount of bound polymer, and M_f represents unbound or free polymer, then the fraction of bound segments, p, is given by:

$$p = \frac{M_b}{M_f + M_b} = \frac{M_b}{M_t} \tag{1.26}$$

In this dissertation, the materials of interest were acrylate and methacrylate polymers, which contained carbonyl groups as an active functional group, and fumed silica used as a substrate. The interaction at the solid interface was from hydrogen bonding between carbonyl groups and silanol groups on the silica surface. The segments attached to the surface, therefore, were also called "*bound carbonyls*" in our study. The interaction at the polymer-solid interface and the degree of adsorption can affect physical properties of the polymer composites, especially a thermal property like the T_g of the adsorbed polymers.[80, 97] The effect can also be observed by using modulated differential scanning calorimetry (MDSC).

1.5.3. Modulated Differential Scanning Calorimetry (MDSC). MDSC is a fairly new thermal analysis technique that has been widely used for determining physical properties of polymers. The properties include glass transition temperatures (T_g), melt temperatures (T_m), crystalline temperatures (T_c), and degradation temperatures (T_D), as well as heat capacities. The concept of MDSC is based on measuring temperatures and heat flows associated with transitions in material, as a function of temperature and time. The basic theory of MDSC can be easily understood by comparing it to conventional DSC.

In conventional DSC, the difference in the amount of energy (heat) absorbed or released by a sample is measured and compared to a reference, as a function of temperature and time. Both the sample and reference are maintained in the same environment. The heat flow rate can be calculated by Equation (1.31):[98]

$$\frac{dQ}{dt} = C_p \frac{dT}{dt} + f(t,T) \tag{1.31}$$

where *dQ/dt* is the total heat flow, C_p is the reversing heat capacity, *dT/dt* is heating rate, *f(t, T)* is related to kinetic responses due to physical or chemical transformations, and T_b is the temperature of the sample, which can be obtained from Equation (1.32).[99]

$$T_b = T_0 + qt \tag{1.32}$$

where T_0 is the initial temperature, q is the programmed heating rate (°C/min), and t is the heating time. Therefore, the signal from DSC will contain information that depends on the temperature and the heat flow rate. Increasing the heating rate will increase the ratio of the signal to noise (S/N) ratio. To improve the S/N by increasing the heating rate, however, results in a poorer sample temperature resolution. Hence, the identification of the overlapped/hidden transition would be rather difficult or impossible.

Modulated DSC (MDSC) was introduced by Reading[100] to overcome the limitations mentioned above. Not only was the same information as that of the conventional DSC obtained, but the S/N also improved with higher resolution. Moreover, the MDSC provided more benefits than the conventional method since the quasi-isothermal heat capacity could be measured using MDSC.

MDSC is conventional DSC with the exception of the sinusoidal perturbation of the linear heating program. Equation (1.32) becomes:

$$T_b = T_0 + qt + B\sin(wt) \tag{1.33}$$

where w is the frequency, and B is the amplitude of the temperature modulation. Hence, two heating rates are used in MDSC: the average heating rate, and the sinusoidal heating rate. The MDSC signal can be described as in the following equation:

$$\frac{dQ}{dt} = C_p q + f'(t,T) + C_p Bw\cos(wt) + C\sin(wt) \qquad (1.34)$$

The first two terms in Equation (1.34) provide information on the total heat flow as obtained from conventional DSC. The additional terms provide information concerning the heat capacity from the heat flow that responds to the rate of temperature change.

The signal obtained from MDSC can be more easily interpreted than the one from conventional DSC, which makes possible the analysis of complex transitions in materials so that MDSC becomes a technique that is useful for studying polymer thin films. The MDSC gives a high resolution signal that yields a distinguishable transition of a polymer at an interface, which is useful for both qualitative and quantitative analysis.[10]

1.6 REFERENCES

1. Keddie, J. L.; Jones, R. A. L.; Cory, R. A., *Europhys. Lett.* **1994,** 27, 59.
2. Keddie, J. L., Jones, R. A. L., Cory, R. A., *Faraday Discuss* **1994,** 98, 219.
3. Zhang, B.; Blum, F. D., *Macromolecules* **2003,** 36, 8522.
4. Kim, J. H.; Jang, J.; Zin, W.-C., *Langmuir* **2000,** 16, 4064.
5. See, Y.-K.; Cha, J.; Chang, T.; Ree, M., *Langmuir* **2000,** 16, 2351.
6. Kanaya, T.; Inoue, R.; Kawashima, K.; Miyazaki, T.; Tsukushi, I.; Shibata, K.; Matsuba, G.; Nishida, K.; Hino, M., *J. Phys. Soc. Japan* **2009,** 78, 041004.
7. Tsui, O. K. C.; Russell, T. P.; Hawker, C. J., *Macromolecules* **2001,** 34, 5535.
8. Kanaya, T.; Miyazaki, T.; Watanabe, H.; Nishida, K.; Yamano, H.; Tasaki, S.; Bucknall, D. B., *Polymer* **2003,** 44, 3769.
9. Wünderlich, B., American Society for Testing and Materials: Philadelphia, 1994; p 17-31.
10. Blum, F. D.; Young, E. N.; Smith, G.; Sitton, O. C., *Langmuir* **2006,** 22, 4741.
11. Fukao, K., Miyamoto, Y., *Phys. Review E* **2000,** 61, 1743.

12. Labahn, D.; Mix, R.; Schonhals, A., *Phys. Review E* **2009,** 79, 011801.

13. Dalnoki-Veress, K.; Forrest, J. A.; Murray, C.; Gigault, C.; Dutcher, J. R., *Phys. Review E* **2001,** 63, 031801.

14. Forrest, J. A.; Dalnoki-Veress, K.; Stevens, J. R.; Dutcher, J. R., *Phys. Rev. Lett.* **1996,** 77, 2002.

15. Forrest, J. A.; Dalnoki-Veress, K.; Dutcher, J. R., *Phys. Review E* **1997,** 56, 5705.

16. Tsui, O. K. C.; Wang, X. P.; Ho, J. Y. L.; Ng, T. K.; Xiao, X., *Macromolecules* **2000,** 33, 4198.

17. Erichsen, J., Dolgner, K., Zaporojtchenko, V., Faupel, F., *Macromolecules* **2004,** 37, 8813.

18. DeMaggio, G. B.; Frieze, W. E.; Gidley, D. W.; Zhu, M.; Hristov, H. A.; Yee, A. F., *Phys. Rev. Lett.* **1997,** 78, 1524.

19. Fryer, D. S.; Nealey, P. F.; de Pablo, J. J., *Macromolecules* **2000,** 33, 6439.

20. Ellison, C. J.; Torkelson, J. M., *Nat Mater* **2003,** 2, 695.

21. Roth, C. B.; McNerny, K. L.; Jager, W. F.; Torkelson, J. M., *Macromolecules* **2007,** 40, 2568.

22. Kulkeratiyut, S.; Kulkeratiyut, S.; Blum, F. D., *J. Polym. Sci., Part B: Polym. Phys.* **2006,** 44, 2071.

23. Urban, M. W.; Koenig, J. L., *Applied Spectroscopy* **1986,** 40, 513.

24. Keddie, J. L.; Jones, R. A. L.; Cory, R. A., *Faraday Discuss.* **1994,** 98, 219.

25. Shin, H. S.; Jung, Y. M.; Oh, T. Y.; Chang, T.; Kim, S. B.; Lee, D. H.; Noda, I., *Langmuir* **2002,** 18, 5953.

26. Lin, W. Y., Blum, F. D., *Macromolecules* **1998,** 31, 4135.

27. Metin, B. B., F. D., *J. Chem. Phys* **2006,** 124, 054908.

28. Tretinnikov, O. N.; Ohta, K., *Macromolecules* **2002,** 35, 7343.

29. Tretinnikov, O. N., *Macromolecules* **2003,** 36, 2179.

30. Painter, P.; Huang, H., *Macromolecules* **2008,** 41, 2494.

31. Ogura, K.; Kawamura, S.; Sobue, H., *Macromolecules* **1971,** 4, 79.

32. Rössler, E.; Sillescu, H.; Spiess, H. W., *Polymer* **1985,** 26, 203-207.

33. O'Connor, R. D.; Blum, F. D.; Ginsburg, E.; Miller, R. D., *Macromolecules* **1998,** 31, 4852-4861.

34. Rössler, E.; Vogel, M., *J. Phys. Chem. A* **1998,** 102, 2102-2108.

35. Cormier, R. J.; Callaghan, P. T., *J. Chem. Phys* **2002,** 116, 10020-10029.

36. Ngai, K. L.; Roland, C. M., *Macromolecules* **2004**, 37, 2817-2822.

37. Greenfield, M. S.; Ronemus, A. D.; Vold, R. L.; Vold, R. R.; Ellis, P. D.; Raidy, T. E., *J. Magn. Reson.* **1987,** 72, 89.

38. Matyjaszewski, K.; Coessens, V.; Nakagawa, Y.; Xia, J.; Qui, J.; Gaynor, S.; Coca, S.; Jasieczek, C., *ACS Sym. Ser* **1998,** 704, 16.

39. Matyjaszewski, K.; Qiu, J.; Shipp, D. A.; Gaynor, S. G., *Macromol. Symp* **2000,** 155, 15.

40. Shinoda, H.; Matyjaszewski, K., *Macromolecules* **2001,** 34, 3186.

41. Mather, P. T.; Jeon, H. G.; Chun, S. B.; Pyun, J.; Matyjaszewski, K., *Polym. Prep:* **2000,** 41, 582.

42. Darcos, V.; Haddleton, D. M., *Euro. Polm. J* **2003,** 39, 855-862.

43. Matyjaszewski, K.; Coca, S.; Gaynor, S. G.; Y., N.; Jo, D. M. 9801480.

44. Patten, T. E.; Matyjaszewski, K., *Adv. Mater* **1998,** 10, 901.

45. Matyjaszewski, K.; Xia J., *Chem Rev.* **2001,** 101, 2921.

46. Matyjaszewski, K., *Controlled/ Living Radical Polymerization: Progress in ATRP, NMP and RAFT*. American Chemical Society: Washington DC, 2000.

47. Matyjaszewski, K.; Davis, T. P., *Handbook of Radical Polymerization*. Wiley: Hoboken, 2002.

48. Matyjaszewski, K., *Chem. Euro. J.* **1999,** 5, 3095.

49. Kato, M.; Kamigoito, M.; Sawamoto, M.; Higashimura, T., *Macromolecules* **1995,** 28, 1721.

50. Haddleton, D. M.; Jasieczek, C. B.; Hannon, M. J.; Shooter, A. J., *Macromolecules* **1997,** 30, 2190.

51. Grimaud, T.; Matyjaszewski, K., *Macromolecules* **1997,** 30, 2216.

52. Uegaki, H.; Kotani, Y.; Kamigato, M.; Sawamoto, M., *Macromolecules* **1995,** 28, 1721.

53. Ando, T.; Kamigaito, M.; Sawamoto, M., *Macromolecules* **1997,** 30, 4507.

54. Granel, C.; Dubois, P.; Jérôme, R.; Teyssié, P., *Macromolecules* **1996,** 29, 8576.

55. Moineau, G.; Minet, M.; Dubois, P.; Teyssié, P.; Senninger, T.; Jérôme, R., *Macromolecules* **1999,** 32, 27.

56. Lecomte, P.; Drapier, I.; Teyssié, P.; Jérôme, R., *Macromolecules* **1997,** 30, 7631.

57. Louie, J.; Grubbs, R. H., *Chem. Commun* **2000**, 1479.

58. Matyjaszewski, K.; Jo, S. M.; Paik, H.-j.; Shipp, D. A., *Macromolecules* **1999,** 32, 6431.

59. Matyjaszewski, K.; Jo, S. M.; Paik, H.-j.; Gaynor, S. G., *Macromolecules* **1997,** 30, 6398.

60. Matyjaszewski, K.; Patten, T. E.; Xia, J., *J. Am. Chem. Soc.* **1997,** 119, 674.

61. Matyjaszewski, K.; Wei, M.; Xia, J.; McDermott, N. E., *Macromolecules* **1998,** 31, 6756.

62. Wang, J. S.; Matyjaszewski, K., *Macromolecules* **1995,** 28, 7970.

63. Kotani, Y.; Kamigaito, M.; Sawamoto, M., *Macromolecules* **1999,** 32, 2420.

64. Kotani, Y.; Kamigaito, M.; Sawamoto, M., *Macromolecules* **2000,** 33, 6746.

65. Percec, V.; Barboiu, B.; Kim, H.-J., *J. Am. Chem. Soc.* **1998,** 120, 305.

66. Xia, J.; Matyjaszewski, K., *Macromolecules* **1997,** 30, 7697.

67. Percec, V.; Barboiu, B., *Macromolecules* **1995,** 28, 7970.

68. Davis, K.; Paik, H.-j.; Matyjaszewski, K., *Macromolecules* **1999,** 32, 1767.

69. Xia, J.; Gaynor, S. G.; Matyjaszewski, K., *Macromolecules,* **1998,** 31, 5958.

70. Teodorescu, M.; Gaynor, S. G.; Matyjaszewski, K., *Macromolecules* **2000,** 33, 2335.

71. Ashford, E. J.; Naldi, V.; O'Dell, R.; Billingham, N. C.; Armes, S. P., *Chem. Commun.* **1999**, 1285.

72. Koji, F.; Yoshihisa, M., *Phys. Review E* **2001,** 64, 011803.

73. Fleer, G. J.; Cohen Stuart, M. A.; Scheutjens, J. M. H. M.; Cosgrove, T.; Vincent, B., *Polymers at Interfaces*. Capman and Hall: London, U.K., 1993.

74. Kawaguchi, M.; Aoki, M.; Takahashi, A., *Macromolecules* **2002,** 16, 635.

75. Kawaguchi, M.; Hayakawa, K.; Takahashi, A., *Macromolecules* **2002,** 16, 631.

76. Scheutjens, M. H. M.; Fleer, G. J., *J. Phys. Chem* **1979,** 83, 1619.

77. Scheutjens, J. M. H. M.; Fleer, G. J., *J. Phys. Chem.,* **1980,** 84, 178.

78. Sanchez, I. C., *Physics of Polymer Surfaces and Interfaces*. Butterworth-Heinemann: Boston, 1992.

79. Porter, C. E.; Blum, F. D., *Macromolecules* **2000,** 33, 7016.

80. Kabomo, M. T.; Blum, F. D.; Kulkeratiyut, S.; Kulkeratiyut, S.; Krisanangkura, P., **2008,** 46, 649.

81. Metin, B.; Blum, F. D., *J. Chem. Phys.* **2006,** 124, 054908/1.

82. Nambiar, R. R.; Blum, F. D., *Macromolecules* **2008,** 41, 983.

83. Okuom, M. O.; Metin, B.; Blum, F. D., *Langmuir* **2008,** 24, 2539.

84. Langmuir, I., *J. Am. Chem. Soc.* **1981,** 40, 1361.

85. Jones, R. A. L.; Richards, R. W., *Polymers at Surfaces and Interfaces*. Cambridge University Press: U.K, 1999.

86. Mathias, L. J., *Solid State NMR of Polymers*. Plenum Press,: New York, 1991.

87. Ulrich, A. S.; Grage, S. L., Solid State NMR of Polymers. In *Solid State NMR of Polymers*, Ando, I.; Asakura, T., Eds. Elsevier: New York, 1998; Vol. 84, p 190.

88. Spiess, H. W., *Colloid Polym. Sci.* **1983,** 261, 193.

89. Grohens, Y.; Prud'homme, R. E.; Schultz, J., *Macromolecules* **1998,** 31, 2545.

90. Koenig, J. L.; William, H. W. In *Probing polymer structures*, the 174th meeting of the American Chemical Society Chicago, Illinois, August 29-September 2, 1977, 1979; Koenig, J. L., Ed. American Chemical Society: Chicago, Illinois, 1979; pp 99-139.

91. Fontana, B. J.; Thomas, J. R., *J. Phys. Chem.* **1961,** 65, 480.

92. Berquier, J.-M.; Arribart, H., *Langmuir* **1998,** 14, 3716.

93. Sakai, H.; Imamura, Y., *Bull. Chem. Soc. Jpn.* **1980,** 53, 1749.

94. Sakai, H.; Fujimori, T.; Imamura, Y., *Bull. Chem. Soc. Jpn.* **1980,** 53, 3457.

95. Johnson, H. E.; Granick, S., *Macromolecules* **1990,** 23, 3367.

96. Koenig, J., L.; Kormos, D., *Applied Spectroscopy* **1979,** 33, 349.

97. Blum, F. D.; Krisanangkura, P., *Thermochimica Acta* **2009,** 492, 55.

98. Reading, M.; Luget, A.; Wilson, R., *Thermochimica Acta* **1994,** 238, 295.

99. Sandler, R. S.; Karo, W.; Bonesteel, J.; Pearce, M. E., *Polymer Synthesis and Characterization: A Laboratory Manual*. Academic Press: San Diego, 1998.

100. Reading, M., *Trends Polym. Sci.* **1993,** 1, 248.

PAPER 1: DYNAMICS OF BULK AND ADSORBED POLY(ISOPROPYL ACRYLATE-D_7) ON A SILICA SURFACE USING ^{2}H NMR

Piyawan Krisanangkura and Frank D. Blum

Department of Chemistry and Materials Research Center, Missouri University of Science and Technology, Rolla, Missouri 65409-0010, USA

1.1 ABSTRACT

The segmental dynamics of bulk and adsorbed poly(isopropyl acrylate)-d_7 (PIPA-d_7) was studied as a function of temperature using quadrupole echo ^{2}H solid-state NMR. The spectra of both bulk and surface PIPA-d_7 showed superimposed powder patterns due to two methyl groups and a methine group on the polymer side chain. The experimental spectra were fitted using superimpositions of calculated spectra, which were simulated from the MXQET program, with different jump rates. The simulated spectra for the methine were produced using a jump model based on positions on the vertices of a truncated icosahedron (soccer ball model), whereas the set for methyl motions was created from a combination of the soccer ball model and a two-site hop model with a tetrahedral angle. In the ^{2}H NMR spectra for the adsorbed sample, the residual powder pattern at the higher temperatures indicated that some of the polymer segments were strongly bound to the silica surface, which was consistent with an increase in the glass transition temperature (T_g) of the PIPA-d_7-silica composite. The change in the thermal

behavior of the adsorbed PIPA-d_7 was also probed with modulated differential scanning calorimetry (MDSC) experiments.

1.2 INTRODUCTION

Polymer composite systems have been studied extensively to determine and understand their physical properties. A significant topic in this area of interest is the behavior of the glass transition temperatures (T_gs)[1] for polymers adsorbed on solid substrates. Changes in the thermal properties of composite materials may be due to several factors, including, the properties of the polymers[2] or the polymer molecular mass.[3, 4] Fillers and their interaction with polymers[5-8] are also a major contributor to changes in the thermal behavior of polymers. If there is a strong attractive interaction, such as hydrogen bonding between the polymer and the surface, the T_g of the composites would be expected to increase.[9, 10] On the contrary, the T_g would be lower than that of the bulk polymer if the interaction at the interface is weak or repulsive,[11, 12] which could result in more mobile polymers.[13, 14] Numerous methods, such as ellipsometry,[15, 16] modulated differential scanning calorimetry (MDSC),[17] and nuclear magnetic resonance (NMR),[18] have been used to probe this phenomena.

^{2}H solid state NMR is a powerful tool for investigating molecular motion to assist in understanding polymer behavior at an interface. The NMR technique has been used for studying the motion of polymers in various systems, and labeled species provide specific probes in different parts of polymer segments. Jelinski et al. studied the motion of the backbone of polyurethanes through ^{2}H labeling of the methylene group of polyurethanes chains.[19] Aromatic-d_4 poly(butylene terephthalate) was deuterated on an aromatic ring to study the flip of the aromatic ring.[20-23] These studies focused on the movement of the

backbone only. In some cases, especially for polymers with side chains, the size of the polymer side chain would be expected to affect the adsorption process, as well as the molecular motion. Steric hindrance may restrict the movements of the bulk polymer coils and polymer segments on the surface. Recently, some polymers with different kinds of side chains, such as poly(methyl acrylate)-d_3 (PMA-d_3),[4, 24, 25] and poly(vinyl acetate)- d_3 (PVAc- d_3),[26] were studied using this technique.

Wide line ^{2}H NMR spectra provided both qualitative and quantitative information on segmental dynamics of the polymer. The ^{2}H NMR lineshapes consisted of powder patterns of randomly oriented C-D bonds from different angles that were combined to yield the full spectrum. Each type of molecular motion yielded different shapes of ^{2}H NMR spectra.[27] The lineshapes also changed along with the motion of the C-D bonds.[28] The motion of glassy polymers was rather slow, or there were effectively no movements of the C-D bonds on the ^{2}H NMR timescale, resulting in a broad solid powder pattern. The spectra became narrower with increasing motional rates, and the powder pattern collapsed and became a single resonance with molecules that had fast isotropic motions. The single sharp resonance indicated that the compound acted in a liquid-like manner. The T_g region was identified as the temperature range at which the ^{2}H NMR spectrum started to collapse until it became a single resonance.

The simulation of ^{2}H NMR lineshapes, based on specific jump models, can provide more insight on segmental dynamics. The theoretical quadrupolar powder patterns can be calculated using ^{2}H solid-state NMR theory. Various computation programs have been written and developed for routine analysis, including Witterbort,[29] MXQET,[30, 31] and EXPRESS.[32] By varying some specific parameters like the number of

exchange sites and rates of motion, NMR spectra can be generated and matched the experimental ones. Weight fractions of each simulated spectrum used for fitting provided approximate information as to what and how much of each component had been combined in the segmental dynamics.

This work focuses on using solid-state ^{2}H NMR to study the mobility of bulk and adsorbed poly(isopropyl acrylate) (PIPA- d_7) on a silica surface. PIPA- d_7 consists of a branched chain with two methyl groups and a methine attached on the same carbon atom. With larger bulky groups on the polymer side chain, as compared to PMA (one methyl group), the deuteration of the side chain in PIPA gave different segment mobility from that shown by previous studies.[18, 26, 33] Lineshapes for bulk and adsorbed PIPA- d_7, obtained at different temperatures, are presented. The MXQET program was selected as the method to be used for generating simulated lineshapes. Different kinds of jump models and various numbers of exchange sites were tested to determine the best fits for the bulk PIPA- d_7 spectra. A series of simulated lineshapes with different jump rates were superimposed on the experimental spectra. Least-square fit methods were applied, and the weight factors[3] were calculated for each of the simulated spectra using MATLAB (The Mathworks, Inc. Natick, MA).

1.3 EXPERIMENTAL

1.3.1. Chemicals. Acryloyl chloride (96%), was purchased from Aldrich Chemical (Milwaukee, WI). Isopropanol-d_8 (99% D) was purchased from CIL (Andover, MA). Isopropanol (AR grade) was obtained from Fisher Scientific. Triethylamine (99.9%) was obtained from Alfa Aesar (Ward Hill, MA). Ethyl 2-bromopropionate (2-

EBP) (99%), *N, N, N´, N˝, N˝*-pentamethyl-diethylenetriamine (PMDETA) (99%), and Cu(I)Br (98%) were purchased from Aldrich. Acryloyl chloride was purified by vacuum distillation at 70 ºC before use. Other chemicals were AR grade and used as received.

1.3.2. Synthesis of Isopropyl Acrylate. The structures of isopropyl and heptadeutero-isopropyl acrylate are shown in Figure 1.1.

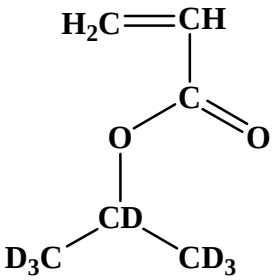

Figure 1.1. The structure of isopropyl acrylate-d_7

Deuterated isopropyl acrylate monomer was prepared from acryloyl chloride and isopropanol-d_8, is shown in the following reaction:

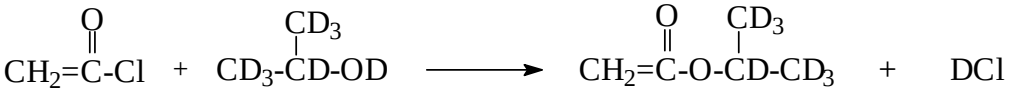

Figure 1.2. The deuteration of isopropyl acrylate.

Purified acryloyl chloride (2.5 ml, 0.4 mole) in 25 mL of toluene was added dropwise into a stirred mixture of 30.6 mL (0.4 mole) of isopropanol-d_8 (CIL, D, 99%), 53.8 mL (0.4 mole) of triethylamine and toluene. The product was transferred to a 1000 mL funnel to be separated, washed three times with a 5% sodium hydrogen carbonate

solution and three times with deionized water. Traces of water in the toluene extract were removed by slowly adding calcium hydride at 0 ºC while stirring continuously until no hydrogen gas came out. The mixture was stirred and maintained at 0 ºC for 1 h, and then stirred and kept at room temperature for 24 h, then purified by vacuum distillation using a rotational evaporator. The product yield was approximately 70%.

1.3.3. Polymerization. Poly(isopropyl acrylate)-d_7 was synthesized by atom transfer radical polymerization (ATRP). The optimum conditions for isopropyl acrylate polymerization were studied at various temperatures. At 75 ºC, the ratio (in moles) of ligand to initiator was 2:1, and polymerization of the isopropyl acrylate monomer by the ATRP technique was achieved within 10 h. The amounts of monomer, initiator, ligand, and catalyst were varied according to the desired molecular mass of the polymer. The degree of polymerization was estimated from $DP_n = \Delta[M]/ [I]_0$. Ethyl 2-bromopropionate (2-EBP) (Aldrich, 99%), *N, N, N´, N˝, N˝*-pentamethyl-diethylenetriamine (PMDETA) (Aldrich, 99%), and Cu(I)Br (Aldrich, 98%), which were used as the initiator, ligand, and catalyst, respectively. All chemicals were used as received. Monomer, PMDETA, Cu(I)Br and toluene were added into a 100 ml round bottom flask and then tightly closed with a septum. The mixture was purged with nitrogen gas for 15 min, then 2-EBP was added to the mixture and purging was continued for another 10 min. Bulk polymerization of poly(isopropyl acrylate) was performed at 75 ºC in an oil bath. The viscosity of the mixture increased gradually over several hours. After, the reaction was completed (approximately 10 h), Cu(I)Br was removed from the polymer by column chromatography using a column packed with alumina. Acetone was used as an eluent.

The polymer was kept under a vacuum in an oven at room temperature for 36 h to remove solvent.

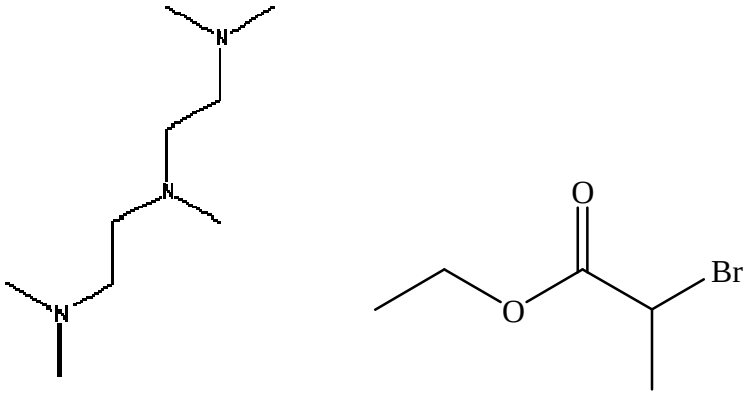

(a) (b)

Figure 1.3. The structures of (a) *N, N, N´, N˝, N˝*-pentamethyldiethylenetriamine (PMDETA) and (b) ethyl 2-bromopropionate (2-EBP).

1.3.4. Polymer Adsorption. Adsorbed samples were prepared by depositing PIPA-d_7 onto amorphous fumed silica, Cab-O-Sil M5P (Cabot Corp., Tuscola, IL), with a surface area of 200 m^2/g. The silica was dried in a furnace at 450 ºC before use. Various concentrations of PIPA-d_7 in toluene were freshly prepared and mixed with 0.3 g silica in a test tube. The tightly closed test tubes of the mixture were placed in and shaken in a mechanical shaker for 72 h. The sample tubes were centrifuged at 2500 rpm for 1 h after shaking, and then the supernatant was decanted. The polymer-adsorbed silica was dried by passing air through the gel samples until they became a dull white (dry) powder. Then all samples were dried in a vacuum oven at room temperature for 36 h, or until there was no trace of solvent. The amount of PIPA-d_7 adsorbed on the silica was determined using

thermogravimetric analysis (TGA) (Hi-Res Thermogravimetric Analyzer 2950, TA Instruments, New Castle, DE).

1.3.5. Characterization.

1.3.5.1 Polymer molecular mass and refractive index increment (dn/dC). The refractive index increment of poly(isopropyl acrylate) in tetrahydrofuran (THF) at 690 nm at room temperature was 0.0398 mL/g, measured using an OPTILAB DSP Interferometer Refractometer (Wyatt Technology, Santa Barbara, CA). The polymer molecular mass and polydispersity were determined by gel permeation chromatography (GPC) in THF at room temperature. The measurements were performed using an OPTILAB DSP Interferometer Refractive Index Detector and a DAWN EOS Light Scattering Instrument (Wyatt Technology, Santa Barbara, CA), connecting to a gel permeation column and isocratic pump.

1.3.5.2 Glass-transition temperature (T_g). The T_gs of bulk polymers were obtained by modulated differential scanning calorimeter (MDSC) (TA Instrument, New Castle, DE). Three scans, two heating scans and one cooling scan, were performed on each of the bulk samples at a heating rate of 2.5 ºC/min, from -40 to 70 ºC, with modulation amplitude of ± 0.5 ºC and a period of 60 seconds. The T_gs of adsorbed samples were performed with the same procedure. A MDSC thermogram obtained from the second heating cycle was used for T_g analysis.

1.3.5.3 ^{2}H solid-state. The ^{2}H NMR spectra of both bulk polymers were recorded using a VARIAN VXR-400/S spectrometer with an Oxford 400 89 mm magnet. The quadruple echo pulse sequence (delay-90_y-tau-90_x-τ -acquisition) at ^{2}H frequency of 61.39 MHz was used for 1D-spectra. The 90º pulse width was 2.8 μs with an echo time of

27 μs and 1 s of delay time. Temperature was controlled by an Oxford VT controller. The spectra were obtained from -40 to 70 ºC with a 5 ºC increment. Liquid nitrogen was used to cool the probe at temperatures lower than 20 ºC. The number of scans used for the bulk and the adsorbed samples was 256 and 1024, respectively. The echo data were analyzed by the Mestre-C software package (Santiago de Compostela University, Spain).

1.3.5.4 Spectral simulation. The MXQET program[30, 31] was used to simulate experimental lineshapes. Jump models with methyl rotations (3-site jump for the symmetry axis of the methyl group) were included in the program package, and a soccer ball model (60-site jump with vertices defined based on a truncated icosahedron structure, as shown in Figure 1.4A) were developed by Metin et al.[3, 18] These were primarily used to simulate motions of the methyl and methine groups in PIPA-d_7. Additionally, a 2-site hop (with the symmetry axis of the methyl group) and a combination of each model were used to create the lineshapes to make the ones closest to the experimental spectrum. A quadrupole-coupling constant (QCC) of 150 kHz was used for the simulations of the static methine, and a reduced QCC of 52 kHz was used for fast rotation of the methyl groups. A 2.8 μs 90º pulse width and a 27 μs pulse spacing were set for the quadrupole-echo pulse sequence in the simulations. A set of simulated lineshapes, with different jump rates, was produced from each of the models. A series of simulated spectra from the models, with the combined 2-site hop and soccer ball models, were selected to fit a part of the experimental spectrum dominated by the two methyl groups. The methine should have the same motions as the methyls; however, the QCC for the methine was much greater. A lineshape fitting program[3] was written and run by using MATLAB (The Mathworks, Inc., Natick, MA). All simulated basic

lineshapes were used, and a least-square fit was applied to find the weight factors for the best fit. Weight factors of the best fit were also estimated from the fitting program.

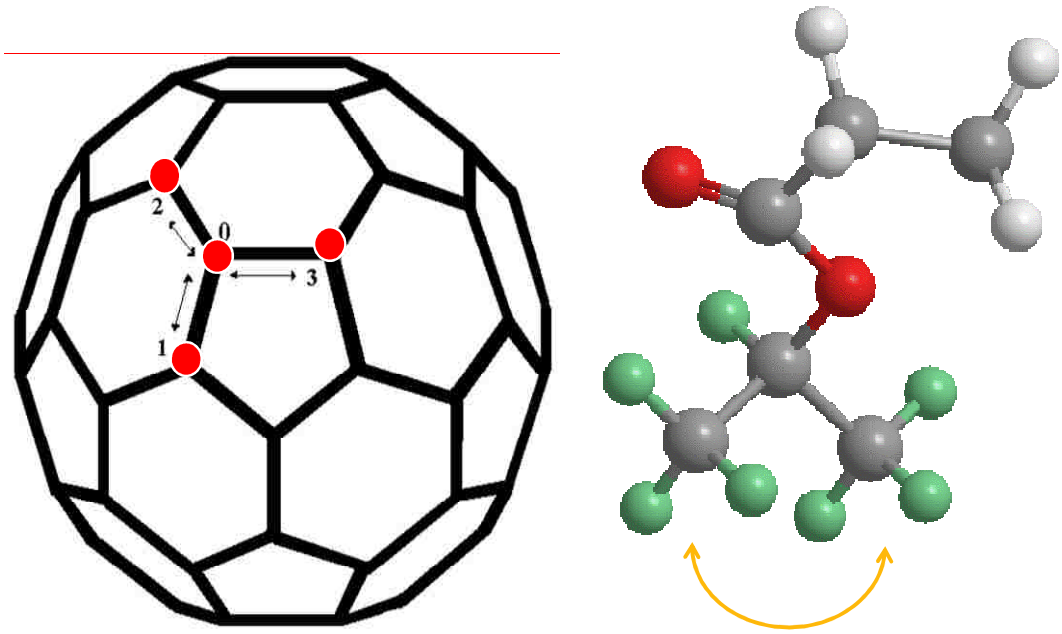

(A) **(B)**

Figure 1.4. The jump models used for the simulation: (A) Geometry of truncated icosahedron (soccer ball). Site 0 can exchange to any of the neighboring sites, 1, 2, or 3 with equal probabilities. (B) Two-site hop with 120º between two methyl groups of PIPA-d_7 side chain.

1.4 RESULTS

1.4.1. Synthesis of Isopropyl Acrylate-d_7 Monomer and Poly(isopropyl acrylate)-d_7.

Poly(isopropyl acrylate)-d_7 (PIPA-d_7) samples were prepared for bulk and adsorbed polymer studies. Isopropyl acrylate-d_7 (PIPA-d_7) was deuterated by reaction between isopropanol-d_8 and acryloyl chloride. For isopropyl alcohol, it was speculated that the process should proceed at a slightly slower rate than that for primary alcohol, due to the two bulky methyl groups. Thus, at 0 ºC, about 6 h were required for the reaction to be complete, compared to the deuterated poly(methyl acrylate)-d_3 (PMA-d_3) which took

3-4 h. ^{1}H and ^{2}H NMR were used to confirm the structure and purity of the product. The isopropyl acrylate-d_7 monomer yields were approximately 65%. PIPA-d_7 was synthesized from the deuterated monomer, and characterized. The molecular mass of PIPA-d_7 was determined to be 89 kDa with a polydispersity of 1.31. The T_g of PIPA-d_7 from MDSC was -11 ºC. The polymer was used to prepare three different adsorbed amounts on silica, 1.02, 2.34, and 3.17 mg/m^2.

1.4.2. ^{2}H NMR. A spectrum of bulk PIPA-d_7 was collected, starting at a temperature of -36 ºC, in this case, which was lower than the bulk T_g. A Pake powder pattern was obtained, indicating that the PIPA-d_7 was in a glassy state on the NMR time scale. The spectrum of PIPA-d_7 at -36 ºC (Figure 1.5) showed an intense powder pattern with a splitting of 37 kHz. This pattern is similar to that expected from a methyl group undergoing rapid motions. This powder pattern was very intense and resulting from the two methyl groups (six deuterons). The magnified portion of the spectrum confirmed that another powder pattern, from the methine was present and consistent with a static C-D bond. The splitting of the outer powder pattern was about 120 kHz.

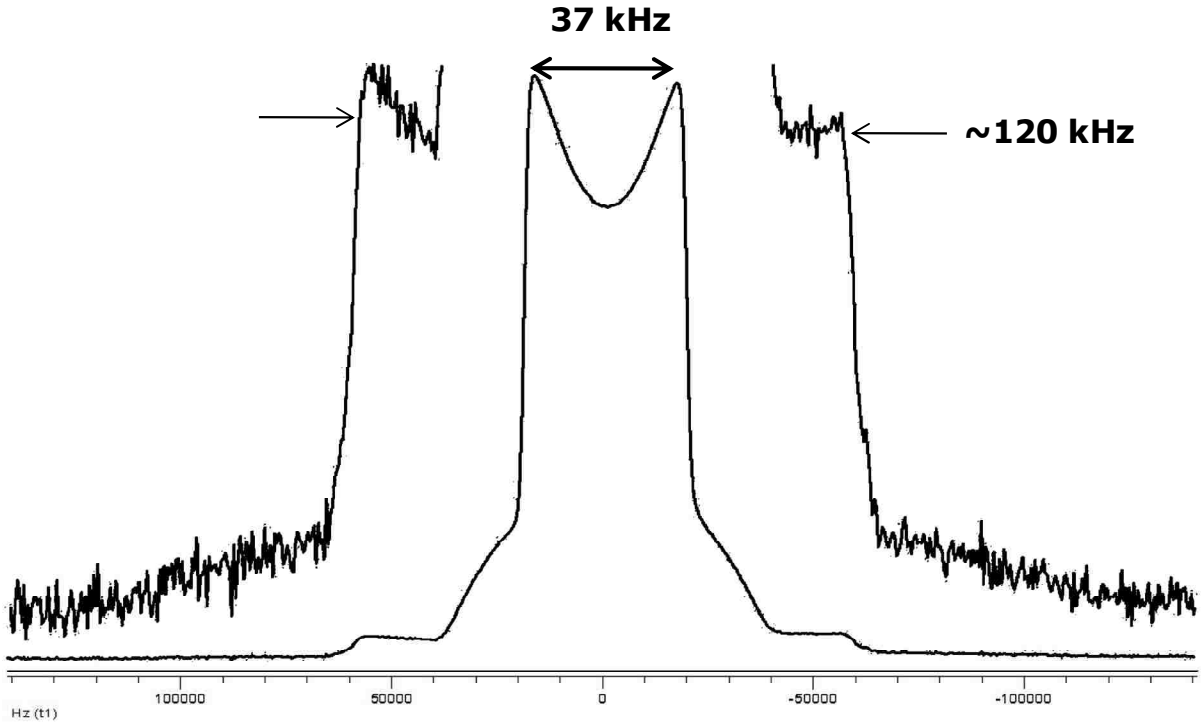

Figure 1.5. ^{2}H NMR spectrum of bulk PIPA-d_7 at -36 ºC. The magnified shoulders of the spectrum show the existence of methine deuteron resonance.

The ^{2}H NMR spectra of bulk PIPA-d_7 were collected as a function of temperature. The mobilities of the bulk polymers were observed, via their NMR spectra. Figure 1.6 shows the experimental ^{2}H NMR spectra of bulk PIPA-d_7 at different temperatures. At low temperatures, the spectra consisted of Pake patterns with splittings between the two main horns. The two horns broadened and collapsed around 16 ºC, where the spectrum became a very broad single resonance. A very small middle peak also showed up at this temperature. This small sharp resonance got more intense, and the spectra became narrower at higher temperatures. At 55 ºC, a sharp single resonance, with no residual of the powder pattern, was observed, indicating that the PIPA-d_7 was completely in a rubbery state.

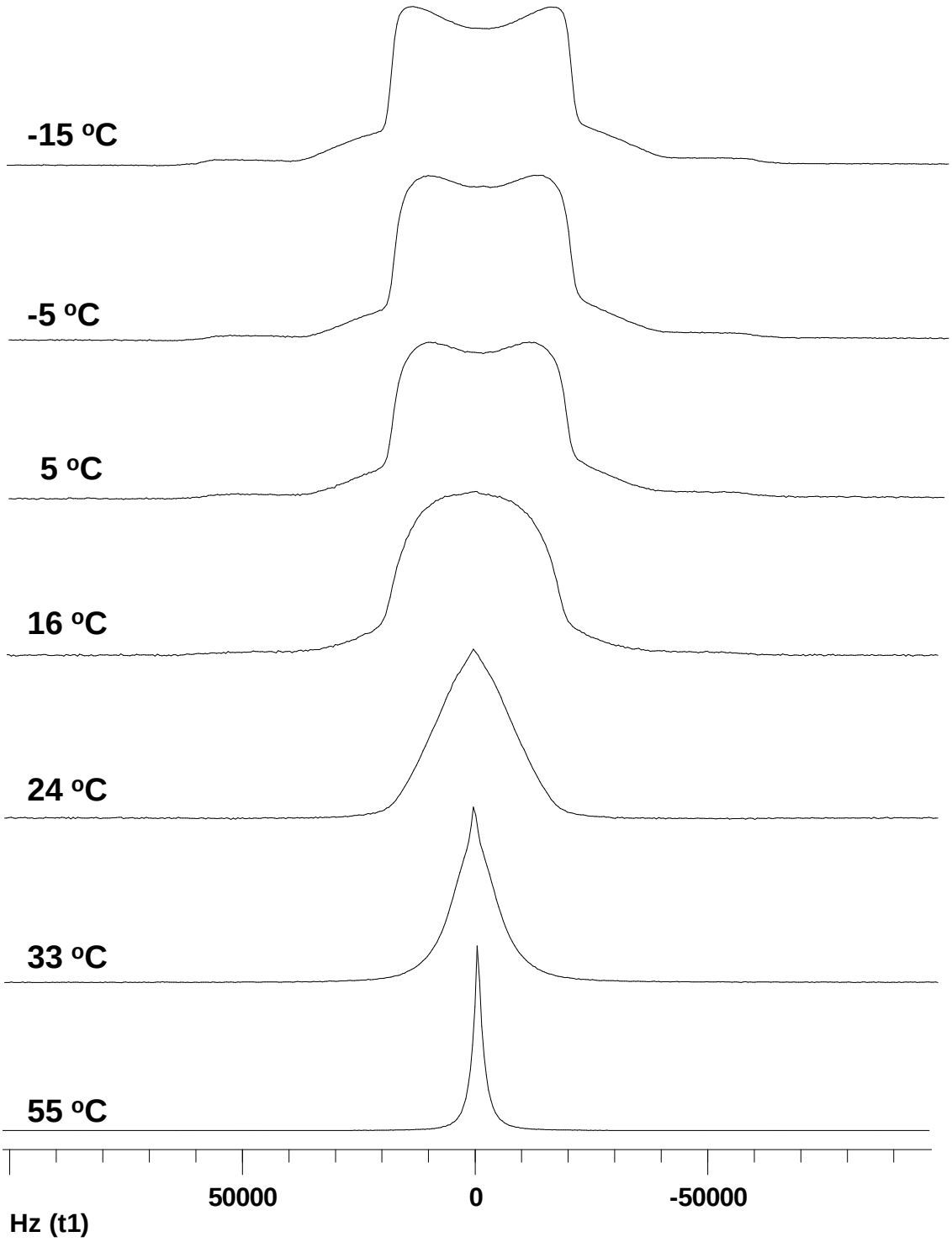

Figure 1.6. ^{2}H solid state NMR spectra of bulk PIPA-d_7 as a function of temperature.

Quadrupole echo NMR spectra for the surface samples, with adsorbed amounts of 1.02, 2.34, and 3.17 mg/m^2, were collected as a function of temperature, as shown in Figure 1.7, 1.8, and 1.9, respectively. With a relatively small adsorbed amount (1.02 mg/m^2 in this case, as shown in Figure 1.7), the surface sample showed behavior different from that of the bulk polymer. A ^{2}H NMR spectrum with a flatted-top powder pattern was obtained at the low temperatures studied. Unlike bulk PIPA-d_7, it is difficult to indicate at what temperature the spectrum of the small adsorbed amount PIPA-d_7 started to collapse. A small middle resonance, however, appeared at 24 ºC, indicating that a mobile component was moving faster and its intensity was increasing as the temperature increased. Although a sharp narrower resonance (that was almost liquid-like) was observed in the spectra of the small adsorbed amount sample at high temperature, the bases of the lineshapes clearly showed the presence of a residual powder pattern, which indicated the presence of some highly restricted segments in the adsorbed sample.

Samples with medium and large adsorbed amounts (shown in Figure 1.8 and 1.9) behaved more like the bulk sample. A broadened Pake pattern lineshape was obtained at a low temperature, and the spectrum was similar to that of the bulk sample. When the temperature increased, flat-top lineshapes were seen. A very broad spectrum with a small spike in the middle of the resonance was observed at 16 ºC. At higher temperatures, this sharp peak increased in intensity and the spectra became narrower. The changes of these spectra with temperature for this adsorbed sample was similar to that of the bulk sample although the residual powder pattern was still detected at higher temperatures.

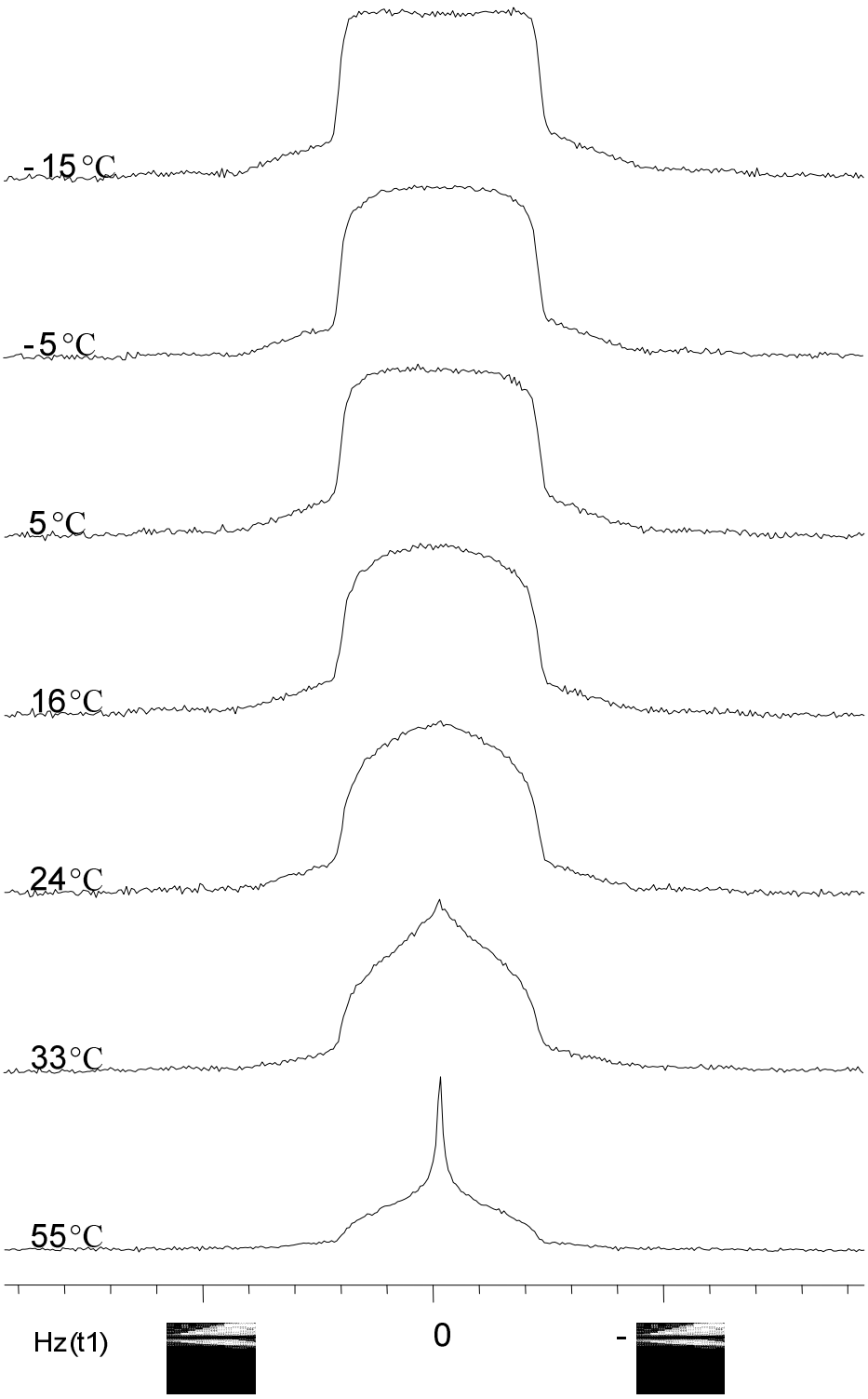

Figure 1.7. ^{2}H solid state NMR spectra of 1.02 mg/m^{2} PIPA-d_7 adsorbed on silica as a function of temperature.

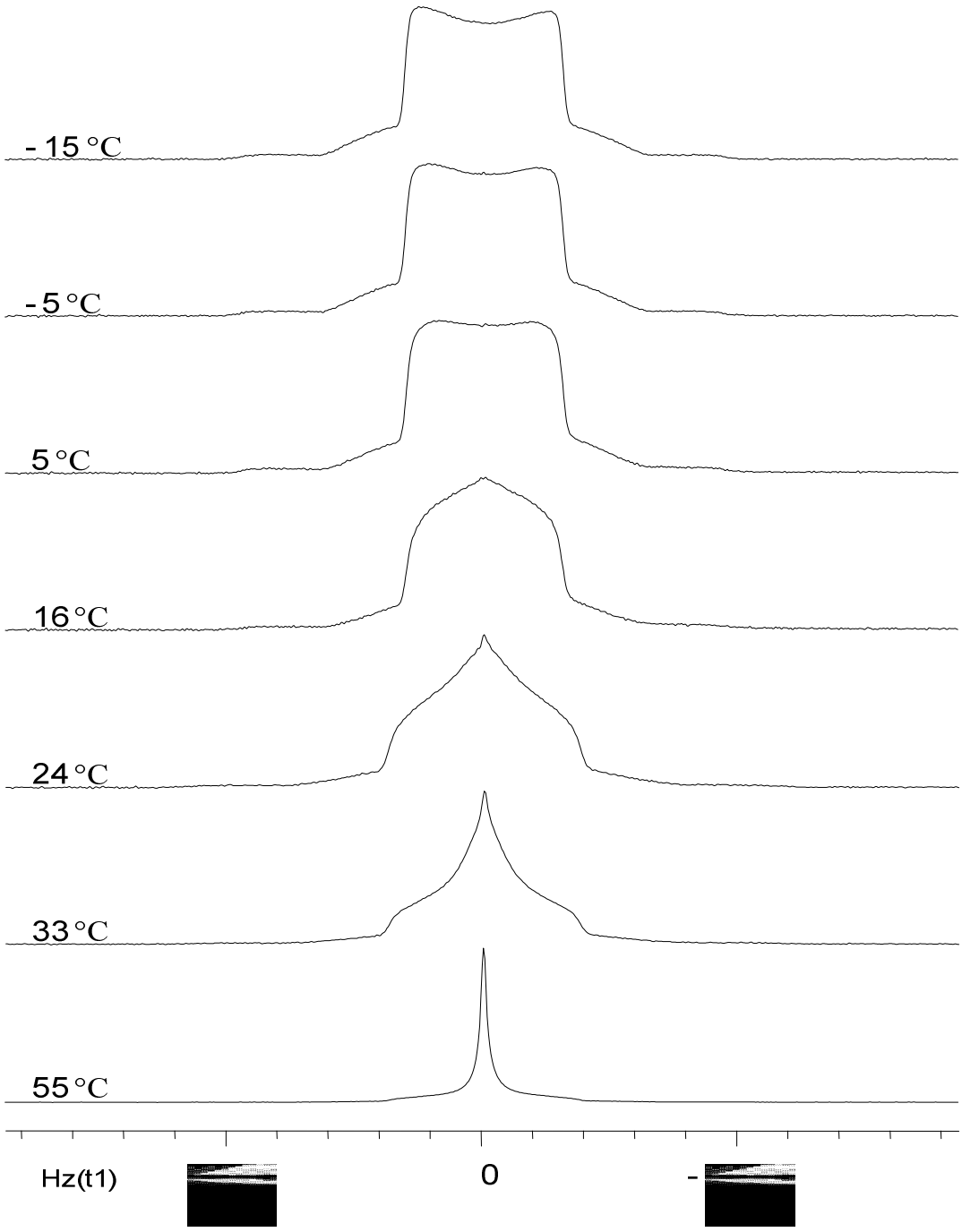

Figure 1.8. ^{2}H solid state NMR spectra of 2.34 mg/ m^2 PIPA-d_7 adsorbed on silica as a function of temperature.

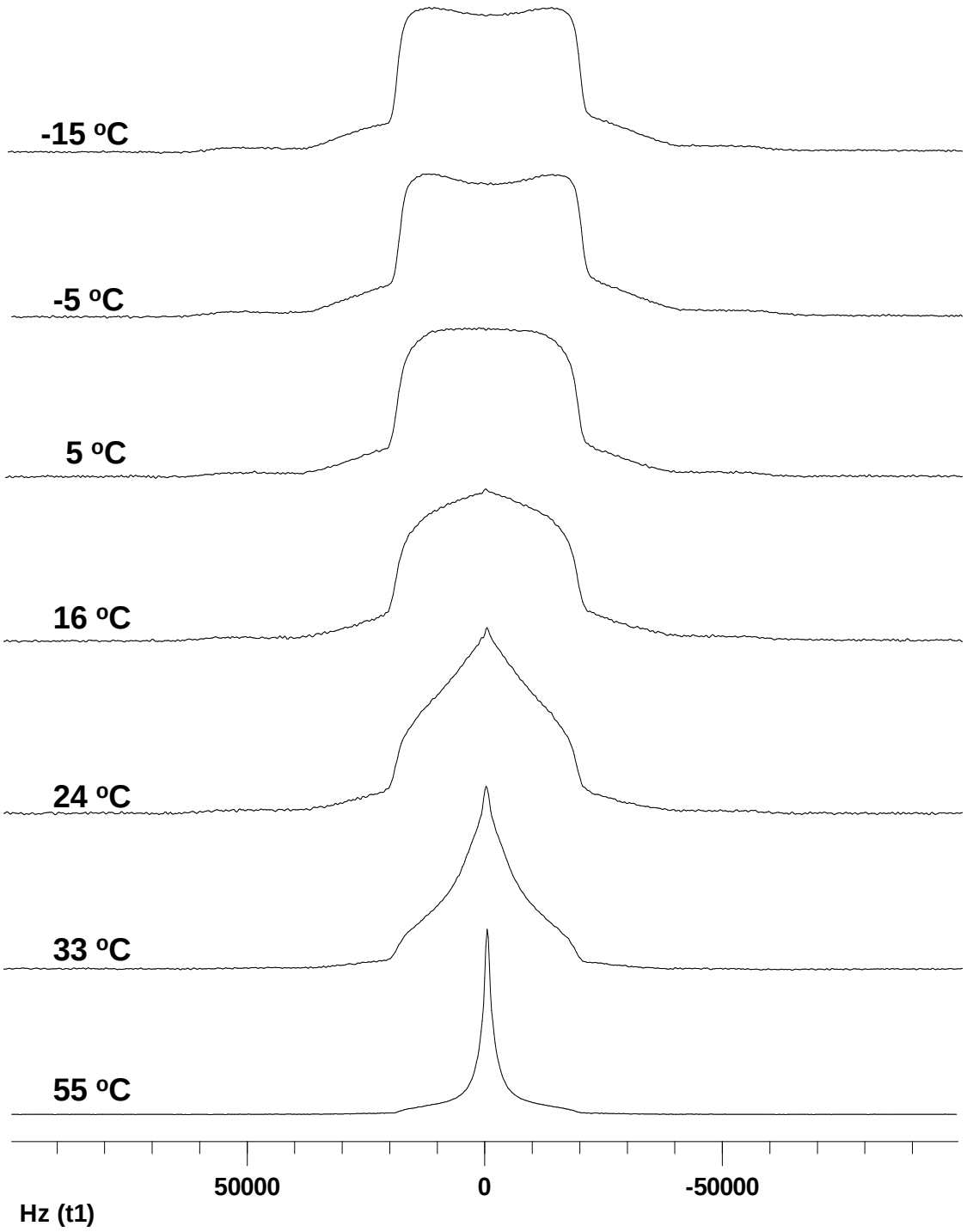

Figure 1.9. ^{2}H solid state NMR spectra of 3.17 mg/ m^{2} PIPA-d_7 adsorbed on silica as a function of temperature.

1.4.3. MDSC. Thermal analysis experiments, using MDSC, were performed on both bulk and adsorbed PIPA-d_7. The derivatives of the reversing heat flow thermograms, with 5 ºC smoothing for all samples, are shown in Figure 1.10. The T_g for the bulk sample was found to be -11 ºC. For a relatively small adsorbed amount of 1.02 mg/m^2, the transition region was indistinguishable in the MDSC thermogram. A big broadened peak at about 0 ˚C was apparent in the thermogram of the samples with adsorbed amounts of 2.34 and 3.17 mg/m^2. A small hump was seen at approximately -10 ºC as well. The intensity for the transition increased as the adsorbed amount increased.

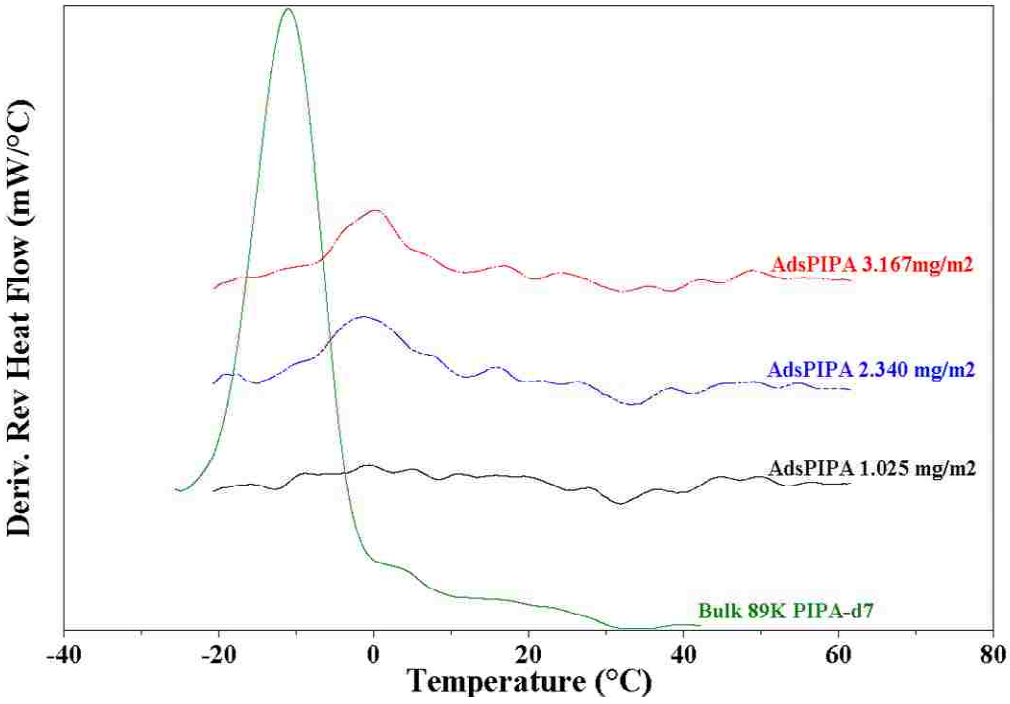

Figure 1.10. MDSC thermograms of the bulk and adsorbed PIPA-d_7 samples. The derivative curves are shown, and the peak is taken as the reported T_g.

1.4.4. Simulation of Bulk PIPA-d_7. The spectrum of bulk PIPA-d_7 in the glassy state (T = -36 ºC) was investigated, and targeted for fitting. Methyl rapid rotation and static methine were the motions that we primarily used for the bulk PIPA-d_7, based on the spectrum in Figure 1.5. Several models were individually used to generate a series of spectra with different jump rates. Those models included a three-site jump (a typical model for methyl rotation), a soccer ball 60-site jump model (developed from previous work on methyl rotation in PMA-d_3[3]) and a two-site hop model (with a dihedral jump angle of 120º). The spectrum from the soccer ball model with the quadrupolar coupling constant of 54 kHz, which modeled the fast methyl rotation from the two methyl groups in bulk PIPA-d_7, gave the best fit for the two horns of the experimental lineshape (Figure 1.11A). However, the middle parts between the simulated and experimental spectra were very different, implying that the PIPA-d_7 side chain probably consisted of at least two kinds of motion.

The two models were combined to fit the center part of the experimental lineshape. For every combination, the jump rates of each model varied individually. A set of spectra produced by combining the soccer ball and two-site hop with the jump angle of 120 º models provided the best fitting for the experimental spectrum bulk for PIPA-d_7 at -36 ºC (Figure 1.11B). The simulated lineshape fit both of the horns with the middle part filled in. With this combination, the center powder pattern of the experimental lineshape dominated by the methyl groups was able to be fit.

The final simulated lineshapes resulted from the addition of the spectra based on methyl fast rotation and the static methine. The inner Pake pattern corresponded to the motion of two methyl groups, which consisted of the fast rotation of each methyl, and

their two-site exchange. The outer part of the spectrum, which was dominated by the methine deuteron, was fit by the simulated spectra generated in the same models, but with the QCC of 150 kHz. Each simulated lineshape was fitted to the experimental one, as in Figure 1.11C, and the sum of the simulations is shown in Figure 1.11D.

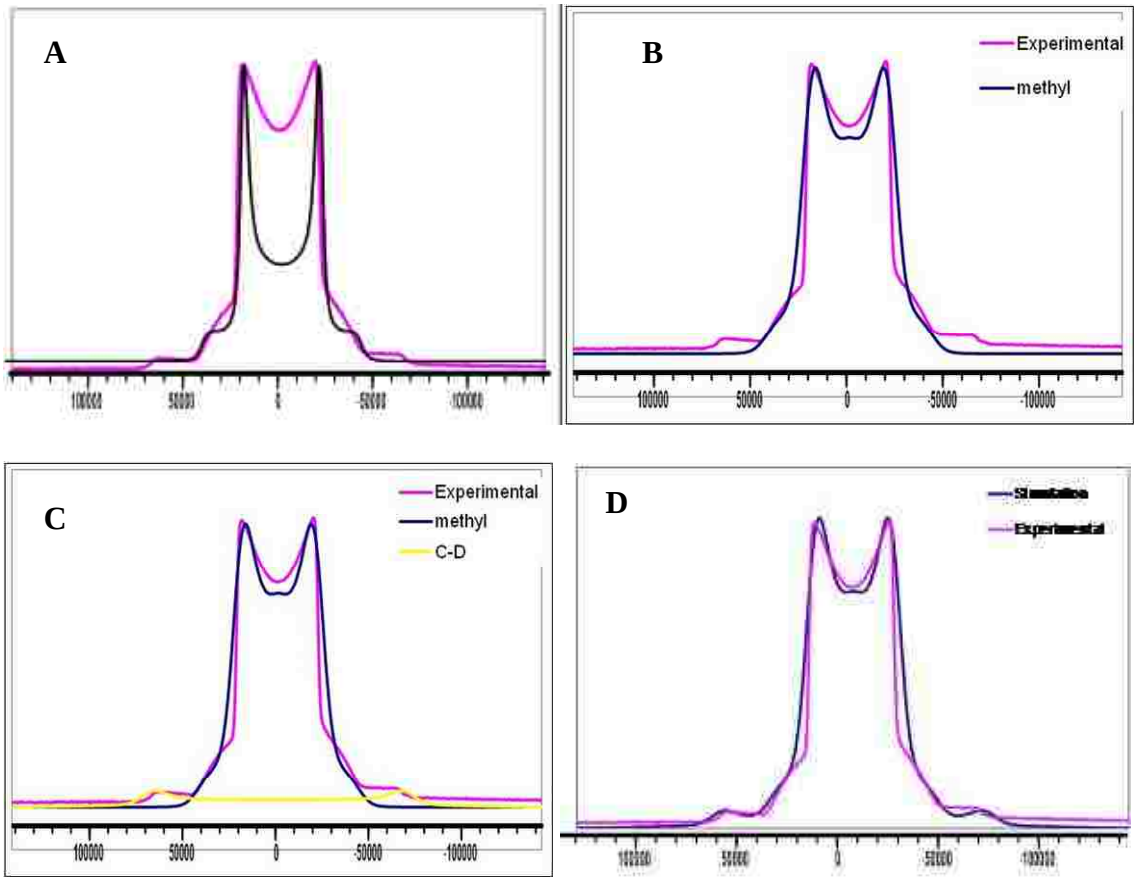

Figure 1.11. Each type of model used in the simulation for bulk PIPA-d_7 at -36 ºC: (A) the soccer ball model with QCC of 54 kHz only, (B) the combination of the soccer ball and the two-site hop models, (C) the combination model and the soccer ball model with QCC of 150 kHz, and (D) the summation of all simulated spectra

A series of spectra for each model (with the various jump rates) was produced to be used as a database for simulations. The final simulated lineshapes resulted from the

superpositions of the simulated spectra. These superpositions and curve fittings were performed using MATLAB. Each fitting was based on a constrained least-square fit to get the best fits for bulk PIPA-d_7 at different temperatures. Then, weighting factors of each simulated spectrum were estimated using MATLAB as well. The simulated and experimental ^{2}H NMR spectra of bulk PIPA-d_7 at different temperatures are shown in Figure 1.12. The simulations are represented by dotted lines. Weight fractions of the simulated spectra used for the bulk sample at various temperatures are summarized in Table 1.1.

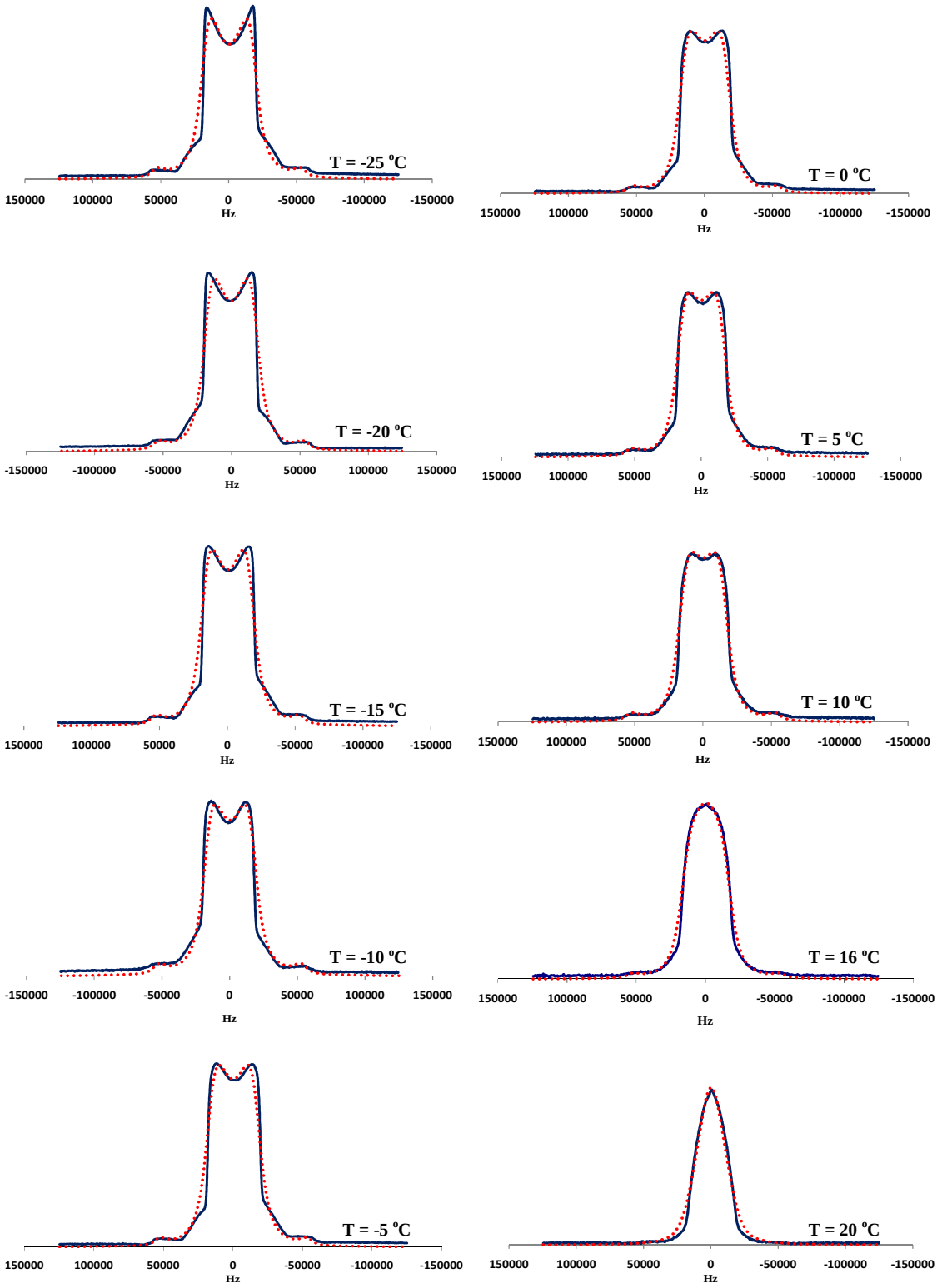

Figure 1.12. Experimental (——) and simulated (•••••) ^{2}H NMR spectra for PIPA-d_7.

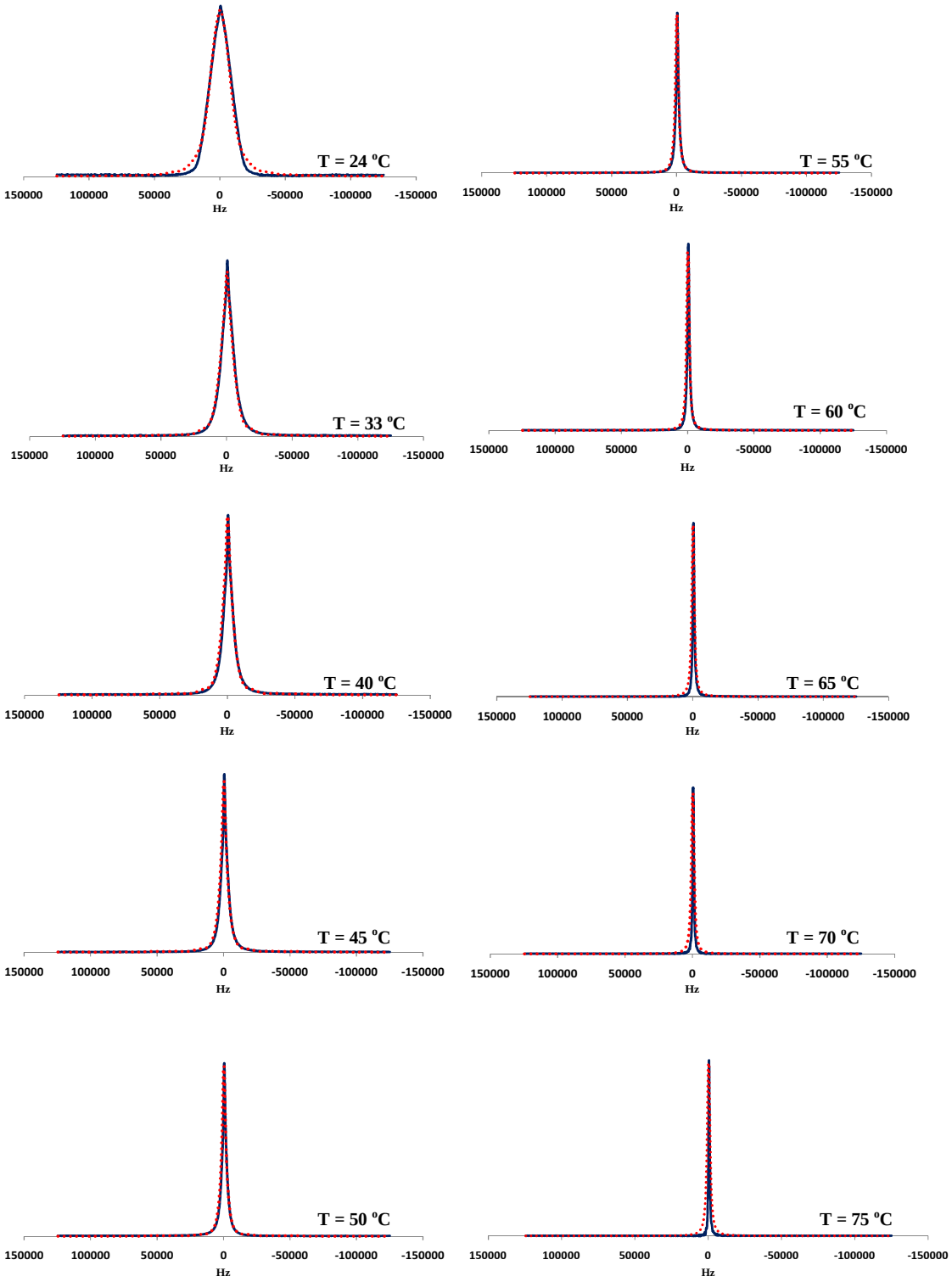

Figure 1.12. Experimental (——) and simulated (••••) ^{2}H NMR spectra for PIPA-d_7 in the higher temperature range. (Continued)

Table 1.1. The weight fractions for the different rates for the methyl (listed first) and methine (listed second) components in the simulated spectra at different temperatures

Rate (Hz)		T (°C)						Rate (Hz)		T (°C)					
2-site	SB	-25		-20		-15		2-site	SB	-25		-20		-15	
0.E+00	0.E+00	--	--	--	--	--	--	1.E+05	1.E+05	--	--	--	--	--	--
0.E+00	1.E+01	--	--	--	--	--	--	1.E+05	5.E+05	--	--	--	--	--	--
1.E+01	0.E+00	--	--	--	--	--	--	1.E+05	1.E+06	--	--	--	--	--	--
1.E+01	1.E+01	0.0057	--	--	--	--	--	5.E+05	1.E+02	--	--	--	--	--	--
1.E+02	1.E+02	--	--	--	--	--	--	5.E+05	1.E+03	--	--	--	--	--	--
1.E+02	1.E+03	--	--	--	--	--	--	5.E+05	5.E+03	--	--	--	--	--	--
1.E+02	5.E+03	--	--	--	--	--	--	5.E+05	1.E+04	--	--	--	--	--	--
1.E+02	1.E+04	--	--	--	--	--	--	5.E+05	5.E+04	--	--	--	--	--	--
1.E+02	5.E+04	--	--	--	--	--	--	5.E+05	1.E+05	--	--	--	--	--	--
1.E+02	1.E+05	--	--	--	--	--	--	5.E+05	5.E+05	--	--	--	--	--	--
1.E+02	5.E+05	--	--	--	--	--	--	5.E+05	1.E+06	--	--	--	--	--	--
1.E+02	1.E+06	--	--	--	--	--	--	5.E+05	5.E+06	--	--	--	--	--	--
1.E+02	5.E+06	--	--	--	--	--	--	1.E+06	1.E+02	--	--	--	--	--	--
1.E+02	1.E+07	--	--	--	--	--	--	1.E+06	1.E+03	--	--	--	--	--	--
1.E+03	1.E+02	--	--	--	--	--	--	1.E+06	5.E+03	--	--	--	--	--	--
1.E+03	1.E+03	--	--	--	--	--	--	1.E+06	1.E+04	--	--	--	--	--	--
1.E+03	5.E+03	--	--	--	--	--	--	1.E+06	5.E+04	--	--	--	--	--	--
1.E+03	1.E+04	--	--	--	0.020	--	0.003	1.E+06	1.E+05	--	--	--	--	--	--
1.E+03	5.E+04	--	--	--	--	--	--	1.E+06	5.E+05	--	--	--	--	--	--
1.E+03	1.E+05	--	--	--	--	--	--	1.E+06	1.E+06	--	--	--	--	--	--
1.E+03	5.E+05	--	--	--	--	--	--	1.E+06	5.E+06	--	--	--	--	--	--
1.E+03	1.E+06	--	--	--	--	--	--	1.E+07	1.E+02	--	--	--	--	--	--
1.E+03	1.E+07	--	--	--	--	--	--	1.E+07	1.E+03	--	--	--	--	--	--
5.E+03	1.E+02	--	--	--	--	--	--	1.E+07	5.E+03	--	--	--	--	--	--
5.E+03	1.E+03	--	--	--	--	--	--	1.E+07	1.E+04	--	--	--	--	--	--
5.E+03	5.E+03	--	--	--	--	--	--	1.E+07	5.E+04	--	--	--	--	--	--
5.E+03	1.E+04	--	0.056	--	0.028	--	0.046	1.E+07	1.E+05	--	--	--	--	--	--
5.E+03	5.E+04	--	--	--	--	--	--	1.E+07	5.E+05	--	--	--	--	--	--
5.E+03	1.E+05	--	--	--	--	--	--	1.E+07	1.E+06	--	--	--	--	--	--
5.E+03	5.E+05	--	--	--	--	--	--	1.E+07	1.E+07	--	--	--	--	--	--
5.E+03	1.E+06	--	--	--	--	--	--	1.E+07	1.E+09	--	--	--	--	--	--
5.E+03	5.E+06	--	--	--	--	--	--	1.E+08	1.E+02	--	--	--	--	--	--
5.E+03	1.E+07	--	--	--	--	--	--	1.E+08	1.E+03	--	--	--	--	--	--
5.E+03	1.E+08	--	--	--	--	--	--	1.E+08	5.E+03	--	--	--	--	--	--
1.E+04	1.E+02	--	--	--	--	--	--	1.E+08	1.E+04	--	--	--	--	--	--
1.E+04	1.E+03	--	--	--	--	--	--	1.E+08	5.E+04	--	--	--	--	--	--
1.E+04	5.E+03	--	--	--	--	--	--	1.E+08	1.E+05	--	--	--	--	--	--
1.E+04	1.E+04	--	--	--	--	--	--	1.E+08	5.E+05	--	--	--	--	--	--
1.E+04	5.E+04	--	--	--	--	--	--	1.E+08	1.E+06	--	--	--	--	--	--
1.E+04	1.E+05	--	--	--	--	--	--	1.E+08	5.E+06	--	--	--	--	--	--
1.E+04	5.E+05	--	--	--	--	--	--	1.E+08	1.E+07	--	--	--	--	--	--
1.E+04	1.E+06	--	--	--	--	--	--	1.E+08	1.E+08	--	--	--	--	--	--
5.E+04	1.E+02	--	--	--	--	--	--	1.E+08	1.E+09	--	--	--	--	--	--
5.E+04	1.E+03	--	--	--	--	--	--	1.E+09	1.E+02	--	--	--	--	--	--
5.E+04	5.E+03	--	--	--	--	--	--	1.E+09	1.E+03	--	--	--	--	--	--
5.E+04	1.E+04	--	--	--	--	--	--	1.E+09	5.E+03	--	--	--	--	--	--
5.E+04	5.E+04	--	--	--	--	--	--	1.E+09	1.E+04	--	--	--	--	--	--
5.E+04	1.E+05	--	--	--	--	--	--	1.E+09	5.E+04	--	--	--	--	--	--
5.E+04	5.E+05	--	--	--	--	--	--	1.E+09	1.E+05	--	--	--	--	--	--
5.E+04	1.E+06	--	--	--	--	--	--	1.E+09	5.E+05	--	--	--	--	--	--
1.E+05	1.E+02	--	--	--	--	--	--	1.E+09	1.E+06	--	--	--	--	--	--
1.E+05	1.E+03	--	--	--	--	--	--	1.E+09	5.E+06	--	--	--	--	--	--
1.E+05	5.E+03	--	--	--	--	--	--	1.E+09	1.E+07	--	--	--	--	--	--
1.E+05	1.E+04	--	--	--	--	--	--	1.E+09	1.E+08	--	--	--	--	--	--
1.E+05	4.E+04	0.88	--	0.34	--	0.027	--	1.E+09	1.E+09	--	--	--	--	--	--
1.E+05	5.E+04	0.062	--	0.61	--	0.92	--			0.94	0.06	0.95	0.05	0.95	0.05
1.E+05	7.E+04	--	--	--	--	--	--		**Total**	**1.0**	**1.0**	**1.0**	**1.0**	**1.0**	**1.0**

Table 1.1. The weight fractions for the methyl and methine components in the simulated spectra at different temperatures reported as (Methyl/Methine) (Continued)

Rate (Hz)		T (°C)						Rate (Hz)		T (°C)					
2-site	SB	-10		-5		0		2-site	SB	-10		-5		0	
0.E+00	0.E+00	--	--	--	--	--	--	1.E+05	1.E+05	--	--	--	--	--	--
0.E+00	1.E+01	--	--	--	--	--	--	1.E+05	5.E+05	--	--	--	--	--	--
1.E+01	0.E+00	--	--	--	--	--	--	1.E+05	1.E+06	--	--	--	--	--	--
1.E+01	1.E+01	--	--	--	--	--	--	5.E+05	1.E+02	--	--	--	--	--	--
1.E+02	1.E+02	--	--	--	--	--	--	5.E+05	1.E+03	--	--	--	--	--	--
1.E+02	1.E+03	--	--	--	--	--	--	5.E+05	5.E+03	--	--	--	--	--	--
1.E+02	5.E+03	--	--	--	--	--	--	5.E+05	1.E+04	--	--	--	--	--	--
1.E+02	1.E+04	--	0.039	--	--	--	--	5.E+05	5.E+04	--	--	--	--	--	--
1.E+02	5.E+04	--	--	--	--	--	--	5.E+05	1.E+05	--	--	--	--	--	--
1.E+02	1.E+05	--	--	--	--	--	--	5.E+05	5.E+05	--	--	--	--	--	--
1.E+02	5.E+05	--	--	--	--	--	--	5.E+05	1.E+06	--	--	--	--	--	--
1.E+02	1.E+06	--	--	--	--	--	--	5.E+05	5.E+06	--	--	--	--	--	--
1.E+02	5.E+06	--	--	--	--	--	--	1.E+06	1.E+02	--	--	--	--	--	--
1.E+02	1.E+07	--	--	--	--	--	--	1.E+06	1.E+03	--	--	--	--	--	--
1.E+03	1.E+02	--	--	--	--	--	--	1.E+06	5.E+03	--	--	--	--	--	--
1.E+03	1.E+03	--	--	--	--	--	--	1.E+06	1.E+04	--	--	--	--	--	--
1.E+03	5.E+03	--	--	--	--	--	--	1.E+06	5.E+04	--	--	--	--	--	--
1.E+03	1.E+04	--	--	--	0.038	--	--	1.E+06	1.E+05	--	--	--	--	--	--
1.E+03	5.E+04	--	--	--	--	--	--	1.E+06	5.E+05	--	--	--	--	--	--
1.E+03	1.E+05	--	--	--	--	--	--	1.E+06	1.E+06	--	--	--	--	--	--
1.E+03	5.E+05	--	--	--	--	--	--	1.E+06	5.E+06	--	--	--	--	--	--
1.E+03	1.E+06	--	--	--	--	--	--	1.E+07	1.E+02	--	--	--	--	--	--
1.E+03	1.E+07	--	--	--	--	--	--	1.E+07	1.E+03	--	--	--	--	--	--
5.E+03	1.E+02	--	--	--	--	--	--	1.E+07	5.E+03	--	--	--	--	--	--
5.E+03	1.E+03	--	--	--	--	--	--	1.E+07	1.E+04	--	--	--	--	--	--
5.E+03	5.E+03	--	--	--	--	--	--	1.E+07	5.E+04	--	--	--	--	--	--
5.E+03	1.E+04	--	--	--	--	--	0.035	1.E+07	1.E+05	--	--	--	--	--	--
5.E+03	5.E+04	--	--	--	--	--	--	1.E+07	5.E+05	--	--	--	--	--	--
5.E+03	1.E+05	--	--	--	--	--	--	1.E+07	1.E+06	--	--	--	--	--	--
5.E+03	5.E+05	--	--	--	--	--	--	1.E+07	1.E+07	--	--	--	--	--	--
5.E+03	1.E+06	--	--	--	--	--	--	1.E+07	1.E+09	--	--	--	--	--	--
5.E+03	5.E+06	--	--	--	--	--	--	1.E+08	1.E+02	--	--	--	--	--	--
5.E+03	1.E+07	--	--	--	--	--	--	1.E+08	1.E+03	--	--	--	--	--	--
5.E+03	1.E+08	--	--	--	--	--	--	1.E+08	5.E+03	--	--	--	--	--	--
1.E+04	1.E+02	--	--	--	--	--	--	1.E+08	1.E+04	--	--	--	--	--	--
1.E+04	1.E+03	--	--	--	--	--	--	1.E+08	5.E+04	--	--	--	--	--	--
1.E+04	5.E+03	--	--	--	--	--	--	1.E+08	1.E+05	--	--	--	--	--	--
1.E+04	1.E+04	--	--	--	--	--	0.023	1.E+08	5.E+05	--	--	--	--	--	--
1.E+04	5.E+04	--	--	--	--	--	--	1.E+08	1.E+06	--	--	--	--	--	--
1.E+04	1.E+05	--	--	--	--	--	--	1.E+08	5.E+06	--	--	--	--	--	--
1.E+04	5.E+05	--	--	--	--	--	--	1.E+08	1.E+07	--	--	--	--	--	--
1.E+04	1.E+06	--	--	--	--	--	--	1.E+08	1.E+08	--	--	--	--	--	--
5.E+04	1.E+02	--	--	--	--	--	--	1.E+08	1.E+09	--	--	--	--	--	--
5.E+04	1.E+03	--	--	--	--	--	--	1.E+09	1.E+02	--	--	--	--	--	--
5.E+04	5.E+03	--	--	--	--	--	--	1.E+09	1.E+03	--	--	--	--	--	--
5.E+04	1.E+04	--	--	--	--	--	--	1.E+09	5.E+03	--	--	--	--	--	--
5.E+04	5.E+04	--	--	--	--	--	--	1.E+09	1.E+04	--	--	--	--	--	--
5.E+04	1.E+05	--	--	--	--	--	--	1.E+09	5.E+04	--	--	--	--	--	--
5.E+04	5.E+05	--	--	--	--	--	--	1.E+09	1.E+05	--	--	--	--	--	--
5.E+04	1.E+06	--	--	--	--	--	--	1.E+09	5.E+05	--	--	--	--	--	--
1.E+05	1.E+02	--	--	--	--	--	--	1.E+09	1.E+06	--	--	--	--	--	--
1.E+05	1.E+03	--	--	--	--	--	--	1.E+09	5.E+06	--	--	--	--	--	--
1.E+05	5.E+03	--	--	--	--	--	--	1.E+09	1.E+07	--	--	--	--	--	--
1.E+05	1.E+04	--	--	--	--	--	--	1.E+09	1.E+08	--	--	--	--	--	--
1.E+05	4.E+04	--	--	--	--	--	--	1.E+09	1.E+09	--	--	--	--	--	--
1.E+05	5.E+04	0.64	--	0.42	--	0.78	--			0.96	0.04	0.96	0.04	0.94	0.06
1.E+05	7.E+04	0.32	--	0.54	--	0.16	--		**Total**	**1.0**	**1.0**	**1.0**	**1.0**	**1.0**	**1.0**

Table 1.1. The weight fractions for the methyl and methine components in the simulated spectra at different temperatures reported as (Methyl/Methine) (Continued)

Rate (Hz)		T (°C)						Rate (Hz)		T (°C)					
2-site	SB	5		10		15		2-site	SB	5		10		15	
0.E+00	0.E+00	--	--	--	--	--	--	1.E+05	1.E+05	--	--	--	--	--	--
0.E+00	1.E+01	--	--	--	--	--	--	1.E+05	5.E+05	--	--	--	--	--	--
1.E+01	0.E+00	--	--	--	--	--	--	1.E+05	1.E+06	--	--	--	--	--	--
1.E+01	1.E+01	--	--	--	--	--	--	5.E+05	1.E+02	--	--	--	--	--	--
1.E+02	1.E+02	--	--	--	--	--	--	5.E+05	1.E+03	--	--	--	--	--	--
1.E+02	1.E+03	--	--	--	--	--	--	5.E+05	5.E+03	--	--	--	--	--	--
1.E+02	5.E+03	--	--	--	--	--	--	5.E+05	1.E+04	--	--	--	--	--	--
1.E+02	1.E+04	--	--	--	--	--	--	5.E+05	5.E+04	--	--	--	--	--	--
1.E+02	5.E+04	--	--	--	--	--	--	5.E+05	1.E+05	--	--	--	--	--	0.26
1.E+02	1.E+05	--	--	--	--	--	--	5.E+05	5.E+05	--	--	--	--	--	--
1.E+02	5.E+05	--	--	--	--	--	--	5.E+05	1.E+06	--	--	--	--	--	--
1.E+02	1.E+06	--	--	--	--	--	--	5.E+05	5.E+06	--	--	--	--	--	--
1.E+02	5.E+06	--	--	--	--	--	--	1.E+06	1.E+02	--	--	--	--	--	--
1.E+02	1.E+07	--	--	--	--	--	--	1.E+06	1.E+03	--	--	--	--	--	--
1.E+03	1.E+02	--	--	--	--	--	--	1.E+06	5.E+03	--	--	--	--	--	--
1.E+03	1.E+03	--	--	--	--	--	--	1.E+06	1.E+04	--	--	--	--	--	--
1.E+03	5.E+03	--	--	--	--	--	--	1.E+06	5.E+04	--	--	--	--	--	--
1.E+03	1.E+04	--	--	--	--	--	0.023	1.E+06	1.E+05	--	--	--	--	--	--
1.E+03	5.E+04	--	--	--	--	--	--	1.E+06	5.E+05	--	--	--	--	--	--
1.E+03	1.E+05	--	--	--	--	--	--	1.E+06	1.E+06	--	--	--	--	--	--
1.E+03	5.E+05	--	--	--	--	--	--	1.E+06	5.E+06	--	--	--	--	--	--
1.E+03	1.E+06	--	--	--	--	--	--	1.E+07	1.E+02	--	--	--	--	--	--
1.E+03	1.E+07	--	--	--	--	--	--	1.E+07	1.E+03	--	--	--	--	--	--
5.E+03	1.E+02	--	--	--	--	--	--	1.E+07	5.E+03	--	--	--	--	--	--
5.E+03	1.E+03	--	--	--	--	--	--	1.E+07	1.E+04	--	--	--	--	--	--
5.E+03	5.E+03	--	--	--	--	--	--	1.E+07	5.E+04	--	--	--	--	--	--
5.E+03	1.E+04	--	0.043	--	0.0052	--	--	1.E+07	1.E+05	--	--	--	--	--	--
5.E+03	5.E+04	--	--	--	--	--	--	1.E+07	5.E+05	--	--	--	--	--	--
5.E+03	1.E+05	--	--	--	--	--	--	1.E+07	1.E+06	--	--	--	--	--	--
5.E+03	5.E+05	--	--	--	--	--	--	1.E+07	1.E+07	--	--	--	--	--	--
5.E+03	1.E+06	--	--	--	--	--	--	1.E+07	1.E+09	--	--	--	--	--	--
5.E+03	5.E+06	--	--	--	--	--	--	1.E+08	1.E+02	--	--	--	--	--	--
5.E+03	1.E+07	--	--	--	--	--	--	1.E+08	1.E+03	--	--	--	--	--	--
5.E+03	1.E+08	--	--	--	--	--	--	1.E+08	5.E+03	--	--	--	--	--	--
1.E+04	1.E+02	--	--	--	--	--	--	1.E+08	1.E+04	--	--	--	--	--	--
1.E+04	1.E+03	--	--	--	--	--	--	1.E+08	5.E+04	--	--	--	--	--	--
1.E+04	5.E+03	--	--	--	--	--	--	1.E+08	1.E+05	--	--	--	--	--	--
1.E+04	1.E+04	--	--	--	0.039	--	--	1.E+08	5.E+05	--	--	--	--	--	--
1.E+04	5.E+04	--	--	--	--	--	--	1.E+08	1.E+06	--	--	--	--	--	--
1.E+04	1.E+05	--	--	--	--	--	--	1.E+08	5.E+06	--	--	--	--	--	--
1.E+04	5.E+05	--	--	--	--	--	--	1.E+08	1.E+07	--	--	--	--	--	--
1.E+04	1.E+06	--	--	--	--	--	--	1.E+08	1.E+08	--	--	--	--	--	--
5.E+04	1.E+02	--	--	--	--	--	--	1.E+08	1.E+09	--	--	--	--	--	--
5.E+04	1.E+03	--	--	--	--	--	--	1.E+09	1.E+02	--	--	--	--	--	--
5.E+04	5.E+03	--	--	--	--	--	--	1.E+09	1.E+03	--	--	--	--	--	--
5.E+04	1.E+04	--	--	--	--	--	--	1.E+09	5.E+03	--	--	--	--	--	--
5.E+04	5.E+04	--	--	--	--	--	--	1.E+09	1.E+04	--	--	--	--	--	--
5.E+04	1.E+05	--	--	--	--	--	--	1.E+09	5.E+04	--	--	--	--	--	--
5.E+04	5.E+05	--	--	--	--	--	--	1.E+09	1.E+05	--	--	--	--	--	--
5.E+04	1.E+06	--	--	--	--	--	--	1.E+09	5.E+05	--	--	--	--	--	--
1.E+05	1.E+02	--	--	--	--	--	--	1.E+09	1.E+06	--	--	--	--	--	--
1.E+05	1.E+03	--	--	--	--	--	--	1.E+09	5.E+06	--	--	--	--	--	--
1.E+05	5.E+03	--	--	--	--	--	--	1.E+09	1.E+07	--	--	--	--	--	--
1.E+05	1.E+04	--	--	--	--	--	--	1.E+09	1.E+08	--	--	--	--	--	--
1.E+05	4.E+04	--	--	--	--	--	--	1.E+09	1.E+09	--	--	--	--	--	--
1.E+05	5.E+04	0.28	--	--	--	--	--			0.96	0.04	0.96	0.04	0.71	0.29
1.E+05	7.E+04	0.68	--	0.96	--	0.71	--		**Total**		**1.0**		**1.0**		**1.0**

Table 1.1. The weight fractions for the methyl and methine components in the simulated spectra at different temperatures reported as (Methyl/Methine) (Continued)

Rate (Hz)		T (°C)						Rate (Hz)		T (°C)					
2-site	SB	20		25		35		2-site	SB	20		25		35	
0.E+00	0.E+00	--	--	--	--	--	--	1.E+05	1.E+05	--	--	--	--	--	--
0.E+00	1.E+01	--	--	--	--	--	--	1.E+05	5.E+05	--	--	--	--	--	--
1.E+01	0.E+00	--	--	--	--	--	--	1.E+05	1.E+06	--	--	--	--	--	--
1.E+01	1.E+01	--	--	--	--	--	--	5.E+05	1.E+02	--	--	--	--	--	--
1.E+02	1.E+02	--	--	--	--	--	--	5.E+05	1.E+03	--	--	--	--	--	--
1.E+02	1.E+03	--	--	--	--	--	--	5.E+05	5.E+03	--	--	--	--	--	--
1.E+02	5.E+03	--	--	--	--	--	--	5.E+05	1.E+04	--	--	--	--	--	--
1.E+02	1.E+04	--	--	--	--	--	--	5.E+05	5.E+04	--	--	--	--	--	--
1.E+02	5.E+04	--	--	--	--	--	--	5.E+05	1.E+05	--	--	0.19	--	0.28	--
1.E+02	1.E+05	--	--	--	--	--	--	5.E+05	5.E+05	--	0.71	--	0.79	--	0.17
1.E+02	5.E+05	--	--	--	--	--	--	5.E+05	1.E+06	--	--	--	--	--	--
1.E+02	1.E+06	--	--	--	--	--	--	5.E+05	5.E+06	--	--	--	--	--	--
1.E+02	5.E+06	--	--	--	--	--	0.35	1.E+06	1.E+02	--	--	--	--	--	--
1.E+02	1.E+07	--	--	--	--	--	--	1.E+06	1.E+03	--	--	--	--	--	--
1.E+03	1.E+02	--	--	--	--	--	--	1.E+06	5.E+03	--	--	--	--	--	--
1.E+03	1.E+03	--	--	--	--	--	--	1.E+06	1.E+04	--	--	--	--	--	--
1.E+03	5.E+03	--	--	--	--	--	--	1.E+06	5.E+04	--	--	--	--	--	--
1.E+03	1.E+04	--	--	--	--	--	--	1.E+06	1.E+05	--	--	--	--	--	--
1.E+03	5.E+04	--	--	--	--	--	--	1.E+06	5.E+05	--	--	--	--	--	--
1.E+03	1.E+05	--	--	--	--	--	--	1.E+06	1.E+06	--	--	--	--	--	--
1.E+03	5.E+05	--	--	--	--	--	--	1.E+06	5.E+06	--	--	--	--	--	--
1.E+03	1.E+06	--	--	--	--	--	--	1.E+07	1.E+02	--	--	--	--	--	--
1.E+03	1.E+07	--	--	--	--	--	--	1.E+07	1.E+03	--	--	--	--	--	--
5.E+03	1.E+02	--	--	--	--	--	--	1.E+07	5.E+03	--	--	--	--	--	--
5.E+03	1.E+03	--	--	--	--	--	--	1.E+07	1.E+04	--	--	--	--	--	--
5.E+03	5.E+03	--	--	--	--	--	--	1.E+07	5.E+04	--	--	--	--	--	--
5.E+03	1.E+04	--	--	--	--	--	--	1.E+07	1.E+05	--	--	--	--	--	--
5.E+03	5.E+04	--	--	--	--	--	--	1.E+07	5.E+05	--	--	--	--	--	--
5.E+03	1.E+05	--	--	--	--	--	--	1.E+07	1.E+06	--	--	--	--	--	--
5.E+03	5.E+05	--	--	--	--	--	--	1.E+07	1.E+07	--	--	--	--	--	--
5.E+03	1.E+06	--	--	--	--	--	--	1.E+07	1.E+09	--	--	--	--	--	--
5.E+03	5.E+06	--	--	--	--	--	--	1.E+08	1.E+02	--	--	--	--	--	--
5.E+03	1.E+07	--	--	--	--	--	--	1.E+08	1.E+03	--	--	--	--	--	--
5.E+03	1.E+08	--	--	--	--	--	--	1.E+08	5.E+03	--	--	--	--	--	--
1.E+04	1.E+02	--	--	--	--	--	--	1.E+08	1.E+04	--	--	--	--	--	--
1.E+04	1.E+03	--	--	--	--	--	--	1.E+08	5.E+04	--	--	--	--	--	--
1.E+04	5.E+03	--	--	--	--	--	--	1.E+08	1.E+05	--	--	--	--	--	--
1.E+04	1.E+04	--	--	--	--	--	0.0029	1.E+08	5.E+05	--	--	--	--	--	--
1.E+04	5.E+04	--	--	--	--	--	--	1.E+08	1.E+06	--	--	--	--	--	--
1.E+04	1.E+05	--	--	--	--	--	--	1.E+08	5.E+06	--	--	--	--	--	--
1.E+04	5.E+05	--	--	--	--	--	--	1.E+08	1.E+07	--	--	--	--	--	--
1.E+04	1.E+06	--	--	--	--	--	--	1.E+08	1.E+08	--	--	--	--	--	--
5.E+04	1.E+02	--	--	--	--	--	--	1.E+08	1.E+09	--	--	--	--	--	--
5.E+04	1.E+03	--	--	--	--	--	--	1.E+09	1.E+02	--	--	--	--	--	--
5.E+04	5.E+03	--	--	--	--	--	--	1.E+09	1.E+03	--	--	--	--	--	--
5.E+04	1.E+04	--	--	--	--	--	--	1.E+09	5.E+03	--	--	--	--	--	--
5.E+04	5.E+04	--	--	--	--	--	--	1.E+09	1.E+04	--	--	--	--	--	--
5.E+04	1.E+05	--	--	--	--	--	--	1.E+09	5.E+04	--	--	--	--	--	--
5.E+04	5.E+05	--	--	--	--	--	--	1.E+09	1.E+05	--	--	--	--	--	--
5.E+04	1.E+06	--	--	--	--	--	--	1.E+09	5.E+05	--	--	--	--	--	--
1.E+05	1.E+02	--	--	--	--	--	--	1.E+09	1.E+06	--	--	--	--	--	--
1.E+05	1.E+03	--	--	--	--	--	--	1.E+09	5.E+06	--	--	--	--	--	--
1.E+05	5.E+03	--	--	--	--	--	--	1.E+09	1.E+07	--	--	--	--	--	--
1.E+05	1.E+04	--	--	--	--	--	--	1.E+09	1.E+08	--	--	--	--	--	--
1.E+05	4.E+04	--	--	--	--	--	--	1.E+09	1.E+09	--	--	0.020	--	0.19	--
1.E+05	5.E+04	--	--	--	--	--	--			0.29	0.71	0.21	0.79	0.48	0.52
1.E+05	7.E+04	0.29	--	--	--	0.0030	--		**Total**		**1.0**		**1.0**		**1.0**

Table 1.1. The weight fractions for the methyl and methine components in the simulated spectra at different temperatures reported as (Methyl/Methine) (Continued)

Rate (Hz)		T (°C)						Rate (Hz)		T (°C)					
2-site	SB	40		45		50		2-site	SB	40		45		50	
0.E+00	0.E+00	--	--	--	--	--	--	1.E+05	1.E+05	--	--	--	--	0.040	--
0.E+00	1.E+01	--	--	--	--	--	--	1.E+05	5.E+05	--	--	--	--	--	--
1.E+01	0.E+00	--	--	--	--	--	--	1.E+05	1.E+06	--	--	--	--	--	--
1.E+01	1.E+01	--	--	--	--	--	--	5.E+05	1.E+02	--	--	--	--	--	--
1.E+02	1.E+02	--	--	--	--	--	--	5.E+05	1.E+03	--	--	--	--	--	--
1.E+02	1.E+03	--	--	--	--	--	--	5.E+05	5.E+03	--	--	--	--	--	--
1.E+02	5.E+03	--	--	--	--	--	--	5.E+05	1.E+04	--	--	--	--	--	--
1.E+02	1.E+04	--	--	--	--	--	--	5.E+05	5.E+04	--	--	--	--	--	--
1.E+02	5.E+04	--	--	--	--	--	--	5.E+05	1.E+05	0.16	--	0.11	--	--	--
1.E+02	1.E+05	--	--	--	--	--	--	5.E+05	5.E+05	--	0.050	--	--	--	--
1.E+02	5.E+05	--	--	--	--	--	--	5.E+05	1.E+06	--	--	--	--	--	--
1.E+02	1.E+06	--	--	--	--	--	--	5.E+05	5.E+06	--	0.26	--	0.22	--	--
1.E+02	5.E+06	--	0.24	--	--	--	--	1.E+06	1.E+02	--	--	--	--	--	--
1.E+02	1.E+07	--	--	--	0.28	--	0.36	1.E+06	1.E+03	--	--	--	--	--	--
1.E+03	1.E+02	--	--	--	--	--	--	1.E+06	5.E+03	--	--	--	--	--	--
1.E+03	1.E+03	--	--	--	--	--	--	1.E+06	1.E+04	--	--	--	--	--	--
1.E+03	5.E+03	--	--	--	--	--	--	1.E+06	5.E+04	--	--	--	--	--	--
1.E+03	1.E+04	--	--	--	--	--	--	1.E+06	1.E+05	--	--	--	--	--	--
1.E+03	5.E+04	--	--	--	--	--	--	1.E+06	5.E+05	--	--	--	--	--	--
1.E+03	1.E+05	--	--	--	--	--	--	1.E+06	1.E+06	--	--	--	--	--	--
1.E+03	5.E+05	--	--	--	--	--	--	1.E+06	5.E+06	--	--	--	--	--	--
1.E+03	1.E+06	--	--	--	--	--	--	1.E+07	1.E+02	--	--	--	--	--	--
1.E+03	1.E+07	--	--	--	--	--	--	1.E+07	1.E+03	--	--	--	--	--	--
5.E+03	1.E+02	--	--	--	--	--	--	1.E+07	5.E+03	--	--	--	--	--	--
5.E+03	1.E+03	--	--	--	--	--	--	1.E+07	1.E+04	--	--	--	--	--	--
5.E+03	5.E+03	--	--	--	--	--	--	1.E+07	5.E+04	--	--	--	--	--	--
5.E+03	1.E+04	--	--	--	--	--	--	1.E+07	1.E+05	--	--	--	--	--	--
5.E+03	5.E+04	--	--	--	--	--	--	1.E+07	5.E+05	--	--	--	--	--	--
5.E+03	1.E+05	--	0.00068	--	--	--	--	1.E+07	1.E+06	--	--	--	--	--	--
5.E+03	5.E+05	--	--	--	--	--	--	1.E+07	1.E+07	--	--	--	--	--	--
5.E+03	1.E+06	--	--	--	--	--	--	1.E+07	1.E+09	--	--	--	--	--	--
5.E+03	5.E+06	--	--	--	--	--	--	1.E+08	1.E+02	--	--	--	--	--	--
5.E+03	1.E+07	--	--	--	--	--	--	1.E+08	1.E+03	--	--	--	--	--	--
5.E+03	1.E+08	--	--	--	--	--	--	1.E+08	5.E+03	--	--	--	--	--	--
1.E+04	1.E+02	--	--	--	--	--	--	1.E+08	1.E+04	--	--	--	--	--	--
1.E+04	1.E+03	--	--	--	--	--	--	1.E+08	5.E+04	--	--	--	--	--	--
1.E+04	5.E+03	--	--	--	0.0033	--	0.0029	1.E+08	1.E+05	--	--	--	--	--	--
1.E+04	1.E+04	--	0.0038	--	--	--	--	1.E+08	5.E+05	--	--	--	--	--	--
1.E+04	5.E+04	--	--	--	--	--	--	1.E+08	1.E+06	--	--	--	--	--	--
1.E+04	1.E+05	--	--	--	--	--	--	1.E+08	5.E+06	--	--	--	--	--	--
1.E+04	5.E+05	--	--	--	--	--	--	1.E+08	1.E+07	--	--	--	--	--	--
1.E+04	1.E+06	--	--	--	--	--	--	1.E+08	1.E+08	--	--	--	--	--	--
5.E+04	1.E+02	--	--	--	--	--	--	1.E+08	1.E+09	--	--	--	--	--	--
5.E+04	1.E+03	--	--	--	--	--	--	1.E+09	1.E+02	--	--	--	--	--	--
5.E+04	5.E+03	--	--	--	--	--	--	1.E+09	1.E+03	--	--	--	--	--	--
5.E+04	1.E+04	--	--	--	--	--	--	1.E+09	5.E+03	--	--	--	--	--	--
5.E+04	5.E+04	--	--	--	--	--	--	1.E+09	1.E+04	--	--	--	--	--	--
5.E+04	1.E+05	--	--	--	0.0010	--	0.00055	1.E+09	5.E+04	--	--	--	--	--	--
5.E+04	5.E+05	--	--	--	--	--	--	1.E+09	1.E+05	--	--	--	--	--	--
5.E+04	1.E+06	--	--	--	--	--	--	1.E+09	5.E+05	--	--	--	--	--	--
1.E+05	1.E+02	--	--	--	--	--	--	1.E+09	1.E+06	--	--	--	--	--	--
1.E+05	1.E+03	--	--	--	--	--	--	1.E+09	5.E+06	--	--	--	--	--	--
1.E+05	5.E+03	--	--	--	--	--	--	1.E+09	1.E+07	--	--	--	--	--	--
1.E+05	1.E+04	--	--	--	--	--	--	1.E+09	1.E+08	--	--	--	--	--	--
1.E+05	4.E+04	--	--	--	--	--	--	1.E+09	1.E+09	0.28	--	0.38	--	0.60	--
1.E+05	5.E+04	--	--	--	--	--	--			0.44	0.56	0.49	0.51	0.64	0.36
1.E+05	7.E+04	0.0050	--	0.0066	--	0.0029	--		**Total**		**1.0**		**1.0**		**1.0**

Table 1.1. The weight fractions for the methyl and methine components in the simulated spectra at different temperatures reported as (Methyl/Methine) (Continued)

Rate (Hz)		T (°C)						Rate (Hz)		T (°C)					
2-site	SB	55		60		65		2-site	SB	55		60		65	
0.E+00	0.E+00	--	--	--	--	--	--	1.E+05	1.E+05	0.0071	--	--	--	--	--
0.E+00	1.E+01	--	--	--	--	--	--	1.E+05	5.E+05	--	--	--	--	--	--
1.E+01	0.E+00	--	--	--	--	--	--	1.E+05	1.E+06	--	--	--	--	--	--
1.E+01	1.E+01	--	--	--	--	--	--	5.E+05	1.E+02	--	--	--	--	--	--
1.E+02	1.E+02	--	--	--	--	--	--	5.E+05	1.E+03	--	--	--	--	--	--
1.E+02	1.E+03	--	--	--	--	--	--	5.E+05	5.E+03	--	--	--	--	--	--
1.E+02	5.E+03	--	--	--	--	--	--	5.E+05	1.E+04	--	--	--	--	--	--
1.E+02	1.E+04	--	--	--	0.00040	--	--	5.E+05	5.E+04	--	--	--	--	--	--
1.E+02	5.E+04	--	--	--	--	--	--	5.E+05	1.E+05	--	--	--	--	--	--
1.E+02	1.E+05	--	--	--	0.0011	--	--	5.E+05	5.E+05	--	--	--	--	--	--
1.E+02	5.E+05	--	--	--	--	--	--	5.E+05	1.E+06	--	--	--	--	--	--
1.E+02	1.E+06	--	--	--	--	--	--	5.E+05	5.E+06	--	--	--	--	--	--
1.E+02	5.E+06	--	--	--	--	--	--	1.E+06	1.E+02	--	--	--	--	--	--
1.E+02	1.E+07	--	0.14	--	--	--	--	1.E+06	1.E+03	--	--	--	--	--	--
1.E+03	1.E+02	--	--	--	--	--	--	1.E+06	5.E+03	--	--	--	--	--	--
1.E+03	1.E+03	--	--	--	--	--	--	1.E+06	1.E+04	--	--	--	--	--	--
1.E+03	5.E+03	--	--	--	--	--	--	1.E+06	5.E+04	--	--	--	--	--	--
1.E+03	1.E+04	--	--	--	--	--	--	1.E+06	1.E+05	--	--	--	--	--	--
1.E+03	5.E+04	--	--	--	--	--	--	1.E+06	5.E+05	--	--	--	--	--	--
1.E+03	1.E+05	--	--	--	--	--	--	1.E+06	1.E+06	--	--	--	--	--	--
1.E+03	5.E+05	--	--	--	--	--	--	1.E+06	5.E+06	--	--	--	--	--	--
1.E+03	1.E+06	--	--	--	--	--	--	1.E+07	1.E+02	--	--	--	--	--	--
1.E+03	1.E+07	--	--	--	--	--	--	1.E+07	1.E+03	--	--	--	--	--	--
5.E+03	1.E+02	--	--	--	--	--	--	1.E+07	5.E+03	--	--	--	--	--	--
5.E+03	1.E+03	--	--	--	--	--	--	1.E+07	1.E+04	--	--	--	--	--	--
5.E+03	5.E+03	--	--	--	--	--	--	1.E+07	5.E+04	--	--	--	--	--	--
5.E+03	1.E+04	--	--	--	--	--	--	1.E+07	1.E+05	--	--	--	--	--	--
5.E+03	5.E+04	--	--	--	--	--	--	1.E+07	5.E+05	--	--	--	--	--	--
5.E+03	1.E+05	--	--	--	--	--	--	1.E+07	1.E+06	--	--	--	--	--	--
5.E+03	5.E+05	--	--	--	--	--	--	1.E+07	1.E+07	--	--	--	--	--	--
5.E+03	1.E+06	--	--	--	--	--	--	1.E+07	1.E+09	--	--	--	--	--	--
5.E+03	5.E+06	--	--	--	--	--	--	1.E+08	1.E+02	--	--	--	--	--	--
5.E+03	1.E+07	--	--	--	--	--	--	1.E+08	1.E+03	--	--	--	--	--	--
5.E+03	1.E+08	--	--	--	--	--	--	1.E+08	5.E+03	--	--	--	--	--	--
1.E+04	1.E+02	--	--	--	--	--	--	1.E+08	1.E+04	--	--	--	--	--	--
1.E+04	1.E+03	--	--	--	--	--	--	1.E+08	5.E+04	--	--	--	--	--	--
1.E+04	5.E+03	--	0.0027	--	--	--	--	1.E+08	1.E+05	--	--	--	--	--	--
1.E+04	1.E+04	--	--	--	--	--	--	1.E+08	5.E+05	--	--	--	--	--	--
1.E+04	5.E+04	--	--	--	--	--	--	1.E+08	1.E+06	--	--	--	--	--	--
1.E+04	1.E+05	--	0.00016	--	--	--	--	1.E+08	5.E+06	--	--	--	--	--	--
1.E+04	5.E+05	--	--	--	--	--	--	1.E+08	1.E+07	--	--	--	--	--	--
1.E+04	1.E+06	--	--	--	--	--	--	1.E+08	1.E+08	--	--	--	--	--	--
5.E+04	1.E+02	--	--	--	--	--	--	1.E+08	1.E+09	--	--	--	--	--	--
5.E+04	1.E+03	--	--	--	--	--	--	1.E+09	1.E+02	--	--	--	--	--	--
5.E+04	5.E+03	--	--	--	--	--	--	1.E+09	1.E+03	--	--	--	--	--	--
5.E+04	1.E+04	--	--	--	--	--	--	1.E+09	5.E+03	--	--	--	--	--	--
5.E+04	5.E+04	--	--	--	--	--	--	1.E+09	1.E+04	--	--	--	--	--	--
5.E+04	1.E+05	--	--	--	--	--	--	1.E+09	5.E+04	--	--	--	--	--	--
5.E+04	5.E+05	--	--	--	--	--	--	1.E+09	1.E+05	--	--	--	--	--	--
5.E+04	1.E+06	--	--	--	--	--	--	1.E+09	5.E+05	--	--	--	--	--	--
1.E+05	1.E+02	--	--	--	--	--	--	1.E+09	1.E+06	--	--	--	--	--	--
1.E+05	1.E+03	--	--	--	--	--	--	1.E+09	5.E+06	--	--	--	--	--	--
1.E+05	5.E+03	--	--	--	--	--	--	1.E+09	1.E+07	--	--	--	--	--	--
1.E+05	1.E+04	--	--	--	--	--	--	1.E+09	1.E+08	--	--	--	--	--	--
1.E+05	4.E+04	--	--	--	--	--	--	1.E+09	1.E+09	0.85	--	0.999	--	1.0	--
1.E+05	5.E+04	--	--	--	--	--	--			0.86	0.14	0.999	0.001	1.00	0.00
1.E+05	7.E+04	--	--	--	--	--	--		**Total**		**1.0**		**1.0**		**1.0**

Table 1.1. The weight fractions for the methyl and methine components in the simulated spectra at different temperatures reported as (Methyl/Methine) (Continued)

Rate (Hz)		**T (°C)**				**Rate (Hz)**		**T (°C)**			
2-site	SB	**70**		**75**		**2-site**	**SB**	**70**		**75**	
0.E+00	0.E+00	--	--	--	--	1.E+05	1.E+05	--	--	--	--
0.E+00	1.E+01	--	--	--	--	1.E+05	5.E+05	--	--	--	--
1.E+01	0.E+00	--	--	--	--	1.E+05	1.E+06	--	--	--	--
1.E+01	1.E+01	--	--	--	--	5.E+05	1.E+02	--	--	--	--
1.E+02	1.E+02	--	--	--	--	5.E+05	1.E+03	--	--	--	--
1.E+02	1.E+03	--	--	--	--	5.E+05	5.E+03	--	--	--	--
1.E+02	5.E+03	--	--	--	--	5.E+05	1.E+04	--	--	--	--
1.E+02	1.E+04	--	--	--	--	5.E+05	5.E+04	--	--	--	--
1.E+02	5.E+04	--	--	--	--	5.E+05	1.E+05	--	--	--	--
1.E+02	1.E+05	--	--	--	--	5.E+05	5.E+05	--	--	--	--
1.E+02	5.E+05	--	--	--	--	5.E+05	1.E+06	--	--	--	--
1.E+02	1.E+06	--	--	--	--	5.E+05	5.E+06	--	--	--	--
1.E+02	5.E+06	--	--	--	--	1.E+06	1.E+02	--	--	--	--
1.E+02	1.E+07	--	--	--	--	1.E+06	1.E+03	--	--	--	--
1.E+03	1.E+02	--	--	--	--	1.E+06	5.E+03	--	--	--	--
1.E+03	1.E+03	--	--	--	--	1.E+06	1.E+04	--	--	--	--
1.E+03	5.E+03	--	--	--	--	1.E+06	5.E+04	--	--	--	--
1.E+03	1.E+04	--	--	--	--	1.E+06	1.E+05	--	--	--	--
1.E+03	5.E+04	--	--	--	--	1.E+06	5.E+05	--	--	--	--
1.E+03	1.E+05	--	--	--	--	1.E+06	1.E+06	--	--	--	--
1.E+03	5.E+05	--	--	--	--	1.E+06	5.E+06	--	--	--	--
1.E+03	1.E+06	--	--	--	--	1.E+07	1.E+02	--	--	--	--
1.E+03	1.E+07	--	--	--	--	1.E+07	1.E+03	--	--	--	--
5.E+03	1.E+02	--	--	--	--	1.E+07	5.E+03	--	--	--	--
5.E+03	1.E+03	--	--	--	--	1.E+07	1.E+04	--	--	--	--
5.E+03	5.E+03	--	--	--	--	1.E+07	5.E+04	--	--	--	--
5.E+03	1.E+04	--	--	--	--	1.E+07	1.E+05	--	--	--	--
5.E+03	5.E+04	--	--	--	--	1.E+07	5.E+05	--	--	--	--
5.E+03	1.E+05	--	--	--	--	1.E+07	1.E+06	--	--	--	--
5.E+03	5.E+05	--	--	--	--	1.E+07	1.E+07	--	--	--	--
5.E+03	1.E+06	--	--	--	--	1.E+07	1.E+09	--	--	--	--
5.E+03	5.E+06	--	--	--	--	1.E+08	1.E+02	--	--	--	--
5.E+03	1.E+07	--	--	--	--	1.E+08	1.E+03	--	--	--	--
5.E+03	1.E+08	--	--	--	--	1.E+08	5.E+03	--	--	--	--
1.E+04	1.E+02	--	--	--	--	1.E+08	1.E+04	--	--	--	--
1.E+04	1.E+03	--	--	--	--	1.E+08	5.E+04	--	--	--	--
1.E+04	5.E+03	--	--	--	--	1.E+08	1.E+05	--	--	--	--
1.E+04	1.E+04	--	--	--	--	1.E+08	5.E+05	--	--	--	--
1.E+04	5.E+04	--	--	--	--	1.E+08	1.E+06	--	--	--	--
1.E+04	1.E+05	--	--	--	--	1.E+08	5.E+06	--	--	--	--
1.E+04	5.E+05	--	--	--	--	1.E+08	1.E+07	--	--	--	--
1.E+04	1.E+06	--	--	--	--	1.E+08	1.E+08	--	--	--	--
5.E+04	1.E+02	--	--	--	--	1.E+08	1.E+09	--	--	--	--
5.E+04	1.E+03	--	--	--	--	1.E+09	1.E+02	--	--	--	--
5.E+04	5.E+03	--	--	--	--	1.E+09	1.E+03	--	--	--	--
5.E+04	1.E+04	--	--	--	--	1.E+09	5.E+03	--	--	--	--
5.E+04	5.E+04	--	--	--	--	1.E+09	1.E+04	--	--	--	--
5.E+04	1.E+05	--	--	--	--	1.E+09	5.E+04	--	--	--	--
5.E+04	5.E+05	--	--	--	--	1.E+09	1.E+05	--	--	--	--
5.E+04	1.E+06	--	--	--	--	1.E+09	5.E+05	--	--	--	--
1.E+05	1.E+02	--	--	--	--	1.E+09	1.E+06	--	--	--	--
1.E+05	1.E+03	--	--	--	--	1.E+09	5.E+06	--	--	--	--
1.E+05	5.E+03	--	--	--	--	1.E+09	1.E+07	--	--	--	--
1.E+05	1.E+04	--	--	--	--	1.E+09	1.E+08	--	--	--	--
1.E+05	4.E+04	--	--	--	--	1.E+09	1.E+09	1.0	--	1.0	--
1.E+05	5.E+04	--	--	--	--			1.00	0.00	1.00	0.00
1.E+05	7.E+04	--	--	--	--		**Total**		**1.0**		**1.0**

1.5 DISCUSSIONS

The spectrum of bulk 89K PIPA-d_7 at -36 ºC is compared to 77K PMA-d_3 at 20 ºC from previous studies,[3] as shown in Figure 1.13. Both PIPA-d_7 and PMA-d_3 were found to have similar reduced quadrupolar splittings of 37 kHz. These patterns were dominated by a methyl group undergoing rapid reorientation about its symmetry axis. However, the depth of the region between the horns in the PIPA-d_7 was not as deep as that of PMA-d_3. In the PIPA-d_7 spectrum, an additional superimposed powder pattern was observed as an outer powder pattern with a splitting of 120 kHz. This powder pattern was expected from a static C-D bond. The part of the powder pattern originating from the single methine is indicated in the circle in Figure 1.13. Both resonances in bulk PIPA-d_7 at -36 ^{o}C were found to be the Pake powder patterns with different quadrupole splittings, indicating that the polymer was rigid or in the glassy state at that temperature.

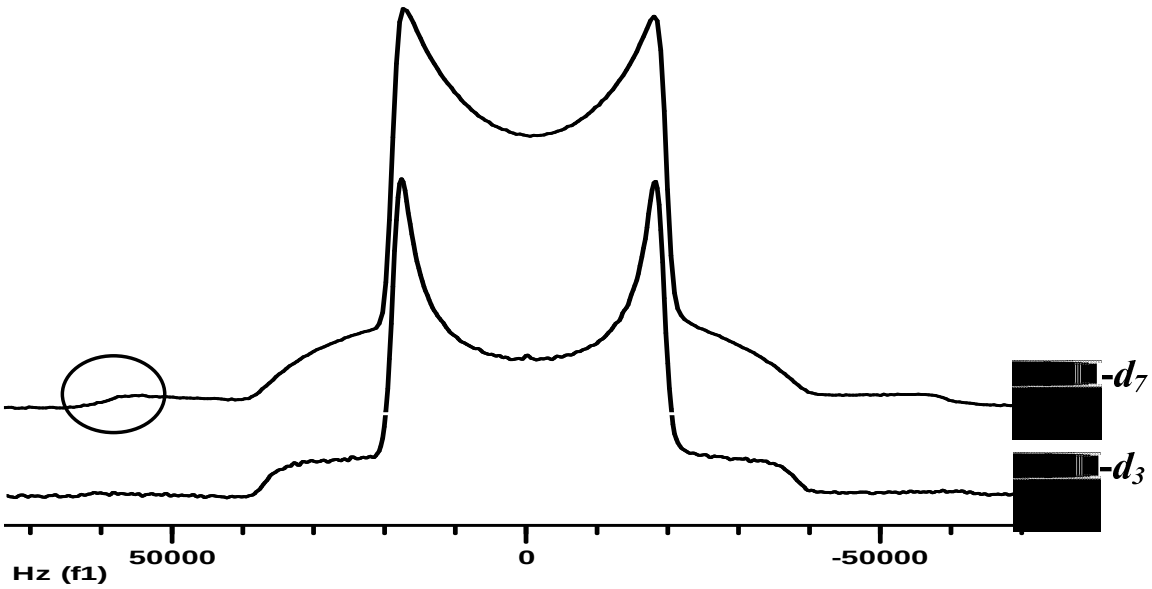

Figure 1.13. ^{2}H NMR spectra of bulk PIPA-d_7 at -36 $^{\circ}$C and bulk PMA-d_3 at 20 $^{\circ}$C.

The powder pattern of bulk PIPA-d_7 obtained at low temperatures collapsed to motionally narrowed resonances as the temperature increased. This was due to changes in the segmental mobility of the polymer. The single sharp resonance suggested that the polymer was very mobile. It was initially observed as a partial collapse of the powder pattern to a broad resonance with the appearance of a small spike at the middle of the spectrum. This small resonance can be attributed to the small number of mobile segments, which could be at the chain end of a polymer, the most mobile part of the polymer.[34] Then, the lineshapes became motionally narrowed with increasing temperature.

The regime for the transition from a glassy to a rubbery state can be defined as the T_g of that polymer. The transition can be observed as the temperature at which a polymer starts having motion that is comparable to the reciprocal of the quadrupole splittings. In Figure 1.5, the T_g of 89K PIPA-d_7 is shown as approximately 16 ºC. The small middle peak is due to the motion of a small fraction of the labeled methyl groups on the polymer, possibly the chain ends, which move rapidly. The segmental mobility was faster when the temperature increased to that around the T_g region. The superposition of the motionally-narrowed component with the broad powder pattern in the spectra of the bulk sample indicated the heterogeneity of the segmental mobility through the glass transition region. The peak intensity increased at approximately this temperature. The resonance eventually became a single sharp peak with no residual powder pattern, indicating that polymer dynamics tend to be more or less homogenous.

Different behavior was found in the PIPA-d_7 adsorbed on silica than that of a bulk sample. There appeared to be at least two different behaviors by the two compositions

existing in the spectra: the sharp edge of the powder pattern represented from the tightly bound chain segment on silica and the mobile part from the free polymer, filled in the middle between the two horns of the flat Pake pattern. Thus, the heterogeneity of the spectra for the adsorbed PIPA-d_7 sample was apparent due to the presence of a motional gradient on the surface.[26] The presence of the middle component on the adsorbed sample indicated that the unbound portions of the polymer segments in the tails and loops were farther away from the restriction due to the surface. The intensity of the "horns" of the powder pattern of the adsorbed sample gradually decreased with temperature. The train conformations, through which the polymers were directly bound to the silica surface through hydrogen bonding, were likely responsible for the broader (more motionally-narrowed) components in the spectra.

By comparing the spectra of bulk and surface samples, there were components that were more mobile in the adsorbed samples than those in the bulk at low temperatures. In contrast, the motions of the deuterium-labeled nuclei were slower or more restricted than those in the bulk PIPA-d_7 at higher temperatures. Hence, the H-bonding[35] at the polymer-silica interface limited the movement of the chain segments and the distribution of the rigid components observed in the spectra, even at higher temperatures. The mobility of the polymer chains in the adsorbed samples increased and behaved more like those in bulk when adsorbed amounts increased due to the more mobile components in the samples. The adsorbed polymers, however, had more motional heterogeneity than the bulk polymer did, even with larger adsorbed amounts in the samples. Rigid components of the spectra near the silica surface were observed, even at the high temperatures.

The phenomena at the interface can also be observed with MDSC. The MDSC thermograms of the adsorbed samples indicated two transitions were found in the adsorbed samples. A transition, that was apparent at a temperature close to the T_g of the bulk PIPA-d_7, is believed to be due to the freely moving chain segments. Another transition that shifted slightly higher than that of the bulk T_g, showed effects of attachment at the polymer-silica interface through H-bonding. The T_gs obtained from MDSC were different from those observed from NMR (approximately 10 ºC lower). Similarity in the differences of the T_gs was found by the intermediate regime of ^{2}H NMR spectra and MDSC measurements for other polymers, including PMA-d_3,[18] poly(vinyl acetate)-d_3 (PVAc-d_3),[26] and poly(methyl methacrylate)-d_3 (PMMA-d_3).[36]

Details about the segmental dynamics in bulk PIPA-d_7 were investigated using simulation. The simulations of the PIPA-d_7 at various temperatures were performed using the MXQET program, with the addition of simulated spectra created from combining the soccer ball and two-site hop models (for two methyls), and spectra from the soccer ball model (for the methine). Small random jumps on the soccer ball geometry validated it as a jump model for amorphous polymer.[3, 37] Hence, the soccer ball model was utilized in this study instead of simple methyl rotation (three-site jump). The ^{2}H NMR lineshapes were fitted with the simulated lineshapes generated based on those models, and the weight factors were calculated using MATLAB.

The weight fractions used for simulating the lineshapes varied with temperature. In the low temperature range (-25 to 10 ºC), approximately 95% (or more) of the simulated spectra from the methyl groups, i.e., these were dominant. The intensities of the inner powder patterns were strong (six deuterons) as compared to a deuteron from methane). In

the temperature range near the T_g, the weight fractions of the methyl and methine components varied, for example, the methyl:methine ratios were 70:30 at 16 ºC, 30:70 at 20 to 24 ºC, and about 50:50 at 33 - 45 ºC. At higher temperatures, the methyl component became more dominant again. At the highest temperatures studied (like 60 to 75 ºC), bulk PIPA-d_7 was completely in a rubbery state, which caused both the methyls and methine to move very fast and freely. The weight fraction should be dominated by both the methyl and methine components with an ideal ratio of 6:1. The weight fractions at those temperatures, however, showed only one lineshape from the methyl component at the highest jump rate (10^9 Hz). This may be due to the limitations of the fitting program. The simulated lineshapes produced from current models did not fit perfectly to the experimental spectra; however, these proposed models provided the reasonably close fitting. The larger number of models used and/or the more complex the jump model, as well as the optimum number of selection conditions for a fitting program will be studied in the future to obtain better fits.

1.6 CONCLUSIONS

PIPA-d_7 was labeled as two methyl groups with a methine on its side chain, and characterized using ^{2}H NMR. At least two types of motion were found in bulk PIPA-d_7, one was the rapid rotational motion of the methyl groups and the other was a static methine deuteron, which resulted in a compound powder pattern. There was less motion of the segmental dynamic at low temperature, whereas greater movement of the ^{2}H labeled groups on PIPA-d_7 was observed at a temperature near the glass transition temperature region. Above the glass transition region, the polymer became rubber-like and the chain had more mobility; therefore, the spectrum obtained consisted of only a

single resonance. Characteristic ^{2}H NMR spectra were found for adsorbed PIPA-d_7 on silica samples. The adsorbed samples showed different behavior than that of the bulk sample. The flat-top powder pattern was obtained at a temperature below the T_g. The presence of at least two motionally different components was noted and, consequently, these indicated the heterogeneity of segmental dynamics on the surface. At a higher temperature, the signal became a sharp resonance, showing that the polymer tended to be more homogeneous. However, a residual powder pattern at higher temperatures indicated the presence of segments with highly restricted mobility on the surface. The T_gs of the adsorbed samples were shifted approximately 10 ºC higher than that of bulk PIPA-d_7. This result was consistent with findings in the MDSC study. The complex spectra of the bulk PIPA-d_7 (especially the part from two methyl groups that dominated at various temperatures) were fitted using the combined small jump and two-site hop models. The simulations fitted quite well to the experimental lineshapes.

1.7 ACKNOWLEDGEMENTS

The authors acknowledge the National Science Foundation (NFS), and Missouri University of Science and Technology for financial support of this research. The authors also would like to thank Professor R. L. Vold for providing the MXQET simulation program, and B. Metin for assisting with the spectral fitting.

1.8 REFERENCES

1. Börjesson, J. M. a. L., *Phys. Review E* **2000,** 62, 5187.

2. Blum, F.; Lin, W.-Y.; Porter, C., *Colloid Polym. Sci.* **2003,** 281, 197.

3. Metin, B.; Blum, F. D., *J. Chem. Phys.* **2006,** 124, 054908/1.

4. Lin, W. Y., Blum, F. D., *Macromolecules* **1998,** 31, 4135.

5. Wallace, W. E.; van Zanten, J. H.; Wu, W., *Phys. Review E* **1995,** 52, R3329.

6. Akabori, K.-I.; Tanaka, K.; Takahara, A.; Kajiyama, T.; Nagamura, T., *The European Physical Journal Special Topics* **2007,** 141, 173.

7. Okuom, M. O.; Metin, B.; Blum, F. D., *Langmuir* **2008,** 24, 2539.

8. Kabomo, M. T.; Blum, F. D.; Kulkeratiyut, S.; Kulkeratiyut, S.; Krisanangkura, P., J. Polym. Sci. B: Polymer Physics 2008, 46, 649.

9. Fryer, D. S.; Nealey, P. F.; de Pablo, J. J., *Macromolecules* **2000,** 33, 6439.

10. van Zanten, J. H.; Wallace, W. E.; Wu, W. L., *Phys. Review E* **1996,** 53, R2053.

11. Reiter, G., *Europhys. Lett.* **1993,** 23, 579.

12. Kawana, S.; Jones, R. A. L., *Phys. Review E* **2001,** 63, 021501.

13. Hammerschmidt, J. A.; Gladfelter, W. L., *Macromolecules* **1999,** 32, 3360.

14. Kerle, T.; Lin, Z.; Kim, H.-C.; Russell, T. P., Macromolecules 2001, 34, 3484-3492.

15. Kim, J. H.; Jang, J.; Zin, W.-C., *Langmuir* **2000,** 16, 4064.

16. See, Y.-K.; Cha, J.; Chang, T.; Ree, M., *Langmuir* **2000,** 16, 2351.

17. Koh, Y. P.; McKenna, G. B.; Simon, S. L., J. Polym. Sci. B: Polymer Physics **2006**, 44, 3518.

18. Metin, B.; Blum, F. D., *J. Chem. Phys.* **2006,** 125, 054707.

19. Jelinski, L. W.; Kintanar, A.; Gancarz, I.; Koberstein, T., Macromolecules 1986, 19, 1876.

20. Jelinski, L. W.; Cholli, A. L.; Dumais, J. J.; Engel, A. K., Macromolecules 1984, 17, 2399.

21. Semin, G. K.; Babushikina, T. A.; Yakobason, G. G., Keter: Jerusalem, 1975.

22. Duer, M. J., Introduction to Solid-State NMR Spectroscopy. Blackwell: Oxford, UK, 2004.

23. Koenig, J., L.; Kormos, D., *Applied Spectroscopy* **1979,** 33, 349.

24. Blum, F. D.; Lin, W. Y., *J. Am. Chem. Soc.* **2001,** 123, 2032.

25. Lin, W.-Y.; Blum, F. D., *Macromolecules* **1997,** 30, 5331.

26. Blum, F. D.; Xu, G.; Liang, M.; Wade, C. G., *Macromolecules* **1996,** 29, 8740.

27. Jelinski, L., W., Methods in Stereochemical Analysis 1986, 7(High Resolut. NMR Spectrosc. Synth. Polym. Bluk), 335.

28. Spiess, H. W., *Colloid Polym. Sci.* **1983,** 261, 193.

29. Wittebolt, R. J.; Olejniczak, E. T.; Griffin, R. G., *J. Chem. Phys* **1987,** 86, 5411.

30. Greenfield, M. S.; Ronemus, A. D.; Vold, R. L.; Vold, R. R.; Ellis, P. D.; Raidy, T. E., J. Magn. Reson. 1987, 72, 89.

31. Vold, R. R.; Vold, R. L., Advances in Magnetic and Optical Resonance 1991, 16, 85.

32. EXPRESS.

33. Lin, W. Y.; Blum, F. D., *Macromolecules* **1997,** 30, 5331.

34. Lin, W. Y.; Blum, F. D., *Macromolecules* **1998,** 31, 4135.

35. Blum, F. D.; Krisanangkura, P., *Thermochimica Acta* **2009,** 492, 55.

36. Kuebler, S. C.; Schaefer, D. J.; Boeffel, C.; Pawelzik, U.; Spiess, H. W., Macromolecules 1997, 30, 6597-6609.

37. Tracht, U.; Heuer, A.; Spiess, H. W., *J. Chem. Phys.* **1999,** 111, 3720.

PAPER 2: EFFECT OF SUBSTRATE SURFACE AREA ON BOUND CARBONYLS IN POLY(ETHYL METHACYLATE)

Piyawan Krisanangkura, Sarah Jackson and Frank D. Blum

Department of Chemistry and Materials Research Center, Missouri University of Science and Technology, Rolla, Missouri 65409-0010, USA

2.1 ABSTRACT

Poly(ethyl methacrylate) (PEMA) was adsorbed onto two similar silicas, with different surface areas, in order to compare fractions of bound carbonyls that were hydrogen bonded to the silica using transmission FTIR. Different adsorbed amounts of PEMA were adsorbed on Cab-O-Sil M-5P and LM-130 with specific surface areas of 200 and 130 m^2/g, respectively. The resonance frequency for the adsorbed carbonyls was observed to shift to a lower frequency than that of the bulk carbonyls. Based on a previously developed model, plots of the ratio of the free and bound carbonyl peak intensities (A_f/A_b), versus the total adsorbed amount (M_t), were found to be linear for both samples and used to estimate the amount of bound polymer (M_b) on the silica. The reported bound fractions, p, were in between 0.07 to 0.10 (over a range of 0.78 to 1.41 mg/m^2 adsorbed PEMA) on M-5P, and 0.04 to 0.06 (over a range of 0.85 to 1.70 mg/m^2 adsorbed PEMA) on LM-130. These values are somewhat less than those previously measured for poly (methyl methacrylate) (PMMA). The differences are believed to be due to a variation in the side chain composition of the polymer.

2.2 INTRODUCTION

Adsorption of polymers from solution onto a surface will result in properties that are altered from those of bulk or unadsorbed polymers. It is important to understand what factors change the properties of materials, and why they do so. In addition to the nature of polymers, which include chain length, blockiness, tacticity, and self-association; interfacial interactions also play a considerable role in the adsorption phenomenon. Moreover, surface modification[1] can affect the strength of interfacial interactions and, in some cases, be tailored to different absorbates to meet specific needs of materials.

Many investigations on interfacial interaction at silica surfaces have been conducted by several researchers.[2-6] Adsorption behavior at the interface can be identified by a variety of spectroscopic techniques, e.g., FTIR,[7-10] UV,[10] NMR,[11, 12] and ESR.[13] Infrared spectroscopy (IR) is, in principle, the simplest method for estimating the fraction of segments bound to a surface. The intermolecular structures that occur before and after the adsorption process can be distinguished via FTIR spectra.

The FTIR technique can be relatively straightforward if the adsorbed species contains appropriate functional groups. It is possible to distinguish certain surface functional groups from internal groups by analysis of the absorption bands when molecules are either chemically or physically adsorbed. Atoms or molecules that are physically adsorbed on a surface through the formation of a new bond, or interaction, could perturb the motions or electron distribution of atoms or molecules of the group, causing shifts in their vibrational frequencies. In IR, the adsorption of molecules on a surface can result in the disappearance of certain features associated with the surface. For example, isolated SiOH stretching vibrations would be expected to disappear, in the case

of silica, when the surface hydroxyls are bound to polymer segments. The appearance of new features, due to adsorbed species, may also be observable as well.[14-16] Some previous studies have focused on the behavior of silanol groups on silica, where it was possible to distinguish between hydrogen bonded and free silanol.[10, 17] For polymers containing carbonyl groups, such as alkyl acrylate or alkyl methacrylate polymers adsorbed on silica, not only can the behavior of the silanol group vibration be observed, but the shift of the carbonyl band is also measurable. These bands can be used to differentiate between free carbonyls and carbonyls associated with the SiOH via hydrogen bonding.[8,9,18-20] Based on these band intensities, the fraction of polymer segments attached to silica surface sites can be estimated.

Previously, we have studied the behavior of adsorbed poly(methyl methacrylate) (PMMA) on silica,[9,20-22] with respect to different aspects of the behavior of adsorbed polymer. In this study, we used FTIR to probe the interaction of poly(ethyl methacrylate) (PEMA) adsorbed on two amorphous silicas with different surface areas. Based on an analysis of the adsorption bands, the ratios of extinction coefficient of bound carbonyls to free carbonyls and the bound fractions (p) of PEMA on both silicas are reported.

2.3 EXPERIMENTAL

2.3.1. Materials. Poly(ethyl methacrylate) (PEMA) (Aldrich, Milwaukee, WI) was used as received. The molecular mass was determined to be 400 kDa with the polydispersity of 1.65 by gel permeation chromatography (GPC). Two different types of silica were used in this study, Cab-O-Sil M-5P fumed silica (Cabot Corp., Tuscola, IL) with a specific surface area of 200 m^2/g and LM-130 (Cabot Corp., Tuscola, IL) with a

specific surface area of 130 m^2/g. The silicas were dried in a furnace at 450 ºC for 24 h, and then used immediately or otherwise, they were stored in a vacuum desiccator. Toluene (HPLC grade, Fisher Scientific, Pittsburgh, PA) was used as received.

2.3.2. Adsorption. Samples of 400 kDa PEMA adsorbed on silica were prepared in test tubes with caps. Different amounts of the PEMA were dissolved in 10 mL of toluene, and silica (0.3 g) was added to each tube. The test tubes filled with silica, solvent, and adsorbed polymer, were shaken in a mechanical shaker for 72 h, centrifuged at 2500 rpm for 1 h, and the supernatants were decanted. The lower layer of PEMA and silica were dried by blowing air through capillary tubes onto the wet samples. The translucent gel (wet) samples turned into a dull white powder after drying. All adsorbed silica samples were put in a vacuum oven for 36 h, at room temperature, for final drying. The amounts of PEMA adsorbed on silica were determined using thermogravimetric analysis with a TGA 2950 (TA Instruments, New Castle, DE) by heating the adsorbed samples to 750 ºC at a heating rate of 20 ºC/min. The organic material started decomposing at around 200 ºC, and completely burned off by 400 ºC. The amounts of adsorbed PEMA were calculated based on weight differences, before and after adsorption. Adsorption curves of PEMA on the two silicas were fitted to Langmuir isotherms, and are given by

$$\Gamma = \frac{\Gamma_m K c}{1 + K c} \tag{2.1}$$

where Γ is the adsorbed amount, c is the equilibrium concentration, and K and Γ_m (maximum adsorbed amount) are constants determined from a fit to the data.

2.3.3. Characterization. FTIR spectra of the adsorbed PEMA on silica were recorded with a Nicolet Nexus 470 Fourier Transform Infrared spectrometer (Nicolet Instruments, Madison, WI). A small amount of dried sample powder (approximately 1-2 mg) was weighed and spread evenly onto a 2.3 cm KBr disk, and then covered with another KBr disk. The two KBr disks were gently clamped together with a holder to keep the sample between them. FTIR spectra of samples with different amounts of PEMA adsorbed on silica were recorded with a 4 cm^{-1} resolution. Curve fitting was done for the carbonyl peaks in all spectra using GRAMS32 software (Thermogalactic, Salem, NH).

2.4 RESULTS

Based on the percentage of weight loss from TGA, the PEMA adsorbed amounts on both silicas were determined. The adsorbed amounts of the polymer were plotted as a function of equilibrium concentrations of the solution, and shown in Figure 2.1. Those curves were fitted to the equation (2.1), and the constants K and Γ_m are reported in Table 2.1. The adsorbed amounts increased with increasing solution concentrations, and then leveled off at around 1.5 mg/m^2 for Cab-O-Sil M-5P and 1.4 mg/m^2 for LM-130. Hence, approximately, 1.5 mg PEMA/m^2 is about the highest uptake by both silicas.

The FTIR spectra of pure M-5P and LM-130 are shown in Figure 2.2. The spectra of the two Cab-O-Sils are similar, as expected. Free or isolated silanols can be observed in pure or unadsorbed silicas, as sharp IR absorptions at 3760 cm^{-1}, with a broad tail to lower frequencies having a maximum of near 3450 cm^{-1}, interpreted as moisture. The moisture adsorption in silica is an indication that silica is a hygroscopic material, and most of it can be removed by heating at 100 ºC or higher before use.[3] However, the water

will re-adsorb under normal laboratory conditions. The FTIR of bulk PEMA is shown in Figure 2.2C. A strong resonance for the carbonyl group in PEMA was observed at 1730 cm^{-1}

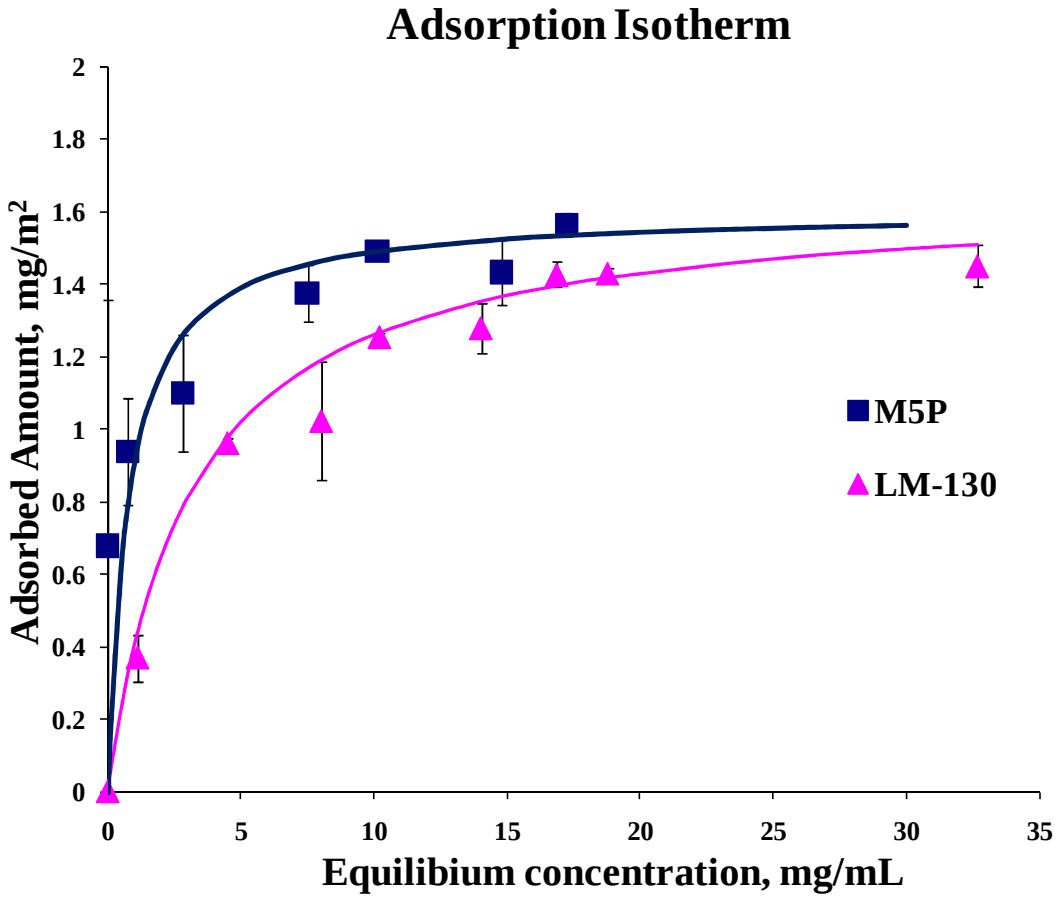

Figure 2.1. The adsorption isotherm from toluene for PEMA adsorbed on Cab-O-Sil M-5P and LM-130.

Table 2.1. The constants from Langmuir adsorption isotherm for PEMA adsorbed on both silicas in the presence of toluene

Silica	K	Γ_m
M5-P	1.46 ± 0.52	1.57 ±0 .09
LM-130	0.32 ± 0.13	1.65 ± 0.15

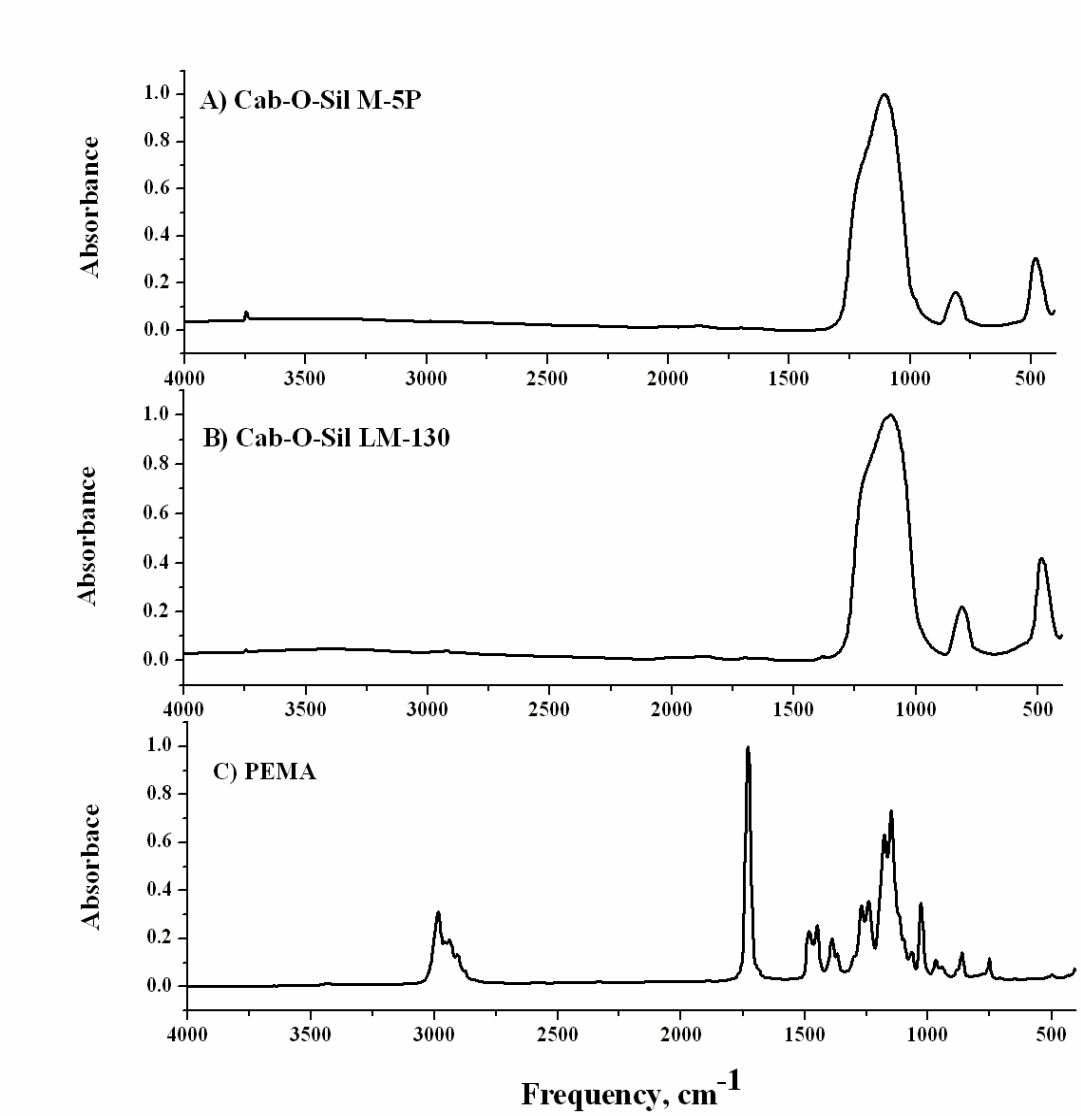

Figure 2.2. FTIR spectra of A) Cab-O-Sil M-5P, B) Cab-O-Sil LM-130, and C) bulk PEMA.

The IR spectra in the region of the hydroxyl stretching are shown in Figure 2.3. The change in intensities of the hydroxyl group resonances before and after adsorption was apparent. It is well-known that polymers containing carbonyl groups can physically adsorb onto silica through hydrogen bond formation with the silanol groups on the surface.[23] The sharp resonance at 3760 cm^{-1} is due to the hydroxyl stretching vibration of

free SiOH on the surface.[3,7] The broader peak at 3550 cm^{-1} becomes stronger in the adsorbed samples due to hydrogen bonding.[24,25] The intensities of the isolated silanol resonances were dramatically decreased in the surface samples due to the interaction with the polymer. The effects of this interaction can also be seen in the carbonyl resonance for the stretching of the C=O bonds.

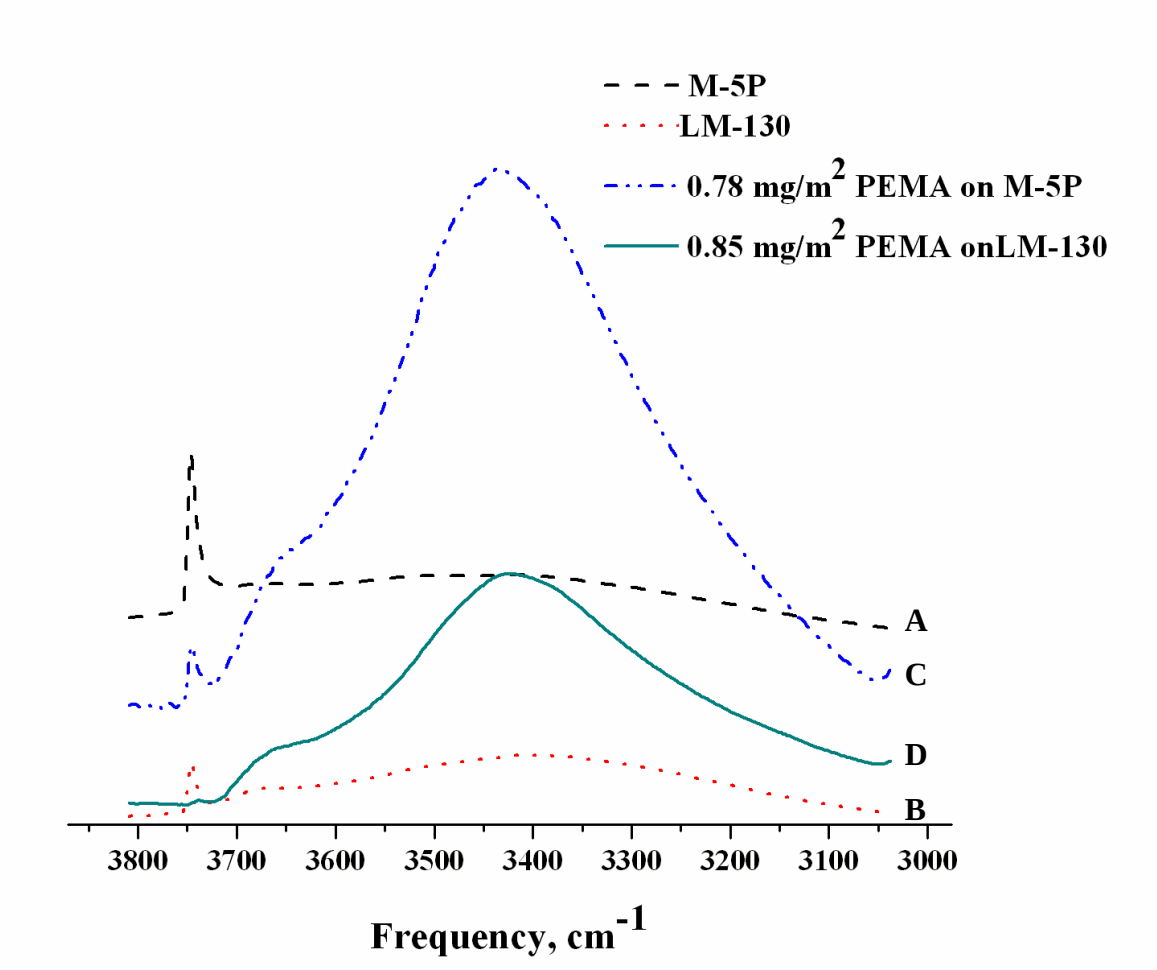

Figure 2.3. Infrared spectra in the –OH stretching region for A) Cab-O-Sil M-5P, B) LM-130, C) 0.71 mg/m^2 PEMA on M-5P, and D) 0.85 mg/m^2 PEMA on LM-130. The vertical scales are scaled and shifted for clarity.

The FTIR spectra of bulk PEMA and adsorbed PEMA on M-5P and LM-130 in the carbonyl region are illustrated in Figure 2.4. As shown in that figure, two strong overlapping IR resonances were observed at 1730 cm^{-1} and 1710 cm^{-1}, which can be assigned to carbonyl stretching mode.[18, 19, 26] The resonance at 1730 cm^{-1} is at the same frequency as that for the bulk PEMA, and is assigned to "free carbonyls". The shift to 1710 cm^{-1}, that was observed here, is due to the carbonyl groups that were hydrogen bonded to the surface silanols.[8] The samples were fairly uniformly placed, in roughly the same amounts, on the salt plate, and hence in the IR beam. It can be seen that the amount of bound carbonyl in PEMA on M-5P was a larger than that of the LM-130 sample at approximately 0.8 mg/m^2 PEMA on silicas.

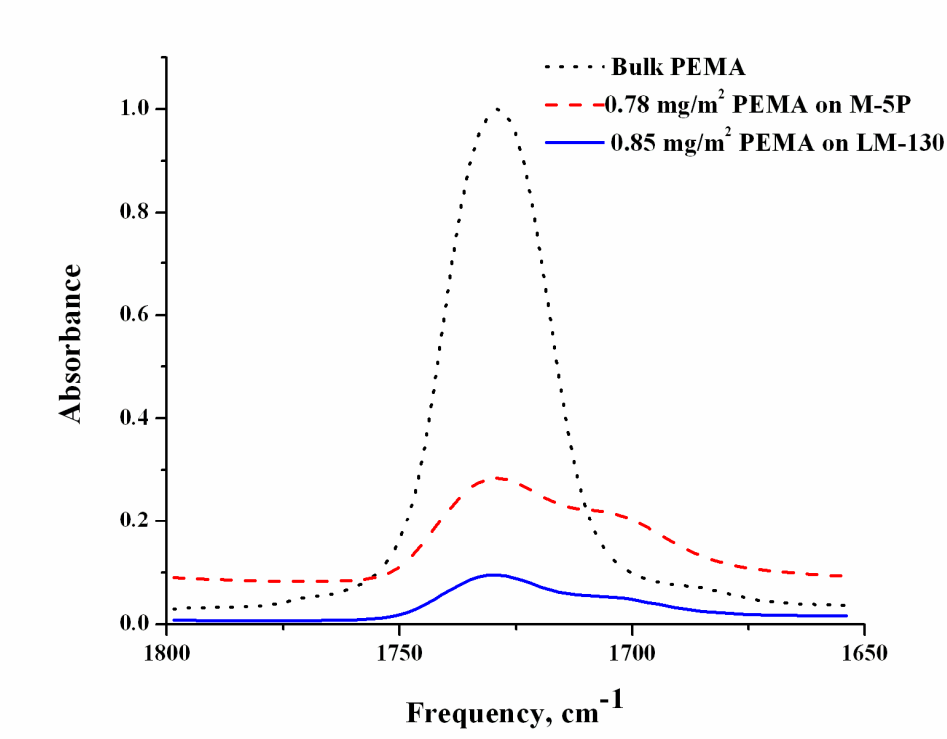

Figure 2.4. Infrared spectra of bulk PEMA, 0.78 mg/m^2 PEMA on M-5P, and 0.85 mg/m^2 PEMA on LM-130. The spectra have been shifted on the vertical scale for clarity. The intensities of the spectra were normalized by OMNIC software (on the instrument).

The relative intensities of bound carbonyl resonances decreased with increased PEMA adsorbed amounts as shown in Figure 2.5 (M-5P) and 2.6 (LM-130). For a certain system, the number of H-bonding (consequently the amount of bound carbonyls) is fixed. The more PEMA added to the silica, the more free carbonyls there will be in the adsorbed polymer. From the figures, it is noted that the fractions of bound carbonyl resonances in PEMA on LM-130, were similar to those on M-5P at the adsorbed amounts lower than 1.0 mg/m^2. At larger adsorbed amounts (greater than 1.0 mg/m^2) LM-130 samples seemed to have a smaller fraction of bound carbonyl resonances. The information from these spectra can be used to determine the fraction of segments that was bound to the surface.

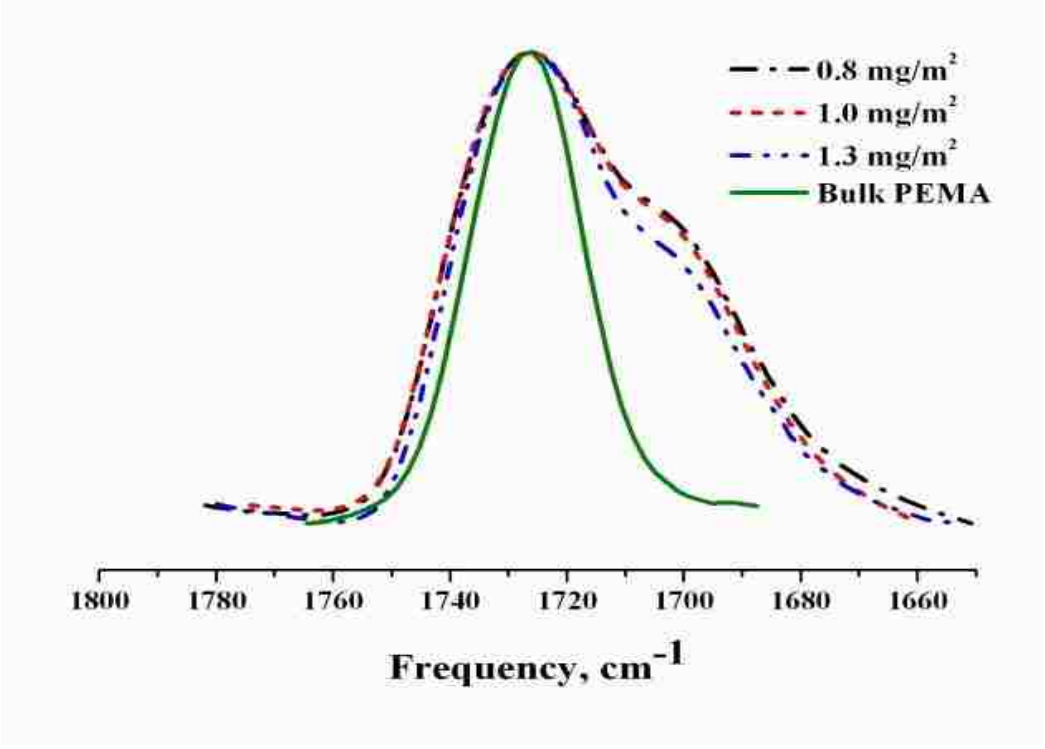

Figure 2.5. FTIR spectra of PEMA adsorbed on M-5P as a function of the adsorbed amount.

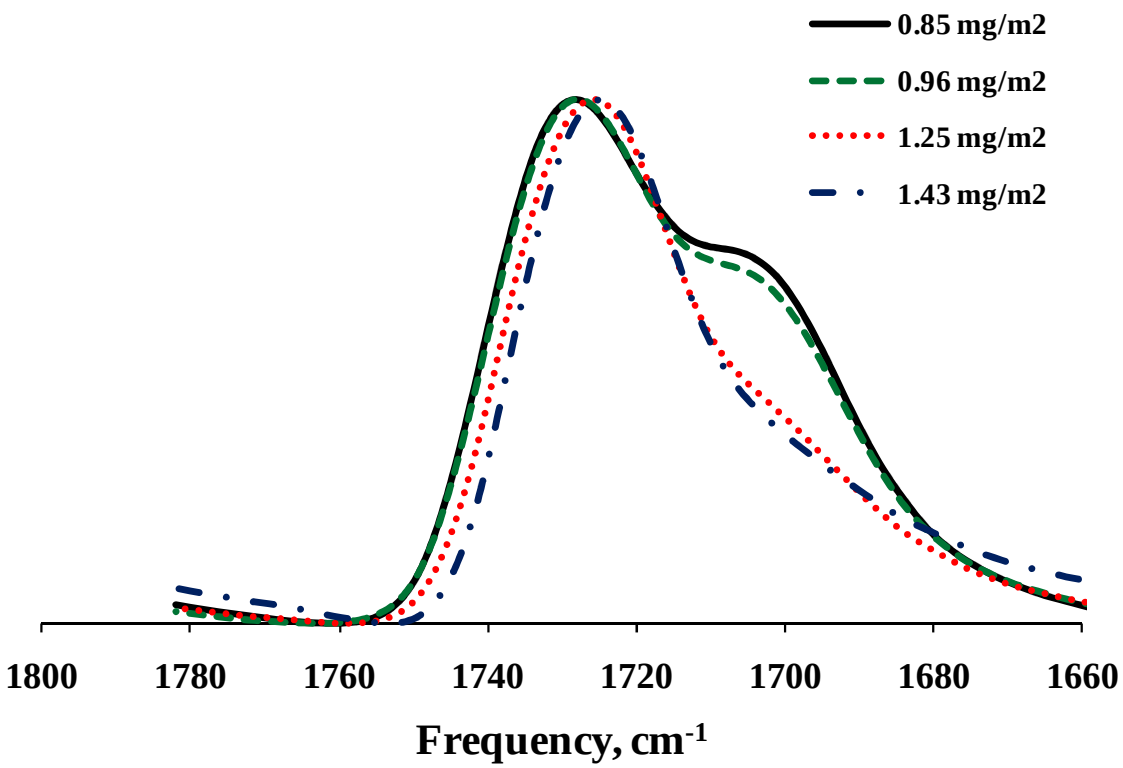

Figure 2.6. FTIR spectra of PEMA adsorbed on LM-130 as a function of the adsorbed amount.

To determine areas under the peaks, the free and bound carbonyl resonances of adsorbed PEMA on both silicas at each adsorbed amount were fitted using GRAMS32 software with Gaussian line shapes. Figures 2.7 and 2.8 show examples of the curve fitting for PEMA adsorbed onto M-5P and LM-130.

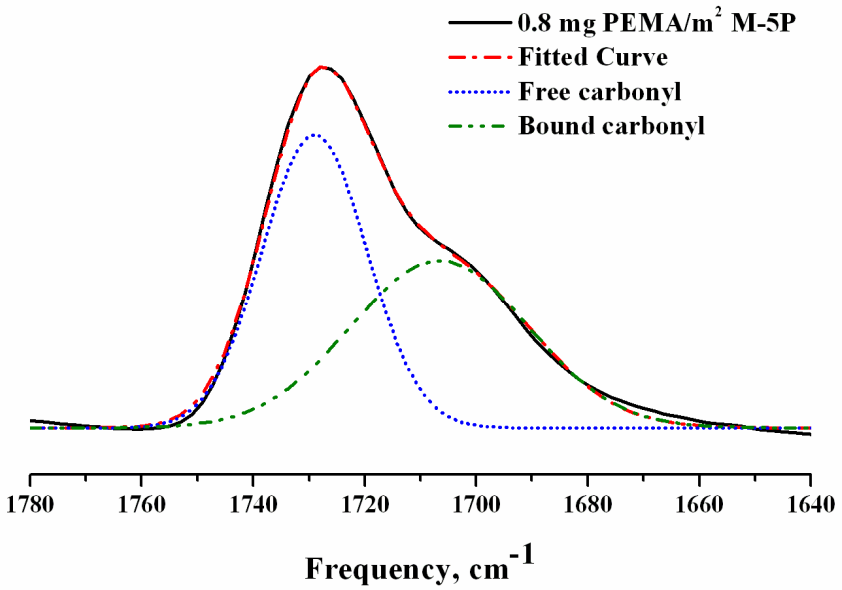

Figure 2.7. Gaussian curve fitting for adsorbed PEMA (0.78 mg/m^2) on M-5P, showing the contribution of the free (~1730 cm^{-1}) and bound (~1710 cm^{-1}) to the experimental spectra.

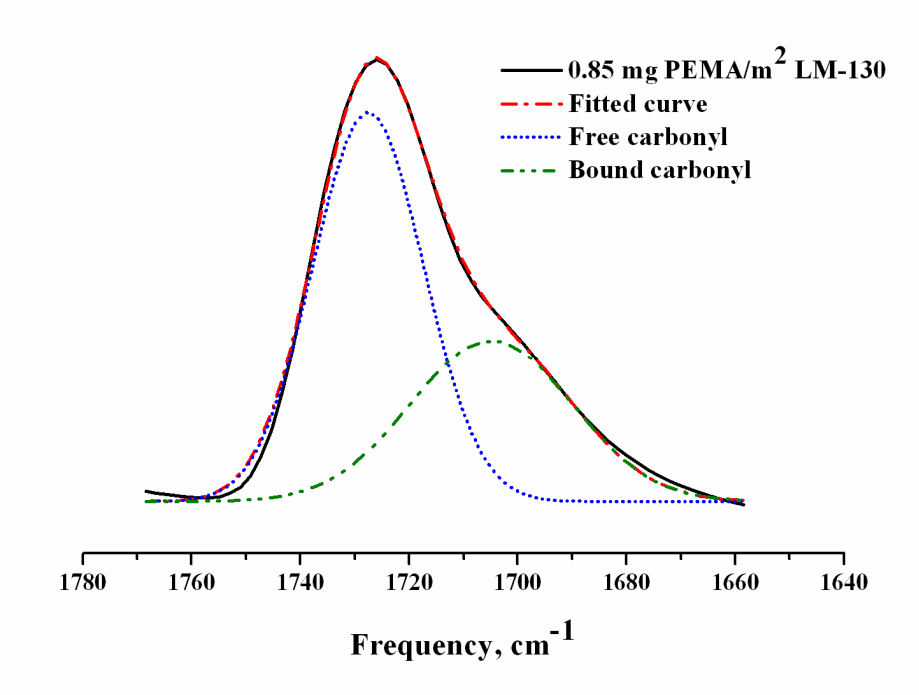

Figure 2.8. Gaussian curve fitting for adsorbed PEMA (0.85 mg/m^2) on LM-130, showing the contribution of the free (~1730 cm^{-1}) and bound (~1710 cm^{-1}) to the experimental spectra..

In these cases, as well as others, the fitted spectra match the experimental ones quite well. However, to estimate the number of bound and free carbonyls, knowledge of the extinction coefficients of each must be taken into consideration. The model proposed by Kulkeratiyut et al.[9] was used to determine the ratio of bound and free carbonyl extinction coefficients (X) and the bound fraction (p).

2.5 DISCUSSION

The strength of an interfacial interaction of a polymer with a metal oxide surface depends on the number of contact points between the polymer chains and the surface. In this case, Cab-O-Sil M-5P and Cab-O-Sil LM-130 with surface areas of 200 m^2/g and 130 m^2/g, respectively, were studied. Basically, both Cab-O-Sil M-5P and LM-130 are untreated fumed silicas that should have similar surface properties, but different surface areas. The primary particle sizes of M-5P and LM-130 were approximately 14 and 21 nm, respectively.[27] The measured adsorption isotherms for PEMA on both silicas were similar. As shown in Figure 2.1, Cab-O-Sil M-5P had slightly higher adsorbed amounts than LM-130 did at similar concentrations. The M-5P curve also reached the maximum adsorbed amounts at lower concentrations than the LM-130, which yielded a higher K value. The particle size and geometry of the substrate also has been observed to affect the adsorption process.[28] On particles with larger particle size (less curvature), polymer chains seemed to prefer train configuration, resulting in a thinner layer. This is in contrast to smaller particles, where the initial adsorption resulted in more tail.[29] However, in our experiments the adsorptions eventually reached the same maximum adsorbed amounts, Γ_m (within experimental error).

The similarity of Γ_m was probably due to the several factors. One factor that might control the number of bound polymer segments is the number of silanol groups on the adsorbent, which is expected to be similar among fumed silicas. The primary particle size of the silica particles may also not have been different enough (14 and 21 nm for Cab-O-Sil M-5P and LM-130, respectively) to cause a significant change in term of Γ_m, as observed in Figure 2.1.

The interfacial interaction between the carbonyls from PEMA and the silanols from the silica can be observed by the frequency shift in the FTIR spectra. An electron donation from the silanol groups to the carbonyl bond weakened the C=O bond. The C=O stretching resonance, therefore, became weaker and was shifted to lower frequency.[30] Two overlapping resonances were found in adsorbed PEMA samples for both silicas, as indicated in Figure 2.4. The resonance centered at 1730 cm^{-1} was assigned to the free carbonyl, and the shoulder resonance centered at around 1710 cm^{-1} was assigned to the bound carbonyl, due to the weakening of the C=O from H-bonding with silanol groups on the silica surface. The positions of those peaks may vary slightly, depending on the environment of the observed system, while the peak intensity should be proportional to the number of carbonyls present in the IR beam. The relative intensities of the bound carbonyl resonances in LM-130 samples were significantly decreased at adsorbed amounts higher than 1.0 mg/m^2. This is probably due to the experimental error from sample preparation that the surface was not uniformly coverage with the polymer for the adsorbed amount more than 1.0 mg/m^2. We can assume that most free silanols on the surface were occupied at the adsorbed amount of 1.0 mg/m^2. The model used is based on the premise that a fixed amount of bound polymer (that associated with bound carbonyl

groups) called "M_b" exists for all adsorbed samples studied.[9] From the model, the fraction of bound carbonyl groups, p, is given by

$$p = \frac{M_b}{M_f + M_b} = \frac{M_b}{M_t} \tag{2.2}$$

where M_b is the adsorbed amount of bound polymer, M_f is unbound or free polymer, and M_t is the total adsorbed amount (all in mg polymer/m^2 surface). Since the resonance intensity is proportional to the number of carbonyls in each case, the M's could be replaced by A_x/α_x (proportional to the concentration), where the A_x is the integrated absorption intensity, α_x is the absorption coefficient, and x is either "b" or "f" for the bound or free carbonyl, respectively. Then, Equation (2.2) can be written as:[9]

$$p = \frac{(A_b / \alpha_b)}{[(A_b / \alpha_b) + (A_f / \alpha_f)]} \tag{2.3}$$

The absorption intensities can be measured, but it is difficult to measure the absorptivity coefficients directly. It is therefore useful to rewrite Equation (2.3) in terms of the ratio $X \ (= \frac{\alpha_b}{\alpha_f})$ or:

$$M_t = M_b (A_b + A_f X) / A_b \tag{2.4}$$

Equation (2.4) can be rewritten as,

$$M_t = (A_f / A_b) X M_b + M_b \tag{2.5}$$

Equation (2.5) is a linear in terms of the total adsorbed amount, M_t, and should vary as the ratio of absorption intensities. From the experimental data, X and M_b can be determined, from which p can be estimated.

Plots of the total adsorbed amount, M_t, on M-5P and LM-130, as a function the ratio of free to bound carbonyl intensities, are illustrated in Figure 2.9. At first glance, both data sets are similar, which is an important conclusion of this work. Linear regressions of the data yielded intercepts of 0.076 +/- 0.019 mg/m^2 for M-5P and 0.062 +/- 0.034 mg/m^2 for LM-130. From the intercepts and the slopes, the values of M_b can be evaluated.

From linear regression of the data, X, M_b, and the bound fractions, p for PEMA on each of the silicas can be determined. The X value for the M-5P surface sample was found to be 10.4 +/- 2.5, and the X for PEMA on LM-130 was 12.5 +/- 3.2. Within experimental error, there are two X values that equivalent for PEMA for both samples, which is consistent with the notion that the adsorption behavior of PEMA on both silicas is similar.

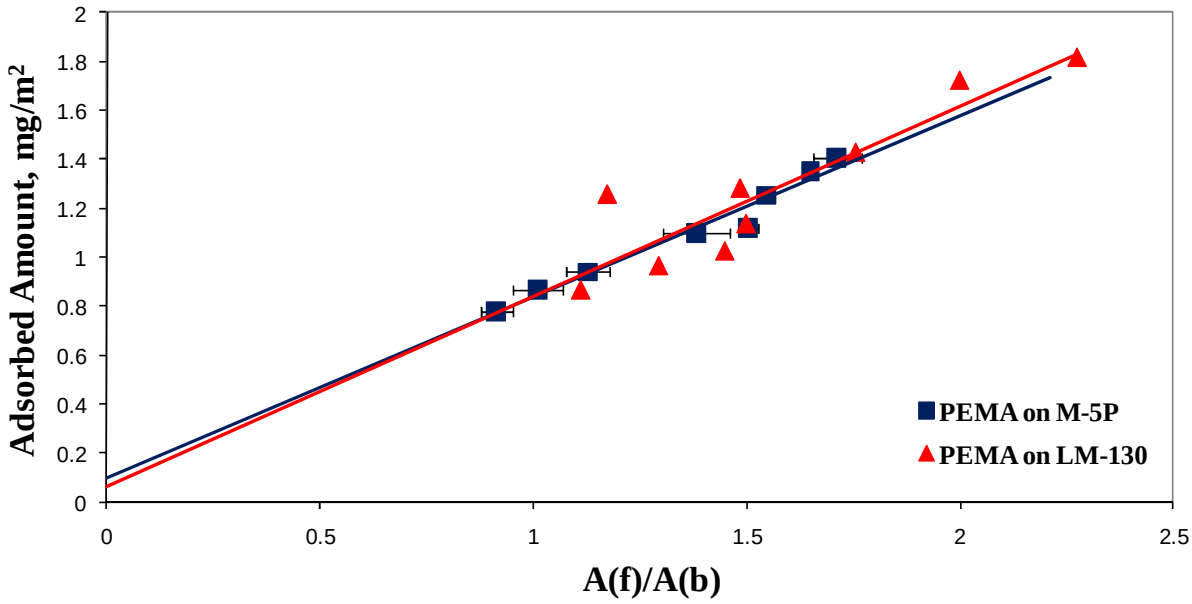

Figure 2.9. The total adsorbed amount, M_t, of PEMA on M-5P and LM-130 as a function of the ratio of free carbonyl to bound carbonyl peak intensities (A_f/A_b).

It is worthwhile to compare the amount of bound PEMA segments on both silicas to previous work on PMMA-M-5P.[9] The amount of tightly bound PEMA segments, M_b, is 0.076 +/- 0.019 mg/m^2 on M-5P, and 0.062 +/- 0.034 mg/m^2 on LM-130. For comparison, the X value for PMMA on M-5P was 7.7 +/- 1.5 and M_b was 0.17 mg/m^2 on M-5P. The M_b value of PEMA on M-5P is obviously lower than that of PMMA, and even lower in the case of LM-130. PEMA has one additional alkyl-unit on the side-chain than PMMA has, which may affect polymer orientation on the surface, leading to fewer bound carbonyls.

The bound fraction, p, can be estimated from the values of M_b and X from

$$p = \frac{A_b}{A_b + A_f X} \tag{2.6}$$

Figure 2.10 shows plots of the bound fractions of adsorbed PEMA on M-5P and LM-130, as a function of adsorbed polymer, M_t. PEMA adsorbed onto LM-130 tended to have a smaller fraction of bound carbonyls than did the sample adsorbed on M-5P. Fractions of bound PEMA were estimated to be between 0.07 to 0.10 over an adsorption range of 0.78 to 1.41 mg/m^2 on M-5P. For LM-130, approximately 0.04 to 0.06 of the bound fractions were reported for an adsorbed amount of 0.85 to 1.70 mg PEMA/m^2. Based on Equation (2.2), theoretical bound fraction curves were shown for comparison. For PEMA adsorbed on M-5P, the experimental data fit the model quite well. Experimental bound fractions of PEMA on LM-130, however, were somewhat different from those of the model, especially at the low adsorbed region amount. The uncertainty in the measurement may have been due to scattering associated with the LM-130 samples, which would be expected to be greater than that for the M5-P, due to their larger size.

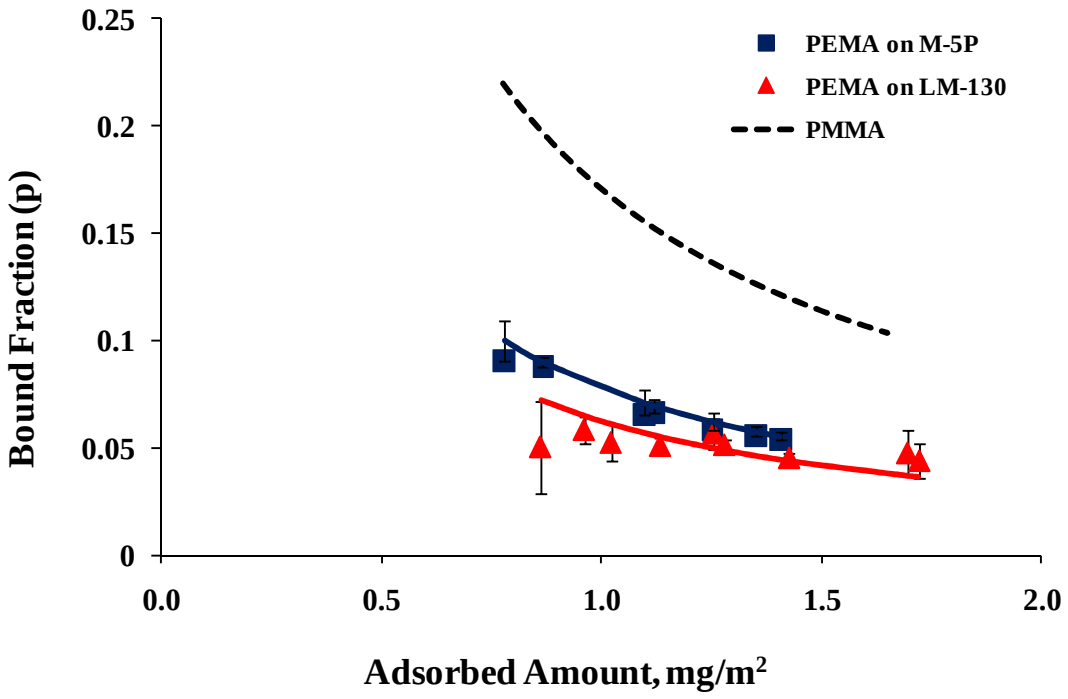

Figure 2.10. Bound fractions of PEMA on M-5P and on LM-130 as a function of the adsorbed amount, compared to PMMA on M-5P.[9]

2.6 CONCLUSIONS

A polymer bound fraction depends upon the nature of both adsorbate and adsorbent. The longer the side chain, the more steric hindrance would be expected for the adsorption process, and consequently, fewer carbonyls may be bound. Characterization of surface behavior can easily be achieved by using an FTIR spectroscopic method. A shift in carbonyl resonance to a lower frequency (approximately 15 – 20 cm^{-1}) for a surface sample is observable, and can be identified as the carbonyl groups bound to SiOH on the surface through H-bonding. The intense nature C=O stretching absorption band made the fitting straightforward and only a Gaussian line-shape was required. The ratio of absorption coefficients (X) for the same types of adsorbate and adsorbent remained

about the same for both silicas, i.e., the X values did not vary with the surface areas. However, the fraction of segments bound to the surface was slightly affected by the size of surface area, but the differences were within the experimental errors of estimating the constants X and M_b. From the proposed model, the bound fractions were found to be 0.07 to 0.10 for an adsorbed amount of 0.78 to 1.41 mg PEMA/m^2 on M-5P, which was lower than that previously found for PMMA.

2.7 ACKNOWLEDGEMENTS

The authors acknowledge the National Science Foundation under grant NSF-0706197 for financial support of this work.

2.8 REFERENCES

1. Lu, X.; Mi, Y., *Macromolecules*, **2005**, *38*, 839.
2. Zhuravlev, L. T., *Langmuir*, **1987**, *3*, 316.
3. Burneau, A.; Barrès, O.; Gallas, J. P.; Lavalley, J. C., *Langmuir*, **1990**, *6*, 1364.
4. Peri, J. B.; Hannan, R. B., *J. Phys. Chem*., **1960**, *64*, 1526.
5. Peri, J. B., *J. Phys. Chem*., **1965**, *69*, 211.
6. Ledoux, R. L.; White, J. L., *Scienc*e, **1964**, *143*, 244.
7. Morrow, B. A.; McFarlan, A. J., *Langmuir*, **1991**, *7*, 1695.
8. Fontana, B. J.; Thomas, J. R., *J. Phys. Chem*., **1961**,*65*, 480.
9. Kulkeratiyut, S.; Kulkeratiyut, S.; Blum, F. D., *J. Polym. Sci. Part B: Polym Phys*, **2006**, *44*, 2071.
10. Kawaguchi, M.; Aoki, M.; Takahashi, A., *Macromolecules*, **1983**, *1*6, 635.
11. Walter, T. H.; Turner, G. L.; Oldfield, E., *J. Mag. Reson*., **1983**, *54*, 121.

12. Grandinetti, P. J.; Baltisberger, J. H.; Farnan, I.; Stebbins, J. F.; Werner, U.; Pines, A., *J. Chem. Phys*., **199**5, *99*, 12341.

13. Sakai, H.; Immaura, Y., *Bull. Chem. Soc. Jpn*., **1987**, *60*, 1261.

14. Hair, M. L., Infrared Spectroscopy in Surface Chemistry, Marcel Dekker, Inc., New York, 1967.

15. Morrow, B. A.; McFarlan, A. J., *J. Phys. Chem*., **1992**, *96*, 1395.

16. Ichikawa, K.; Mori, T.; Kitano, H.; Fukuda, M.; Mochizuki, A.; Tanaka, M., *J. Polym. Sci. Part B: Polym Phys*, **200**1, *39*, 2175.

17. Kobayashi, K.; Araki, K.; Imamura, Y., *Bull. Chem. Soc. Jpn*., **1989**, *62*, 3421.

18. Berquier, J-M.; Arribart, H., *Langmuir*, **1998**, *14*, 3716.

19. Frantz, P.; Granick, S., *Macromolecules*, **1995**, *28*, 6915.

20. Kabomo, M. T.; Blum, F. D.; Kulkeratiyut, S.; Kulkeratiyut, S.; Krisanangkura, P., *J. Polym. Sci. B: Polym Phys*, **2008**, *46*, 649.

21. Porter, C. E.; Blum, F. D., *Macromolecules*, **2000**, *33*, 7016.

22. Blum, F. D.; Young, E., N.; Smith, G.; Sitton, O. C., *Langmuir*, **2006**, *22*, 4741.

23. Korn, M.; Killmann, E.; Eisenlauer, J., *J. Colloid Interface Sci*., **1980**, *76*, 7.

24. Yamagiwa, S.; Kawaguchi, M.; Kato, T.; Takahashi, A., *Macromolecules*, **1989**, *22*, 2199.

25. McFarlan, A. J.; Morrow, B. A., *J. Phys. Chem*., **1991**, *95*, 5388.

26. Johnson, H. E.; Granick, S., *Macromolecules*, **1990**, *23*, 3367.

27. Flick, E. W., Handbook of adhesives raw materials. 2nd ed. Noyes Publications, New Jersey, 1989.

28. Hershkovits, E.; Tannenbaum, A.; Tannenbaum, R., *J. Phys. Chem. C*, **2007**, *111*, 12369.

29. Baker, J. A.; Pearson, R. A.; Berg, J. C., *Langmuir*, **1989**, *5*, 339.

30. Painter, P. C.; Coleman, M. M.; Koenig, J. L., *The theory of vibrational spectroscopy and its application to polymeric materials*. John Wiley & Sons: New York, 1982.

PAPER 3: BOUND FRACTIONS OF METHACRYLATE POLYMERS ADSORBED ON SILICA USING FTIR

*Piyawan Krisanangkura, Alyssa M. Packard, Jacquline Burgher and Frank D. Blum**

Department of Chemistry and Materials Research Center, Missouri University of Science and Technology, Rolla, Missouri 65409-0010, USA

3.1 ABSTRACT

A set of methacrylate polymers was physically adsorbed onto fumed silica and its hydrogen bonding to the silica was monitored using FTIR. The set included poly (alkyl methacrylates), where the alkyl groups were *n*-C_nH_{2n+1} (*n* = 1, 2, 4, and 12) and poly (benzyl methacrylate). A shift in the carbonyl (C=O) vibrational frequency to a lower frequency (approximately 20 cm^{-1}) from that found in the bulk polymer was observed in the adsorbed polymer sample for hydrogen bonded carbonyls. These carbonyl groups were hydrogen bonded through the silanol groups (Si-OH). A series of samples, with different adsorbed amounts (varying from 0.5 to 2.0 mg/m^2) of each polymer was prepared to determine the effect of side-chain length in the H-bonding process. The FTIR spectra of each of the adsorbed methacrylate polymer were obtained and fitted. By taking the ratios of the intensities of the free carbonyl resonances (~1730 cm^{-1}) and the bound carbonyl resonances (~1710 cm^{-1}), the ratios of molar extinction coefficients of bound- to free- carbonyls, X, and the fractions of bound carbonyls, p, were determined. The X values for each polymer were largest for the methyl (shortest side chain) and lauryl

(rubbery) polymer. Bound fractions for the poly(alkyl methacrylate)s were also significantly higher for the methyl and lauryl side chain polymers.

3.2 INTRODUCTION

Composite materials have been extensively studied in order to understand the nature of the properties of systems of interest.[1, 2] Composite materials typically combine some of the advantages of each of the different phases: for example, flexibility, ductility, and processability from the organic phase, plus rigidity and thermal stability from the inorganic phase.[3] These properties not only depend on the properties of individual components, but also upon interfacial interactions. Several studies have reported that the presence of nanosilica in a polymer matrix improved the physical properties,[4, 5] and thermal stability,[6, 7] and the glass transition temperature (T_g) in the composites.[8-10] In some cases, a second T_g was observed at a higher temperature than that of the polymer resin itself.[9, 11] This phenomenon was attributed to the interfacial interactions between the polymer and the surface.

When a polymer is adsorbed on a solid substrate, one may envision different regions of the polymer molecules. One region is that of the polymer at or near the interface with the solid substrate. Due to the restrictions of the polymer on the surface, this part of the polymer would be expected to have reduced mobility, as compared to bulk, if the polymer attaches to the surface. This polymer portion could be considered tightly attached (or tightly bound) to the surface. Another region would be that of the polymer that is next to that tightly bound layer and farther away from the surface. This material would be expected to act more bulk-like. A third region would be that at the air

interface (illustrated in Figure 3.1). The highlighted zone in the figure represents the polymer segments that are tightly bound to the surface (M_b). The polymer segments beyond that zone could move more freely. If the interaction between the polymer matrix and the surface was strong and attractive, the T_g of the polymer at the interface would be elevated,[12] probably resulting in increased thermal stability of the composite.[13] The changes in the T_g and other properties depend upon several factors, such as the nature of the polymer and filler, as well as the amounts of each, and the type of interactions between them.

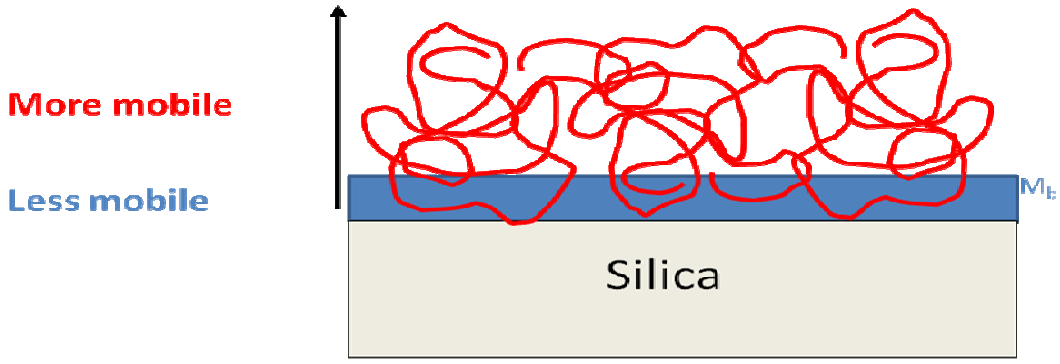

Figure 3.1. Schematic of a polymer adsorbed on a silica surface. The region labeled Mb corresponds to the polymer segments that can be considered tightly bound.

A polymer can undergo adsorption onto a surface via bond formation (either chemical or physical) between the polymer and a solid surface. The strength of the interaction depends upon the nature of the bonding, and the number of points that the polymer can anchor onto the surface. Those properties vary with the types of polymers, as well as substrates. Materials with high specific surface (like fumed silica) are commonly used as a filler. Fumed silica has an extremely large specific surface area, consisting of numerous silanol groups on its surface. These silanol groups can form

hydrogen bonds with a polymer containing functional groups, such as carbonyls like those on acrylate or methacrylate polymers. This interfacial interaction can be monitored by using a technique such as FTIR.

FTIR is a versatile and simple method that can be applied in various ways for studies of polymers. It is used in the polymer field primarily to characterize and identify polymers.[14, 15] FTIR has also been exploited for physical studies of polymers, including measurement of polymer chain conformation and orientation,[16-19] crystallinity, and to determine the T_g of polymers.[20, 21] The utility of FTIR is not limited to bulk polymers, but polymer composites can also be characterized.[22, 23] Quantitative FTIR permits a detailed analysis of many quantities, such as composite composition. A quantitative analysis, however, requires knowledge of a number of parameters as well as calibrations, and the necessary parameters are sometimes difficult to determine. Kulkeratiyut et al.[24] developed a technique of using FTIR to measure adsorbed carbonyls in adsorbed poly(methyl methacrylate) (PMMA).

This work was focused on studying the effect of the nature of the side chains of methacrylate polymers on their adsorption onto silica. For methacrylate polymers, which contain carbonyl groups on the side chains, adsorbed on a silica surface (Figure 3.2), the interfacial interaction is hydrogen bonding between carbonyls on the polymer side chains and silanols on the silica surface, as illustrated in Figure 3.3. Those carbonyls that undergo the hydrogen bonding with silanols (bound carbonyls), can be monitored using FTIR.[25-27] In this study, the R group shown in Figure 3.2 was varied for *n*-C_nH_{2n+1} with n = 1, 2, 4, and 12, and a benzyl group. Then, the fraction of bound carbonyls, p, are compared to determine the effect of the R groups.

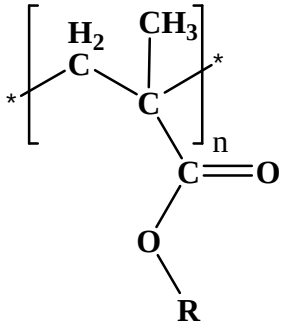

Figure 3.2. The structure of the methacrylate polymers used here where R = methyl, ethyl, n-butyl, dodecyl (lauryl), and benzyl groups.

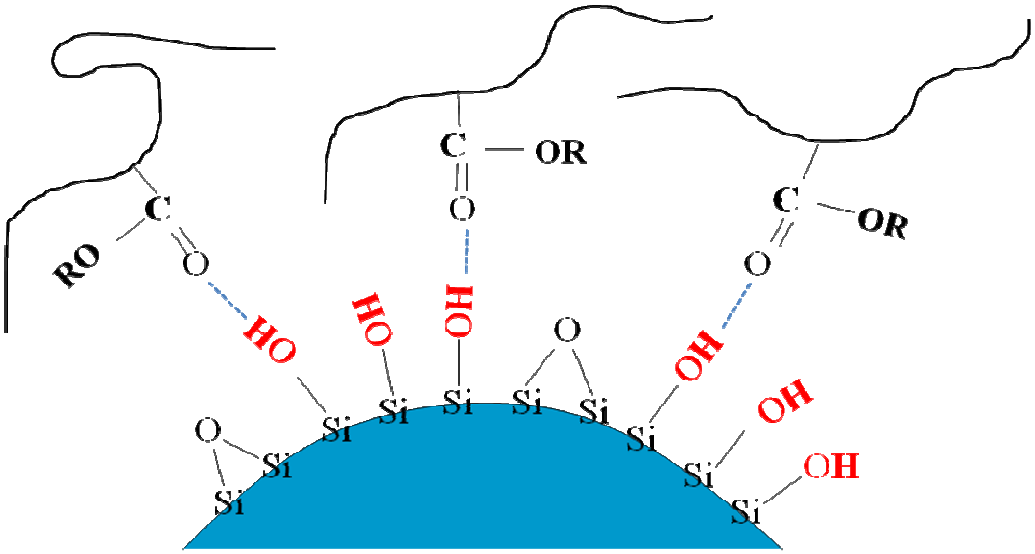

Figure 3.3. Schematic diagram of the hydrogen bonding of the methacrylate polymers with silanol groups residing on an adjacent silica particle.

3.3 EXPERIMENTAL

3.3.1. Materials. The methacrylate polymers studied were purchased from the Aldrich Chemical Co. Ltd. (Milwaukee, WI), and used as received. The molecular mass and polydispersities were determined using a DAWN EOS Light Scattering Instrument (Wyatt Technology, Santa Barbara, CA) and OPTILAB DSP Interferometer Refractive

index detector. The methacrylate polymers used in this study are listed in Table 3.1, along with their glass transition temperatures (T_gs). Cab-O-Sil M-5P fumed silica (Cabot Corp., Tuscola, IL), with a specific surface area of 200 m^2/g, was used as the substrate. The silica, a very high hygroscopic material, was dried at 450 ºC, for at least 24 h before use, in order to eliminate moisture. The dried silica was kept in a vacuum desiccator afterward. Toluene (HPLC grade, Fisher Scientific, Pittsburgh, PA) was used as received as the solvent.

Calorimetric measurements of the bulk polymers, except PLMA, were made using a modulated differential scanning calorimeter (MDSC, TA Instruments, New Castle, DE), with a modulation rate of ± 1 ºC per 60 s and a heating rate of 3 ºC/min. Scan ranges varied from ± 40 ºC from the expected T_g of each polymer. The estimated T_g of PLMA in Table 3.1 was from the report value in the polymer handbook.[28]

Table 3.1. Some properties of the polymers studied

Polymer	M_w (kDa)	PD[a]	*dn*/*dc* (mL/g)[b]	T_g (°C)
Poly(methyl methacrylate) (PMMA)	90	1.6	0.088	110
Poly(ethyl methacrylate) (PEMA)	400	1.65	0.051	65
Poly(n-butyl methacrylate) (PnBMA)	430	1.98	0.046	30
Poly(lauryl methacrylate) (PLMA)	160	2.84	0.120	-70
Poly(benzyl methacrylate) (PbenzylMA)	170	2.28	1.41	55

[a] Polydispersity index (M_w/M_n)
[b] In THF

3.3.2. Adsorption. A series of methacrylate polymer solutions at various concentrations was prepared. From Table 3.1, the molecular masses of polymer studied were quite different; however, the bound fraction was independent with the polymer molecular mass.[24] The clear polymer solutions were added to separate test tubes (with caps) with each containing about 0.3 g of Cab-O-Sil M-5P silica. After shaking the tubes in a mechanical shaker for 72 h, the test tubes (with the mixture of polymer solution and silica) were centrifuged at 2500 rpm for 1 h and the clear supernatants were decanted. The translucent gels (wet) samples were dried by blowing air through capillary tubes onto the wet samples until the gel became dry dull white powders. All adsorbed silica samples were placed in a vacuum oven at 60 ºC for 36 h, for final drying. The amounts of polymer adsorbed on silica were determined using thermogravimetric analysis with a TGA 2950 (TA Instruments, New Castle, DE). The adsorbed samples were heated to 750 ºC with a ramp rate of 20 ºC/min. The polymer content (organic compound) was completely burned off by 400 ºC. The amounts of adsorbed methacrylate polymers were calculated based on mass differences with and without adsorbed polymer.

3.3.3. FTIR Method. A small amount (approximately 1-2 mg) of dried sample powder with adsorbed polymer was spread evenly onto a 2.3 cm KBr disk, and then covered with another KBr disk. The two KBr disks were gently clamped together with a holder to keep the sample between them. FTIR spectra of the adsorbed methacrylate polymer on silica were collected with a Nicolet Nexus 470 Fourier Transform Infrared spectrometer (Nicolet Instruments, Madison, WI). Due to the small polymer-silica particles of the sample studied here, the IR signals did not scatter enough to significantly interfere with the measurement, and the samples appeared to obey the Beer-Lambert law.

FTIR spectra from samples, with different adsorbed amounts in each polymer set, were recorded with a 4 cm^{-1} resolution. The spectra were processed by OMINC EZ software. Curve fitting was done for the carbonyl peaks in all spectra using GRAMS32 software (Thermogalactic, Salem, NH).

3.3.4. Model. If M_t is defined as the total amount of adsorbed polymer, and M_b is the mass of polymer segments with bound carbonyls, the bound carbonyl fraction, p, can be expressed as the following equation.

$$p = \frac{M_b}{M_t} \tag{3.1}$$

The model proposed is the same as that developed by Kulkeratiyut et al.[24] The method is outlined here because the fitted parameters are relevant to the current study. The fraction, p, varies with the adsorbed amount, M_t. The mass of bound carbonyls, M_b, is limited by the number of functional groups on the surface, silanol groups in this case. All silanol groups at the surface are not necessarily hydrogen bonded to the polymer. M_b, may also depend upon the type of polymer. In addition to a certain amount of adsorbed polymer, the number of H-bonds (and consequently, M_b) is fixed for a particular system. The rest of the carbonyls would be unbound or free carbonyls, represented by M_f. These bound- and free- carbonyls are distinguishable by FTIR.[29] The value of M_b represents a pseudo-layer (not a real separable layer) of only bound carbonyls.

In absorption spectroscopy like FTIR, the Beer-Lambert law (Equation (3.2)) is generally applied for quantitative analysis in the linear range. The absorbance, A, is proportional to the molar absorption coefficient, sometimes called the specific

absorptivity, α, the path length of light through the sample or sample thickness, b, and the concentration of the sample, C, or

$$A = \alpha bC \tag{3.2}$$

The absorbance of free- and bound carbonyls can be expressed as,

$$A_f = \alpha_f bC_f \tag{3.3}$$

$$A_b = \alpha_b bC_b \tag{3.4}$$

where subscripts f and b are defined as free-, and bound- carbonyls, respectively.

From Equation (3.3) and (3.4), the specific absorbance for both free- and bound-carbonyls was required to determine the fractions of methacrylate polymers that were bound on silica. Without separate calibration, the absorption coefficients of the carbonyls were difficult to determine because of the nature of the sample. Since these parameters were difficult to determine independently, the ratio of the two absorbances: A_b and A_f, were determined and used. In these terms, the bound fraction of carbonyls can be rearranged as

$$p = (\frac{A_b}{\alpha_b})[\frac{1}{A_b/\alpha_b + A_f/\alpha_f}] \tag{3.5}$$

Equation (3.5) has two parameters, α_b and α_f, which were not independently determined and, therefore, they were reduced to a ratio, X ($=\frac{\alpha_b}{\alpha_f}$). Then p can be expressed as

$$p = \frac{A_b/X}{A_b/X + A_f} \tag{3.6}$$

which requires knowledge of the absorption intensities and X. Equating the right hand side of Equation (3.1) with (3.6), and rearranging them yielded a linear relationship between M_t and the ratio of absorption intensities, or

$$M_t = M_b + \frac{A_f}{A_b} XM_b \qquad (3.7)$$

From a series of measurements at different adsorbed amounts, X and M_b were determined from the slope and intercept of a plot of A_f/A_b against M_t.

3.4 RESULTS

The FTIR spectra of each adsorbed methacrylate polymer sample, at about 1.0 mg polymer/m^2 silica and pure Cab-O-Sil M5P silica, are shown in Figure 3.4. The vertical scales of the spectra were adjusted for clarity. In the Cab-O-Sil M5P silica spectrum (bottom), a big broad intense band at 1000 – 1300 cm^{-1} corresponds to the vibration of Si-O groups on silica. A small, but sharp resonance at 3750 cm^{-1} was due to unassociated (isolated) hydroxyl groups on the silica surface.[30] This resonance became less intense when the adsorbed amounts increased, and eventually disappeared at some adsorbed amounts, indicating that the free or isolated silanol groups on the surface were completely occupied. A broad resonance was centered at about 3400 cm^{-1} due to the presence of small amounts of moisture.

In spectra of samples with adsorbed polymer, resonances from the polymers were also observed, along with those from the silica. The resonances (around 2800 – 3000 cm^{-1}) were from the CH or CC stretching of $–CH_3$, $-CH_2$, and –C=C-; their intensities and structures varied roughly with side chain length. The polymers with longer alkyl groups showed a stronger absorption at 2900 cm^{-1} ($-CH_2$ stretching). The most intense $–CH_2$

resonance was for poly(lauryl methacrylate) (PLMA) because that species has many -CH_2s. For poly(benzyl methacrylate) (PBenzylMA), the peaks at 3000 – 3050 cm^{-1} were from the aromatic species. For the spectra from the adsorbed samples, the apparent broad resonance centered at approximately 3650 cm^{-1} was assigned to the hydrogen bonded hydroxyl groups.[30] The last major peak, observed in adsorbed samples, was the carbonyl peak at approximately 1705 – 1730 cm^{-1}, depending on the types of carbonyls and their environment.

The carbonyl stretching region for each of the adsorbed polymers was expanded (shown in Figure 3.5). Two resonances were clearly found to overlap for each adsorbed polymer. By comparing the resonance frequency of the bulk polymer vibration, it was apparent that the peak centered at ~1730 cm^{-1} in the adsorbed sample represented the free or unassociated carbonyls. The other FTIR band, at the lower wavenumber (roughly at 1710 cm^{-1}), was from the carbonyl groups that were bound to the silica surface.[26, 31]

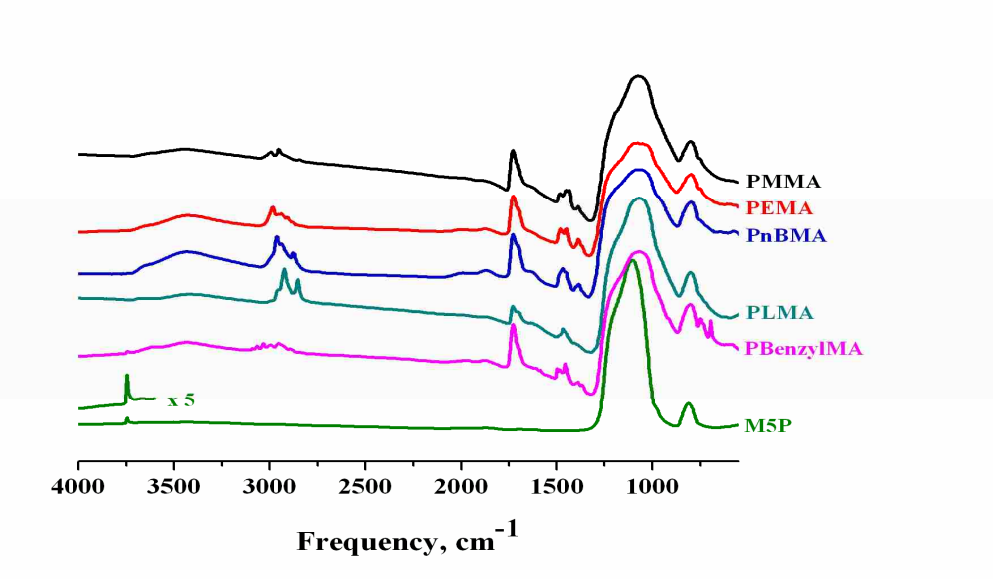

Figure 3.4. FTIR spectra of methacrylate polymers adsorbed on Cab-O-Sil M5P and pure silica. The approximate adsorbed amount for each sample was 1.0 mg/m^2. The spectra are shifted and scaled on the absorbance axis for clarity.

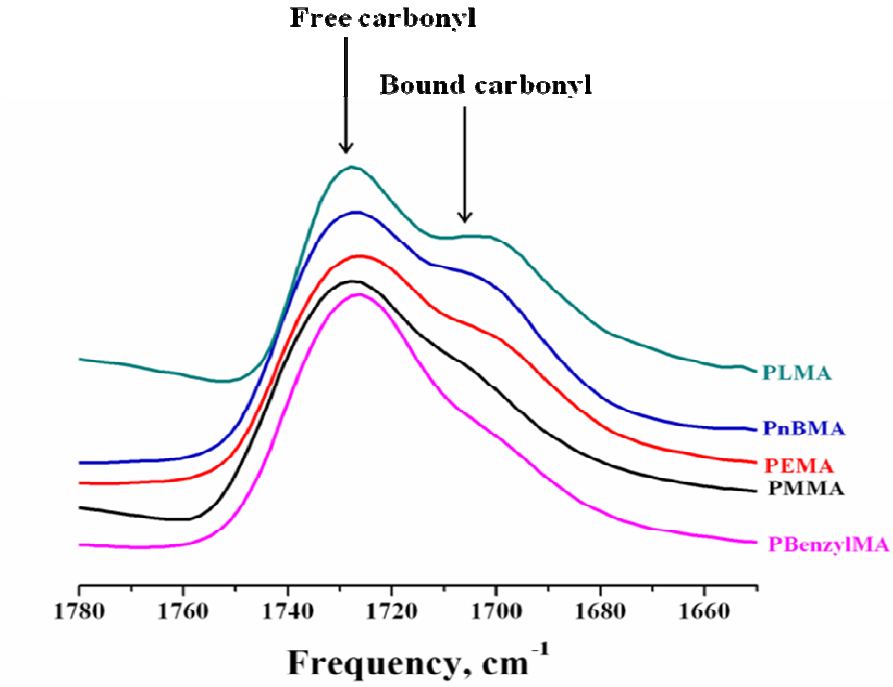

Figure 3.5. FTIR spectra of the adsorbed methacrylate polymers in the carbonyl stretching region. The adsorbed amounts were roughly 1.0 mg/m^2.

The FTIR spectra of three different amounts of adsorbed and bulk PLMA, are shown in Figure 3.6. The relative intensities of the bound carbonyls, compared to the free carbonyls, decreased with an increase in the PLMA adsorbed amounts. The decrease in the relative intensity of the bound carbonyl resonance was due to the smaller fraction of bound carbonyls.

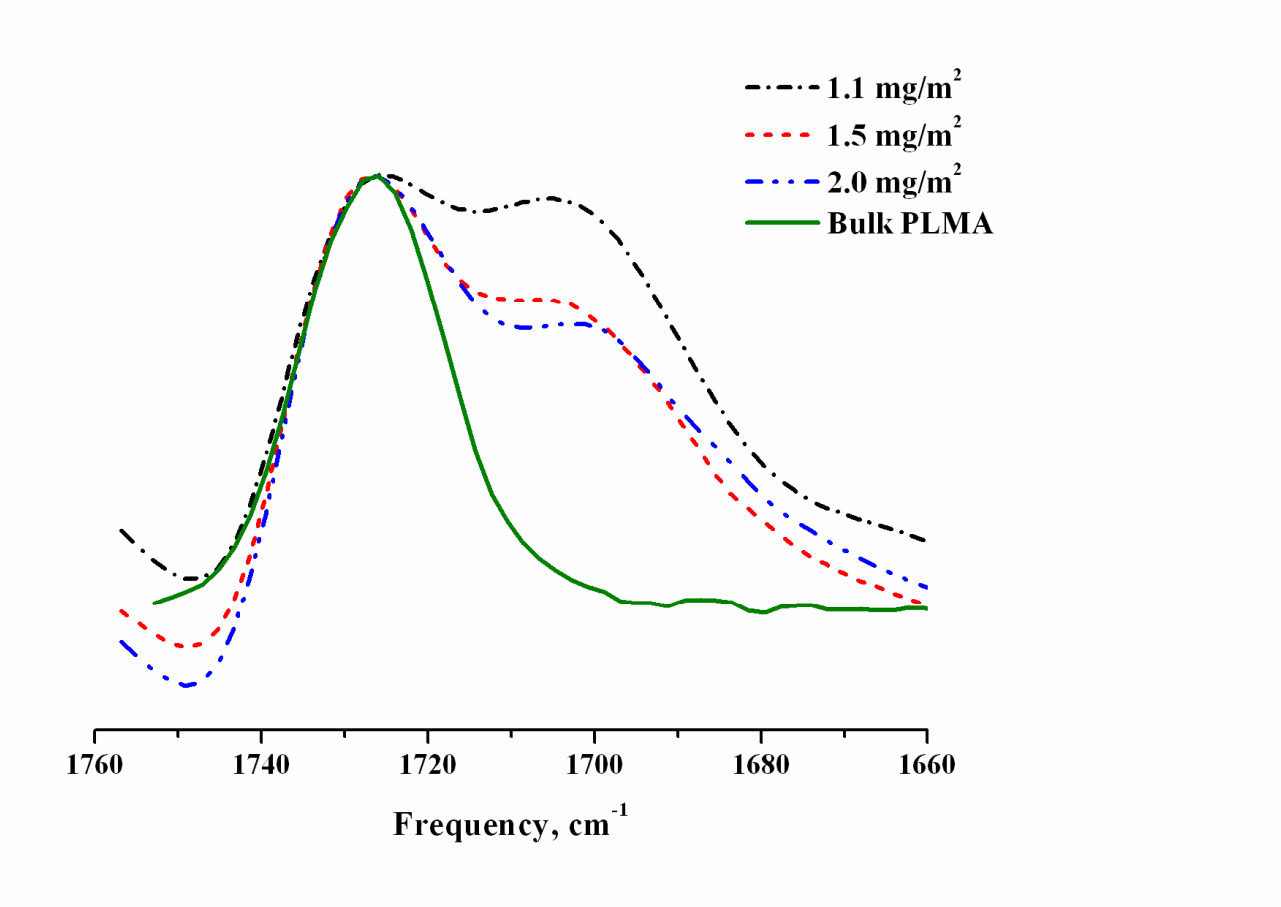

Figure 3.6. FTIR spectra of poly(lauryl methacrylate) (PLMA) as a function of the adsorbed amount and bulk polymer.

An example of the results of carbonyl peak fitting is demonstrated in Figure 3.7. Each free and bound carbonyl peak for the adsorbed methacrylates was fitted individually using a Gaussian lineshape by GRAMS32 to get the best fitted curves. The curve fitting with two components gave a good result for these systems. The fittings were performed in the same manner for all methacrylate polymers at different adsorbed amounts. Determination of peak locations and integration of areas under the peaks of each type of carbonyl were optimized by the software. The peak positions of free and bound carbonyls for each polymer are reported in Table 3.2.

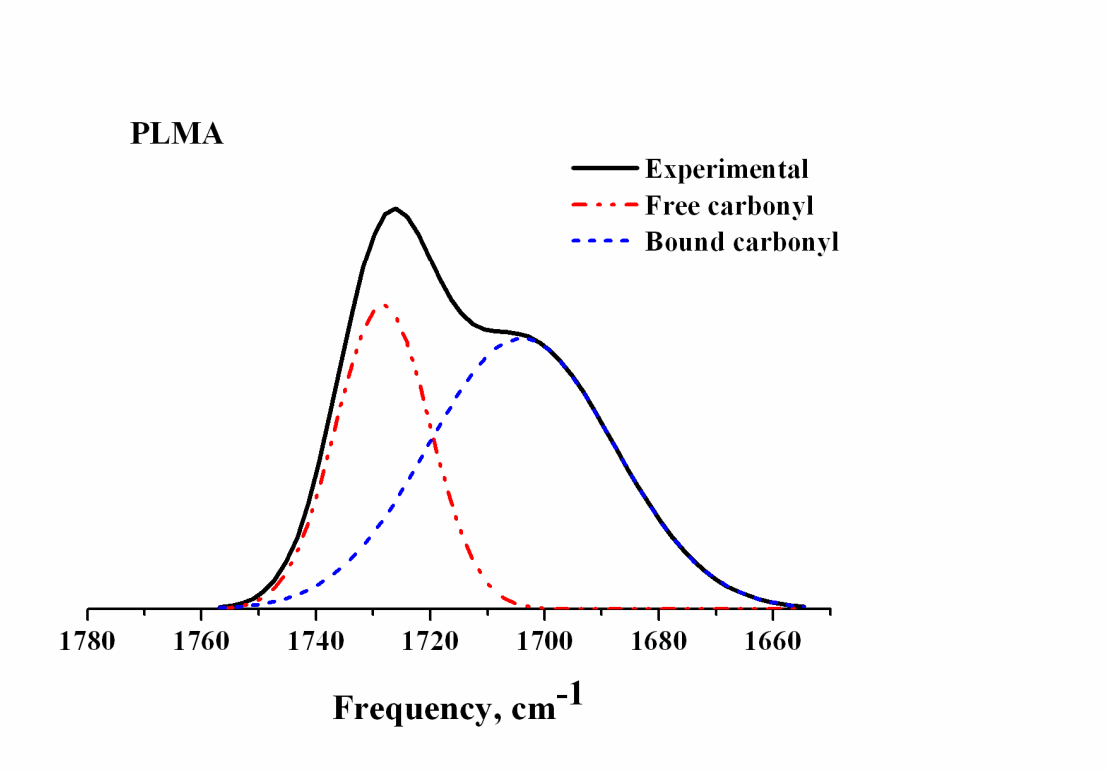

Figure 3.7. Gaussian lineshape fitted carbonyl peaks of 2.0 mg/m^2 adsorbed PLMA by GRAMS32.

Table 3.2. The FTIR resonances of free and bound carbonyl stretching for methacrylate polymers

	Carbonyl stretching frequency (cm^{-1})	
Polymer	**Free**	**Bound**
PMMA	**1736**	**1713**
PEMA	**1731**	**1707**
PnBMA	**1730**	**1706**
PLMA	**1729**	**1706**
PBenzylMA	**1730**	**1707**

By taking the ratios of integrated peak areas of free- (A_f) to bound- (A_b) carbonyls, the ratios of the molar absorptivities for the methacrylate polymers could be calculated from plots of the A_f/A_b as a function of the adsorbed amounts of polymer, M_t. The plots for all methacrylate polymers (with adsorbed amounts up to 2.0 mg/m^2) are

displayed in Figure 3.8. The least square fits were done to calculate X and M_b from Equation (3.7) using Mathematica (Wolfram Research, Inc. Champaign, IL). The calculated best fits for X and M_b are listed in Table 3.3. The uncertainties are given based on ±1 standard deviation of the slopes and intercepts.

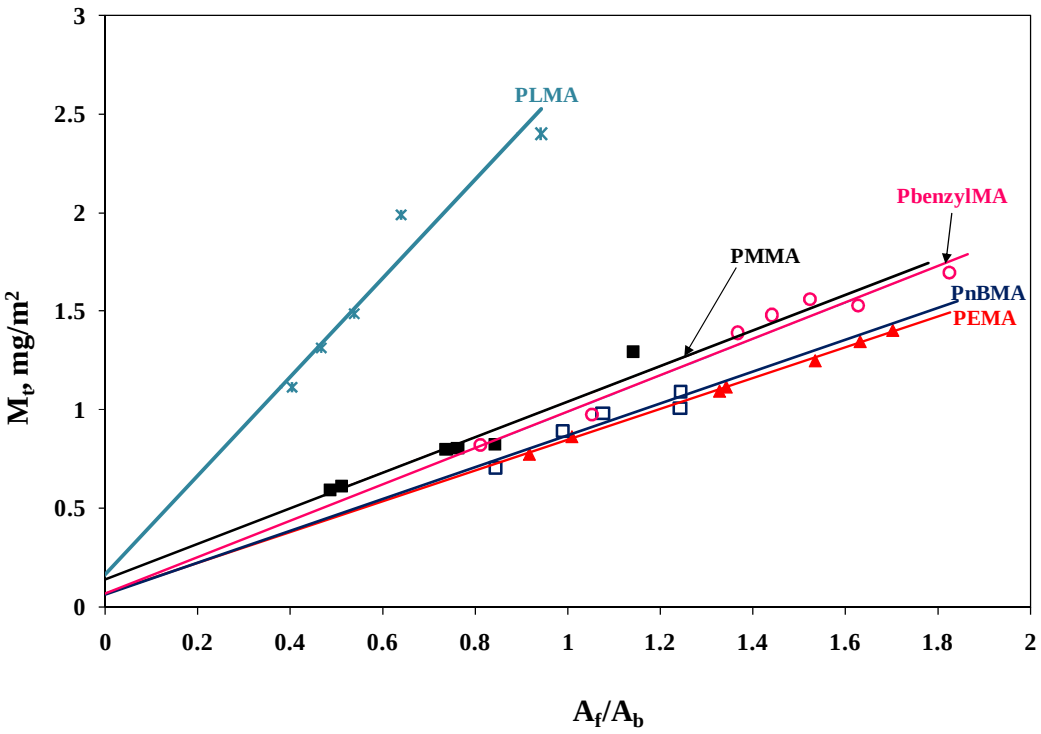

Figure 3.8. Ratios of resonance intensities of free- to bound- carbonyls (A_f/A_b) as a function of the adsorbed amount of polymer for different methacrylate polymers.

Table 3.3. Ratios of the molar extinction coefficients of bound- to free- carbonyls (X) and the calculated masses of methacrylate polymer with bound carbonyls (M_b).

Polymer	X	M_b (mg/m^2)
PMMA	**5.8 ± 1.0**	**0.155 ± 0.023**
PEMA	**10.4 ± 2.5**	**0.076 ± 0.019**
PnBMA	**12.1 ± 4.1**	**0.068 ± 0.023**
PLMA	**11.1 ± 2.9**	**0.213 ± 0.055**
PBenzylMA	**11.8 ± 2.2**	**0.072 ± 0.014**

3.5 DISCUSSION

Frequency shifts with adsorption of polymer were clearly observed for both hydroxyl and carbonyl vibrations. The hydrogen bonds between carbonyls in methacrylate polymers and silanols on a silica surface were detected at approximately 3650 and 1710 cm^{-1} for hydroxyl and carbonyl regions, respectively. Upon adsorption, the intensity of the free silanol peak at 3750 cm^{-1} was also reduced or eliminated due to the hydrogen bonding. This suggests that almost all of the free silanol groups were accessible to the polymers. Therefore, it may be tentatively concluded that hydrogen bonding is part of the adsorption of the polymer on the silica surface.

The carbonyl stretch is particularly useful in analyzing the hydrogen bonding of the polymer to the silica. Using the carbonyl stretch for quantization is advantageous due to the relatively intense resonances, and there are no spectral interferences from moisture, as in the hydroxyl region. The carbonyl stretch region (Figure 3.5) clearly shows that two types of carbonyl resonances overlapped. The variation of the carbonyl resonances at different adsorbed amounts suggested that the resonance at approximately 1730 cm^{-1} corresponded to the unassociated carbonyl groups, whereas the peak at near 1710 cm^{-1} was assigned to the bound carbonyl groups.[26, 32] The center of the resonances varied depending upon the polymers, as listed in Table 3.2. The peak positions were slightly different from those in the literature due to different experimental conditions.[24, 26, 32] For the bound carbonyl peaks, a shift was found to be approximately 20 cm^{-1} lower than the bulk resonance for the bound carbonyl peak. The shift to a lower frequency was due to the electron donating groups release of electrons to the antibonding orbital of the carbonyl, because the hydrogen bonding weakened the carbonyl double bond.[14]

The intensities of the bound carbonyl resonances varied with the amount of the polymer adsorbed. The intensities of the bound carbonyl resonance became smaller with an increase in the adsorbed amounts of the polymers (Figure 3.6), which implied that there were fewer bound carbonyl groups (compared to free carbonyls) when the adsorbed amounts increased. The plots of A_f/A_b versus the adsorbed amount gave a line with a positive slope and intercept. This tendency appeared to be the same for all methacrylate polymers, but the slopes of the plots varied with the types of polymers, as depicted in Figure 3.8. The molar absorption coefficient ratios (X) and the masses of polymer segments with bound carbonyls (M_b) were determined from the slopes and the intercepts of each plot (Table 3.3). The X values of the polymers did not appear to show an obvious pattern, although the M_b values for the methyl and lauryl methacrylate seemed larger than the others.

At the first approximation, all of the M_bs were similar and around 0.1 mg polymer/m^2 silica. More detailed inspection roughly showed that the M_b of the polymethacrylates varied with the size of the side chain, except PLMA. The smallest side chain group (methyl), PMMA, had a larger M_b than PEMA, PnBMA, and PBenzylMA. The M_b of PEMA, PnBMA, and PBenzylMA were quite similar, suggesting a similar effect from these side chains. Unexpectedly, the longest side chain of the methacrylate polymer in this study, PLMA, had the highest M_b of 0.213 mg/m^2 ± 0.055. However, PLMA has a bulk T_g of -70 ^oC, which means that it was in a rubbery state at room temperature. The rubbery polymers move more freely than the glassy ones. One might expect that the polymer chain would be more flexible, and could get closer to the silica

surface, yielding more bound segments in the interfacial polymer, and have a smaller A_f/A_b ratio.

Several studies of polymethacrylates, especially PMMA, adsorbed on a silica surface have been conducted. It was worthwhile to compare the results of X and M_b from this work to those of others. The X and M_b of PMMA found in this study were 5.8 ± 1.0, and 0.155 ± 0.023 mg/m^2, respectively. Granick and coworkers[33] used ATR-FTIR to study the adsorbed PMMA in the presence of solvents (CCl_4). Their X ratio was in the range of 1 to 2. The intensity of ATR-FTIR experiments, however, was expected to be different than that in transmission FTIR. With spectral subtraction, M_b of 0.14 mg/m^2 was estimated by Johnson and Granick.[27] Kulkeratiyut et al.[24] estimated the X to be 7.7 ± 1.5 and M_b as 0.17 ± 0.04 mg/m^2 for dried samples, which is within the experimental error of this work. In the latter study, the suspended adsorbed polymer was used for casting film for FTIR measurement, yielding the difference in the ratio X. Those conditions affected the results of the ratio X and M_b, leading to the different bound fractions, p. In any case, we concluded that the X ratio for the surface adsorbed sample was greater than that in the presence of the solvents.

The bound fractions, p, for all methacrylate polymers studied, were estimated based on the model in Equation (3.6) with the calculated Xs, and plotted as a function of the total adsorbed amounts, M_t. The relationship of bound fractions (shown in Figure 3.9) was based on the assumption that each polymer with adsorbed amounts above their M_b threshold was free (Equation (3.1)). The data points fit the model well for all samples. The value of p, obviously decreased with increasing adsorbed amounts. It was obvious

that the bound fractions for PMMA and PLMA were much greater than those for the others.

The data from this paper was also compared to that for PMMA from the work of Kulkeratiyut et al.[24] using their M_b of 0.17 mg/m^2. Their data showed slightly higher bound carbonyl fractions than the data from this work did, possibly because of different methods of sample preparation. The difference, however, is within acceptable experimental error. The fraction, p, of PEMA and PBenzylMA showed little difference, although it was slightly lower for PnBMA. This may mean that the size of the side chains that were larger than those of the methyl group had little effect.

In contrast to the other samples, PLMA, the methacrylate polymer with the longest alkyl groups (C_{12}) in this study, had the highest bound fractions. This phenomenon could not be simply explained by the side chain length. Other factors, such as the T_g of the polymer, might have accounted for this difference. Nonetheless, the bound fractions of PLMA were much smaller than the ones investigated by Fontana and Thomas.[26] In their work, the ratio X was assumed to be 1, although solvent was present (the samples were measured in gel form). Even though a solvent was present in their study, X could most likely have been expected to be greater than 1 (but probably not as high as 12). We believe that their bound fractions are abnormally high and that, if their bound fractions are correct as reported, a greater number of carbonyls would have to be hydrogen bonded than there are silanols to hydrogen bond with. In any case, a higher ratio X would be more consistent with our work.

The number of moles of bound carbonyl for the methacrylate polymers were estimated based in this work. The calculations were based on the surface silanols and

carbonyl groups available for H-bonding. Generally, surface silanols found in fumed silica (like Cab-O-Sil) are in the range of 2.5 – 3.5 OH/nm^2.[34, 35] Not all of those surface silanols, however, can undergo H-bonding. Morrow et al. reported that 1.4 OH/nm^2 were able to react with hexamethyldisilazane (HMDS) for Cab-O-Sil HS5 (surface area of 325 m^2/g). The number of surface silanols that could undergo the reaction with HMDS would be roughly the same for H-bonding with methacrylate polymers. The value of 1.4 OH/nm^2 for surface silanols, which corresponds to a surface concentration of 2.3×10^{-6}, therefore, was used in the calculation. It was assumed that each silanol only H-bonded with one carbonyl. The number of moles of the carbonyl groups of approximately 1 mg polymethacrylates/m^2 that were bound to the surface silanols are summarized in Table 3.4.

Table 3.4. The number of bound carbonyls for the methacrylate polymers.

Polymer	Adsorbed Amount, mg/m^2	No. of carbonyls, mol/m^2	p	No. of bound carbonyl, mol/m^2	H-bonded silanol, %
PMMA	0.81	8.10×10^{-6}	0.155	1.25×10^{-6}	54
PEMA	1.10	9.63×10^{-6}	0.076	7.30×10^{-7}	31
PnBMA	0.98	6.89×10^{-6}	0.062	4.30×10^{-7}	18
PLMA	1.12	4.40×10^{-6}	0.19	8.38×10^{-7}	35
PBenzylMA	0.98	5.56×10^{-7}	0.075	4.18×10^{-8}	18

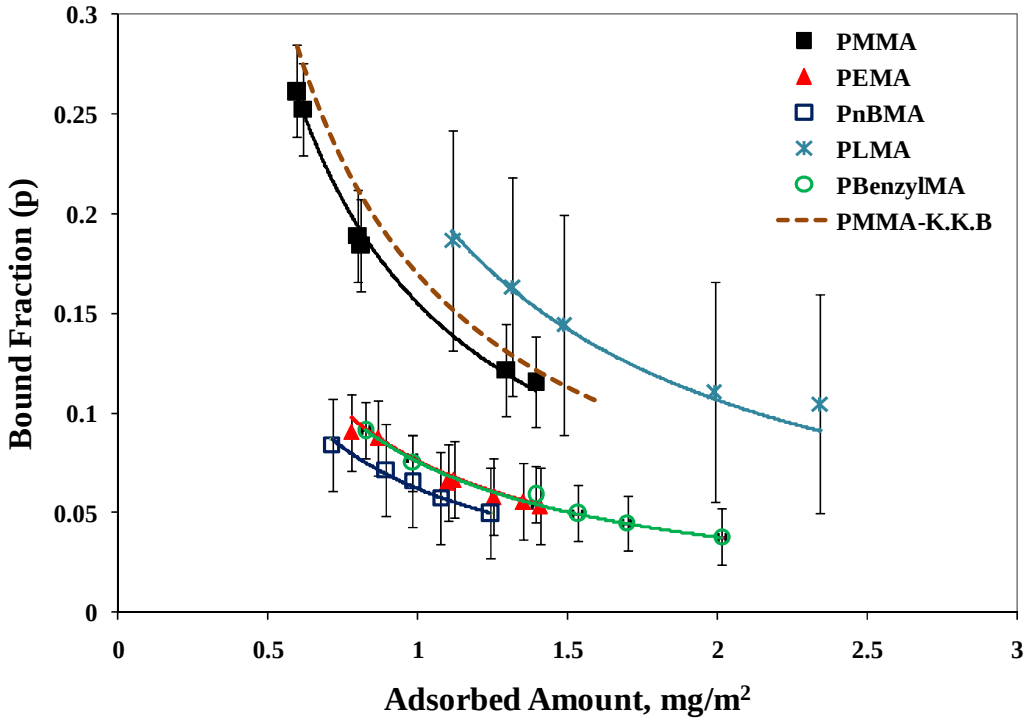

Figure 3.9. Bound fractions, p, of the methacrylate polymers adsorbed on Cab-O-Sil M5P silica as a function of the total adsorbed amounts, M_t. The PMMA-dispersion data is from Kullkeratiyut et al.[24]

The M_b and p can be estimated by using different techniques for probing different parts of the polymer segments. The estimated p curve obtained from MDSC,[9] and ESR[32, 36] are illustrated in Figure 3.10, as a comparison of the results acquired by different methods. For MDSC, the data were calculated from M_b of 1.3 mg/m^2. The M_b obtained from MDSC was considerably higher than the one from FTIR and, consequently, this resulted in much higher bound fractions. The bound fraction curve from ESR was higher than that from FTIR, but slightly lower than that of MDSC. The result from ESR identified the contribution of each polymer segment, including trains, short loops, and long loops. The train contribution could denote the tightly bound segment. The bound segments, however, referred to trains and short loops, according to Fleer and

co-authors.[37] The sum of the contributions of trains and short loops gave a result close to that of MDSC. This difference was due to the various distance scales, to which the experiments are sensitive.[37, 38] The p data attained from FTIR were in the same range as those obtained when they were evaluated on a larger scale (e.g., from MDSC), as demonstrated in Figure 3.10. The MDSC evaluated the adsorption of the entire material, ESR monitors the segments adsorbed in any mechanism, while the FTIR technique is localized on the adsorption of hydrogen bonds between the carbonyl and the silanol only.

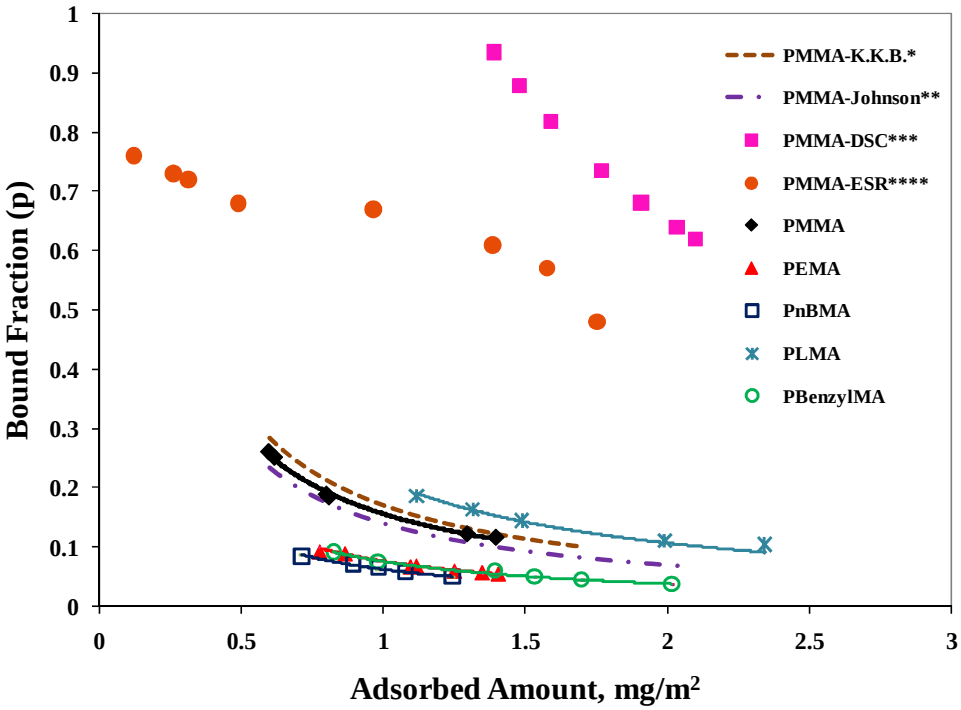

* PMMA from previous study by Kulkeratiyut et al.[24]
** PMMA from ATR-FTIR by Johnson et al.[27]
*** PMMA from MDSC by Blum et al.[9]
**** PMMA from ESR (train contribution) by Sakai et al.[32, 36]

Figure 3.10. The comparison of the bound fractions of the methacrylate polymers on silica using FTIR and other techniques.

3.6 CONCLUSIONS

The determinations of the bound carbonyl fractions in methacrylate polymers were measured by quantitative FTIR using the ratio of the areas under peaks of free- to bound- carbonyl stretching resonances. The amount of polymer bound to the surface varied with the size of the side chains of the polymers. The bound fraction decreased with the length of the side chains, or the more bulky groups, except for PLMA. It appeared that the rubbery PLMA polymer studied had a higher bound fraction than did the glassy polymers, under the same conditions. The fact that the bound fraction obtained from FTIR was smaller than the bound fractions found from MDSC was due to the technique used to probe the hydrogen bonds at the interface only.

Another way to analyze the data would be to conclude that, in the course limit, all of the polymers behaved in more or less the same way. On closer examination, the different polymers showed different behaviors, with PMMA (the shortest side chain) and PLMA (rubbery) having the higher fraction of bound chains. This work verifies that the model proposed and successfully applied to PMMA is also generally applicable to other polymers. We also believe it is consistent with the value of X ($= \alpha_f/\alpha_b$) being significantly greater than unity for hydrogen bonded methacrylates, in the absence of solvent.

3.7 ACKNOWLEDGEMENT

The author would like to thank the National Science Foundation for support provided under grant NSF-0706197, and the Missouri University of Science and Technology for financial support.

3.8 REFERENCES

1. Vaia, R. A.; Maguire, J. F., *Chem Mater* **2007,** 19, 2736.

2. Zou, H.; Wu, S.; Shen, J., *Chem. Rev.* **2008,** 108, 3893.

3. Novak, B. M., Hybrid nanocomposite materials - Between inorganic glasses and organic polymers. *Advanced Materials* **1993,** 5, (6), 422-433.

4. Landry, C. J. T.; Coltrain, B. K.; Landry, M. R.; Fitzgerald, J. J.; K., L. V., *Macromolecules* **1993,** 26, (14), 3702.

5. Reynaud, E.; Jouen, T.; Gauthier, C.; Vigier, G.; Varlet, J., *Polymer* **2001,** 42, (21), 8759.

6. Hsiue, G.-H.; Kuo, W.-J.; Huang, Y.-P.; Jeng, R.-J., *Polymer* **2000,** 41, (8), 2813.

7. Kashiwagi, T.; Morgan, A. B.; Antonucci, J. M.; VanLandingham, M. R.; Harris, R. H.; Awad, W. H.; Shields, J. R., *J. Appl. Pol. Sci.* **2003,** 89, 2072.

8. Porter, C. E.; Blum, F. D., *Macromolecules* **2002,** 35, 7448.

9. Blum, F. D.; Young, E. N.; Smith, G.; Sitton, O. C., *Langmuir* **2006,** 22, 4741.

10. Metin, B.; Blum, F. D., *J. Chem. Phys* **2006,** 124, 054908.

11. Tsagaropoulos, G.; Eisenberg, A., *Macromolecules* **1995,** 28, 396.

12. Porter, C. E.; Blum, F. D., *Macromolecules* **2000,** 33, 7016.

13. Zhang, B.; Blum, F. D., *Thermo. Acta* **2003,** 396, 211.

14. Painter, P. C.; Coleman, M. M.; Koenig, J. L., *The theory of vibrational spectroscopy and its application to polymeric materials*. John Wiley & Sons: New York, 1982.

15. Koenig, J. L., *Spectroscopy of Polymers*. American Chemical Society: Washington, DC, 1992.

16. Grohens, Y.; Prud'homme, R. E.; Schultz, J., *Macromolecules* **1998,** 31, 2545.

17. Tretinnikov, O. N.; Ohta, K., *Macromolecules* **2002,** 35, 7343.

18. Painter, P.; Huang, H., *Macromolecules* **2008,** 41, 2494.

19. Angood, A. C.; Koenig, J. L., *J. Appl. Phys.* **1968,** 39, (11), 4985.

20. Ogura, K.; Kawamura, S.; Sobue, H., *Macromolecules* **1971,** 4, 79.

21. Koenig, J. L.; William, H. W. In *Probing polymer structures*, the 174th meeting of the American Chemical Society Chicago, Illinois, August 29-September 2, 1977, 1979; Koenig, J. L., Ed. American Chemical Society: Chicago, Illinois, 1979; pp 99-139.

22. Urban, M. W.; Koenig, J. L., *Applied Spectroscopy* **1986,** 40, 513.

23. Shin, H. S.; Jung, Y. M.; Oh, T. Y.; Chang, T.; Kim, S. B.; Lee, D. H.; Noda, I., *Langmuir* **2002,** 18, 5953.

24. Kulkeratiyut, S.; Kulkeratiyut, S.; Blum, F. D., *Journal of Polymer Science: Part B: Polymer Physics* **2006,** 44, 2071.

25. Pimentel, G. C.; McClellan, A. L., *The Hydrogen Bond*. W. H. Freeman and company: San Francisco, 1960.

26. Fontana, B. J.; Thomas, J. R., *J. Phys. Chem.* **1961,** 65, 480.

27. Johnson, H. E.; Granick, S., *Macromolecules* **1990,** 23, 3367.

28. Brandrup, J.; Immergut, E. H., *Polymer Handbook*. 3rd ed.; John Wiley &Sons Inc.: New York, 1989.

29. Lee, J. Y.; Painter, P. C.; Coleman, M. M., Hydrogen bonding in polymer blends. 3. Blends involving polymers containing methacrylic acid and ether groups. *Macromolecules* **2002,** 21, (2), 346-354.

30. Morrow, B. A.; McFarlan, A. J., *The Journal of Physical Chemistry* **1992,** 96, 1395.

31. Berquier, J.-M.; Arribart, H., *Langmuir* **1998,** 14, 3716.

32. Sakai, H.; Imamura, Y., *Bull. Chem. Soc. Jpn.* **1980,** 53, 1749.

33. Frantz, P.; Granick, S., *Macromolecules* **1995,** 28, 6915.

34. Morrow, B. A.; McFarlan, A. J., Infrared and gravimetric study of an aerosil and a precipitated silica using chemical and hydrogen/deuterium exchange probes. *Langmuir* **1991,** 7, (8), 1695-1701.

35. Liu, C. C.; Maciel, G. E., The Fumed Silica Surface: A Study by NMR. *Journal of the American Chemical Society* **1996,** 118, (21), 5103-5119.

36. Sakai, H.; Fujimori, T.; Imamura, Y., *Bull. Chem. Soc. Jpn.* **1980,** 53, 3457.

37. Fleer, G. J.; Cohen Stuart, M. A.; Scheutjens, J. M. H. M.; Cosgrove, T.; Vincent, B., *Polymers at Interfaces*. Capman and Hall: London, U.K., 1993.

38. Blum, F. D.; Krisanangkura, P., *Thermochimica Acta* **2009,** 492, 55.

APPENDIX A
CHARACTERIZATION OF SAMPLES STUDIED

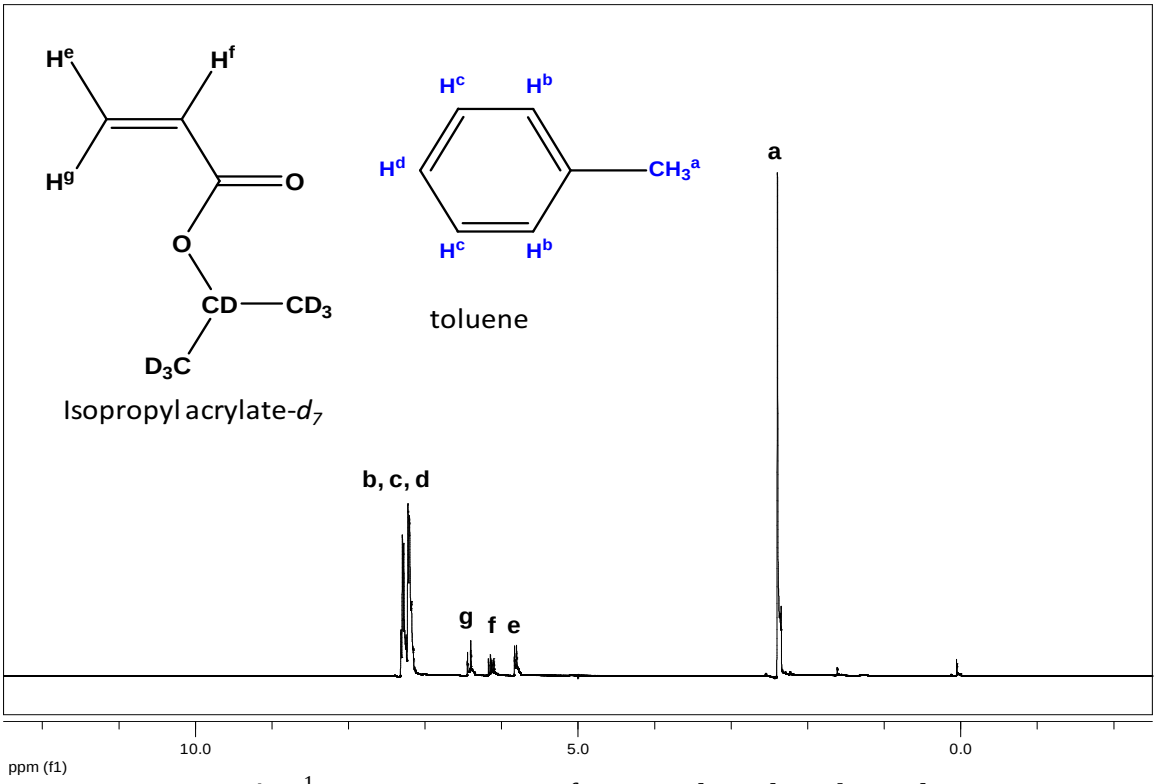

Figure A1. ^{1}H NMR spectrum of isopropyl acrylate-d_7 in toluene.

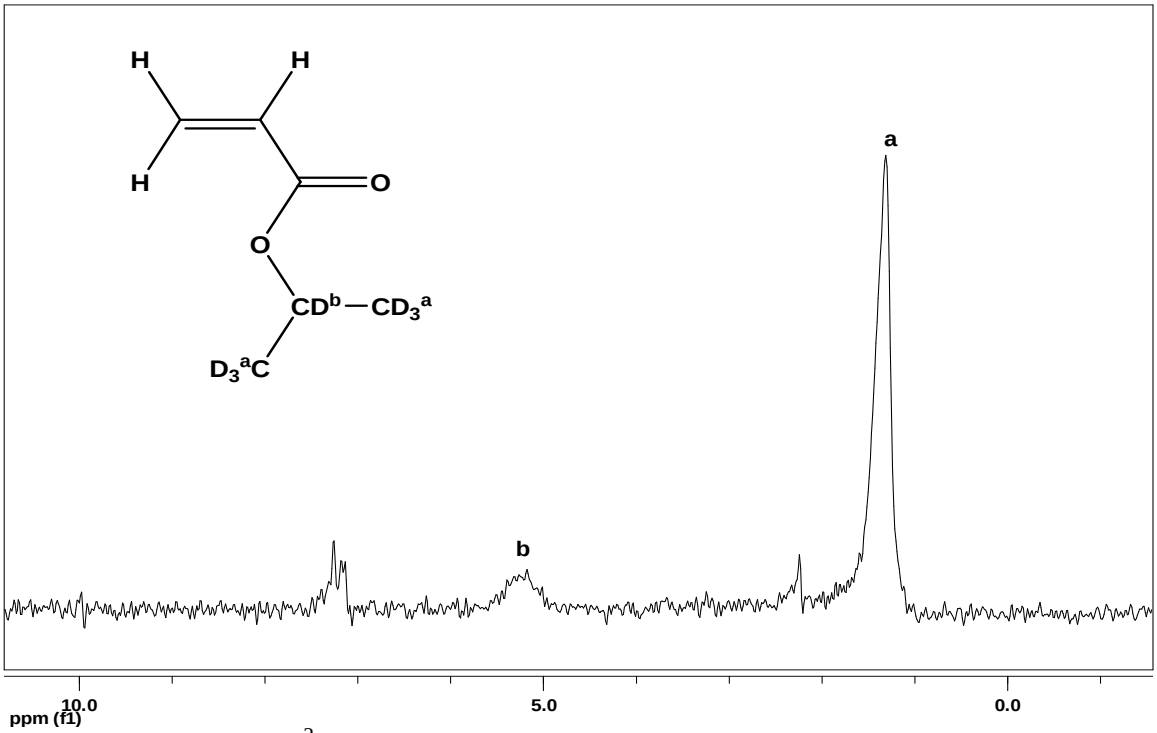

Figure A2. ^{2}H NMR spectrum of isopropyl acrylate-d_7 in toluene.

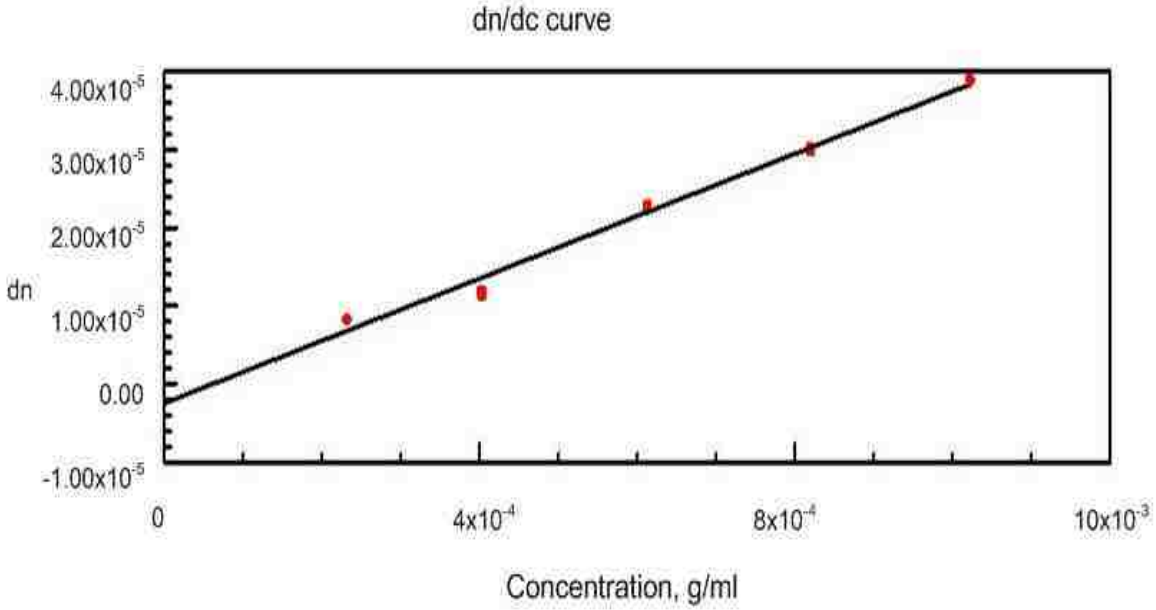

Figure A3. Refractive increment (dn/dc) curve of poly(isopropyl acrylate) in THF measured at 690 nm.

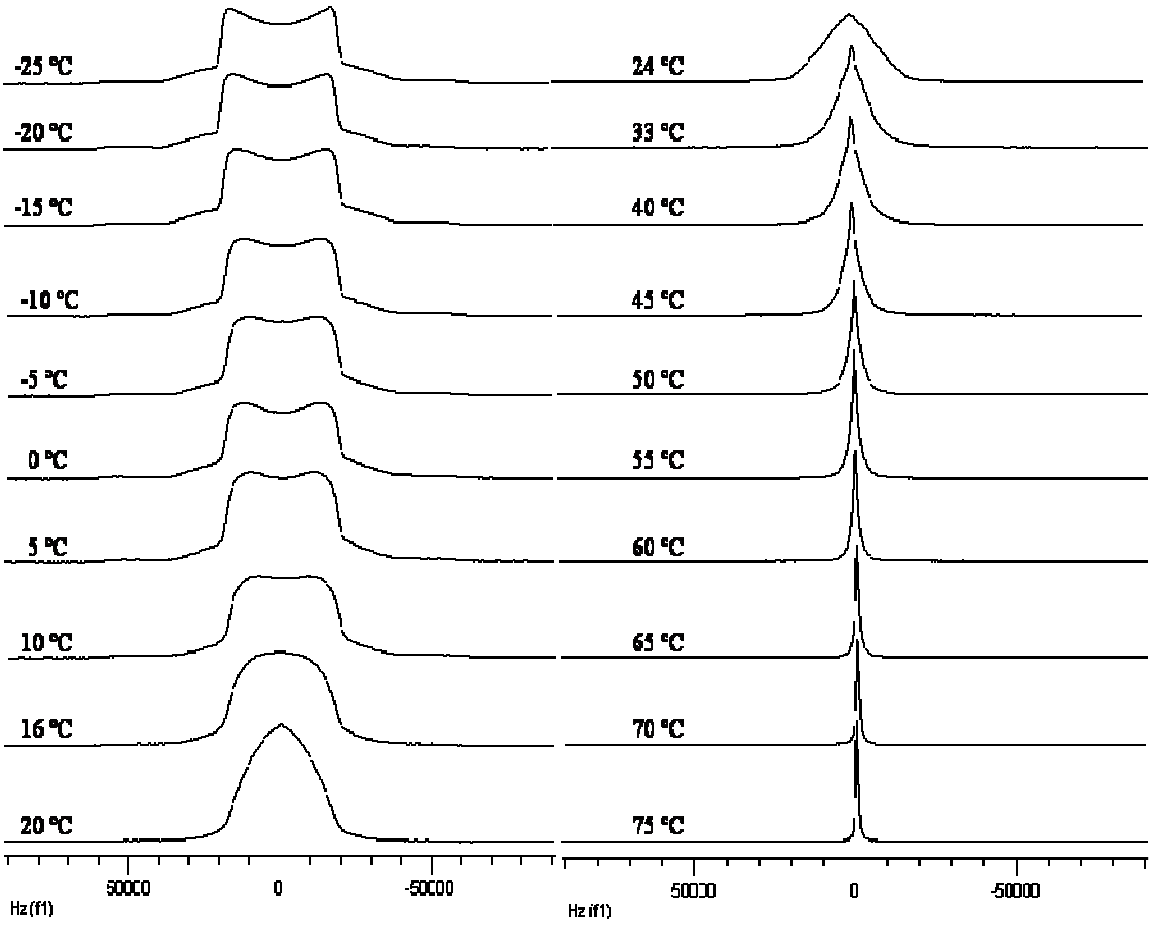

Figure A4. ^{2}H solid-state NMR spectra of bulk PIPA-d_7 as a function of temperature.

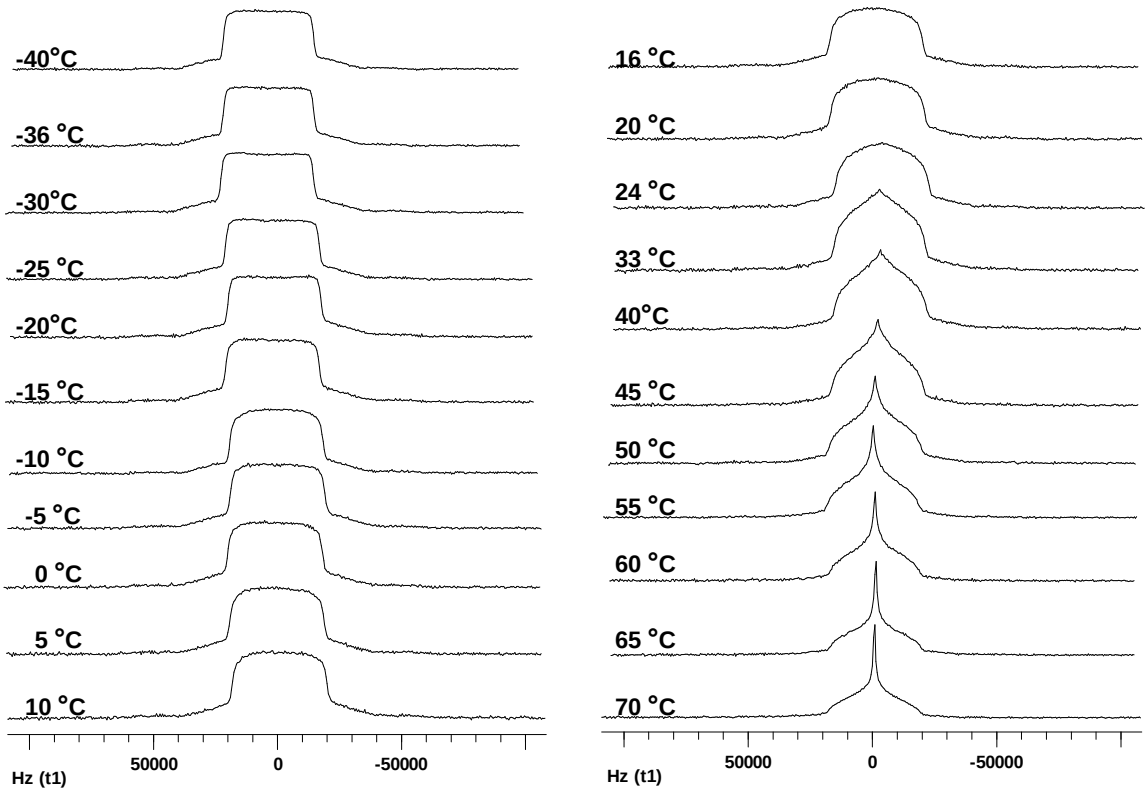

Figure A5. ^{2}H solid-state NMR spectra of 1.02 mg PIPA-d_7 per m^2 silica as a function of temperature.

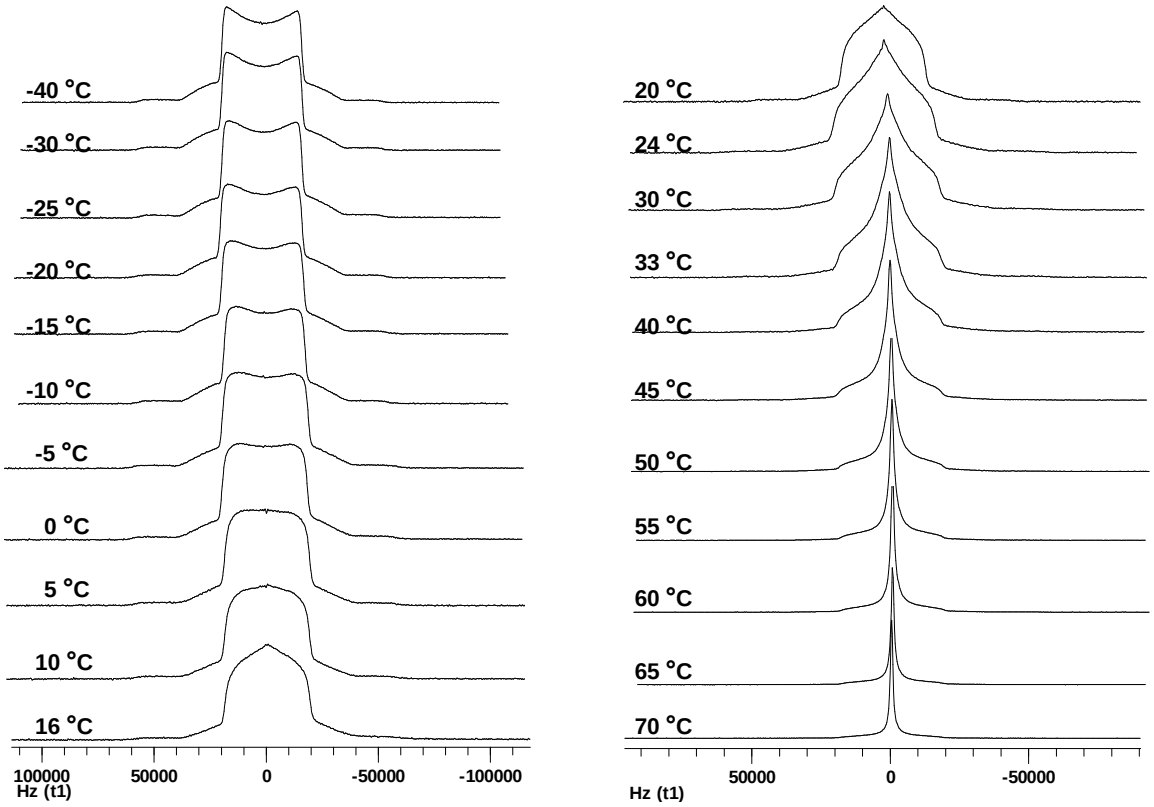

Figure A6. ^{2}H solid-state NMR spectra of 2.34 mg PIPA-d_7 per m^2 silica as a function of temperature.

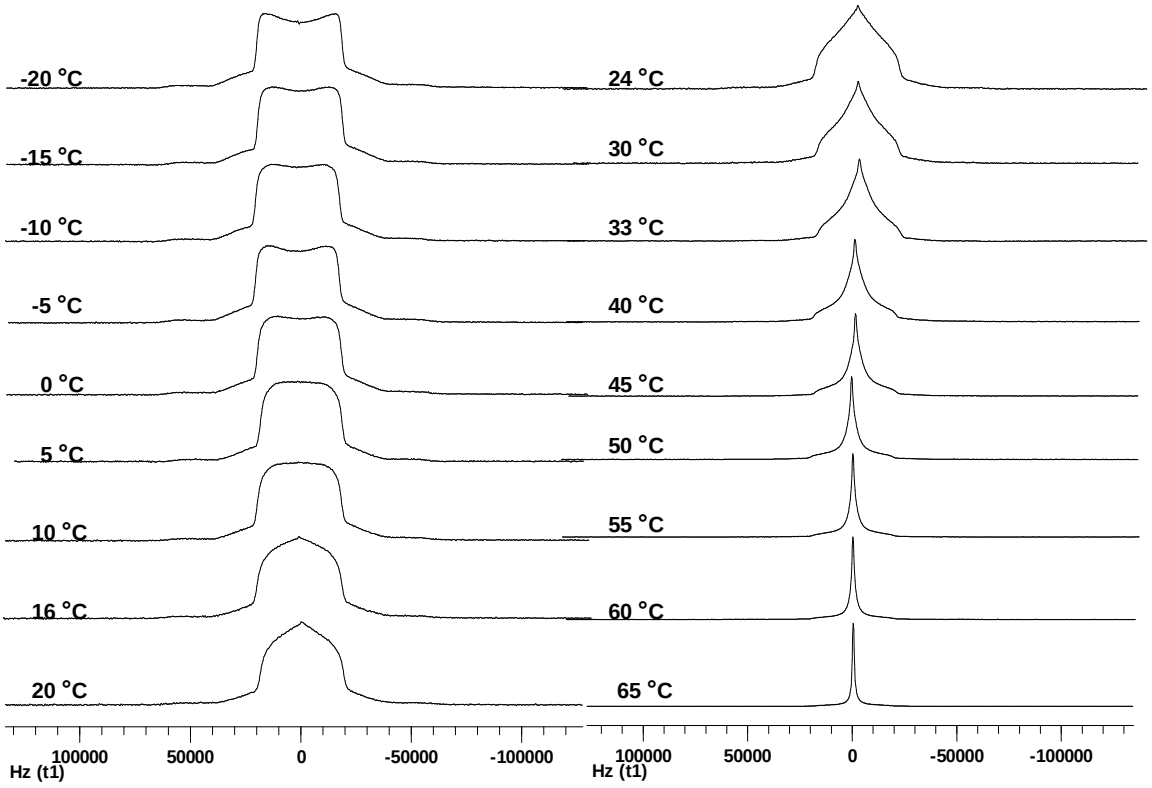

Figure A7. ^{2}H solid-state NMR spectra of 3.17 mg PIPA-d_7 per m^2 silica as a function of temperature.

APPENDIX B

SIMULATION PARAMETER AND RESULTS

THE JUMP COORDINATION USED IN THE SIMULATIONS.

- **Two-site model**

SITE	THETA	PHI	RHO
1	70.5	0	0
2	70.5	120	0

- **Soccer ball model**

SITE	THETA	PHI	RHO	SITE	THETA	PHI	RHO
1	131.02	81.651	0	31	49.5305	83.0491	0
2	148.637	57.422	0	32	130.104	293.748	0
3	136.358	24.2961	0	33	79.2033	146.036	0
4	113.306	28.4304	0	34	114.635	166.976	0
5	101.434	49.4514	0	35	137.436	205.717	0
6	109.19	72.2473	0	36	114.291	209.033	0
7	168.821	94.2426	0	37	130.48	263.046	0
8	136.092	350.381	0	38	108.335	303.229	0
9	100.933	7.7252	0	39	89.392	289.432	0
10	78.1447	49.803	0	40	102.34	187.915	0
11	90.3286	86.1848	0	41	79.0675	187.915	0
12	131.405	112.79	0	42	66.6939	208.43	0
13	65.718	330.957	0	43	67.0361	13.1832	0
14	77.6726	7.9183	0	44	31.2067	60.2275	0
15	42.5642	25.7172	0	45	89.6714	266.184	0
16	65.3798	346.976	0	46	49.8959	113.748	0
17	167.87	281.095	0	47	32.0838	137.21	0
18	112.964	346.816	0	48	108.93	252.839	0
19	42.2736	350.895	0	49	70.2014	302.919	0
20	100.813	326.036	0	50	48.6071	292.79	0
21	147.916	317.21	0	51	101.855	229.792	0
22	71.0703	72.8397	0	52	78.5658	229.451	0
23	90.608	109.432	0	53	43.9209	170.358	0
24	148.793	240.227	0	54	43.6415	204.296	0
25	109.802	122.929	0	55	70.8088	252.263	0
26	149.546	136.375	0	56	12.13	101.095	0
27	71.6737	123.224	0	57	30.4544	316.375	0
28	102.492	145.983	0	58	48.9875	261.651	0
29	137.714	170.899	0	59	11.1786	274.242	0
30	77.5083	325.983	0	60	31.3624	237.422	0

THE EXCHANGE SITE MATRIX FOR SOCCER BALL MODEL (60 × 60)

**** ROW   1 ****
-3.0000,+1.0000,+0.0000,+0.0000,+0.0000,+1.0000,+0.0000,+0.0000,+0.0000,+0.0000
+0.0000,+1.0000,+0.0000,+0.0000,+0.0000,+0.0000,+0.0000,+0.0000,+0.0000,+0.0000
+0.0000,+0.0000,+0.0000,+0.0000,+0.0000,+0.0000,+0.0000,+0.0000,+0.0000,+0.0000
+0.0000,+0.0000,+0.0000,+0.0000,+0.0000,+0.0000,+0.0000,+0.0000,+0.0000,+0.0000
+0.0000,+0.0000,+0.0000,+0.0000,+0.0000,+0.0000,+0.0000,+0.0000,+0.0000,+0.0000
+0.0000,+0.0000,+0.0000,+0.0000,+0.0000,+0.0000,+0.0000,+0.0000,+0.0000,+0.0000

**** ROW   2 ****
+1.0000,-3.0000,+1.0000,+0.0000,+0.0000,+0.0000,+1.0000,+0.0000,+0.0000,+0.0000
+0.0000,+0.0000,+0.0000,+0.0000,+0.0000,+0.0000,+0.0000,+0.0000,+0.0000,+0.0000
+0.0000,+0.0000,+0.0000,+0.0000,+0.0000,+0.0000,+0.0000,+0.0000,+0.0000,+0.0000
+0.0000,+0.0000,+0.0000,+0.0000,+0.0000,+0.0000,+0.0000,+0.0000,+0.0000,+0.0000
+0.0000,+0.0000,+0.0000,+0.0000,+0.0000,+0.0000,+0.0000,+0.0000,+0.0000,+0.0000
+0.0000,+0.0000,+0.0000,+0.0000,+0.0000,+0.0000,+0.0000,+0.0000,+0.0000,+0.0000

**** ROW   3 ****
+0.0000,+1.0000,-3.0000,+1.0000,+0.0000,+0.0000,+0.0000,+1.0000,+0.0000,+0.0000
+0.0000,+0.0000,+0.0000,+0.0000,+0.0000,+0.0000,+0.0000,+0.0000,+0.0000,+0.0000
+0.0000,+0.0000,+0.0000,+0.0000,+0.0000,+0.0000,+0.0000,+0.0000,+0.0000,+0.0000
+0.0000,+0.0000,+0.0000,+0.0000,+0.0000,+0.0000,+0.0000,+0.0000,+0.0000,+0.0000
+0.0000,+0.0000,+0.0000,+0.0000,+0.0000,+0.0000,+0.0000,+0.0000,+0.0000,+0.0000
+0.0000,+0.0000,+0.0000,+0.0000,+0.0000,+0.0000,+0.0000,+0.0000,+0.0000,+0.0000

**** ROW   4 ****
+0.0000,+0.0000,+1.0000,-3.0000,+1.0000,+0.0000,+0.0000,+0.0000,+1.0000,+0.0000
+0.0000,+0.0000,+0.0000,+0.0000,+0.0000,+0.0000,+0.0000,+0.0000,+0.0000,+0.0000
+0.0000,+0.0000,+0.0000,+0.0000,+0.0000,+0.0000,+0.0000,+0.0000,+0.0000,+0.0000
+0.0000,+0.0000,+0.0000,+0.0000,+0.0000,+0.0000,+0.0000,+0.0000,+0.0000,+0.0000
+0.0000,+0.0000,+0.0000,+0.0000,+0.0000,+0.0000,+0.0000,+0.0000,+0.0000,+0.0000
+0.0000,+0.0000,+0.0000,+0.0000,+0.0000,+0.0000,+0.0000,+0.0000,+0.0000,+0.0000

**** ROW   5 ****
+0.0000,+0.0000,+0.0000,+1.0000,-3.0000,+1.0000,+0.0000,+0.0000,+0.0000,+1.0000
+0.0000,+0.0000,+0.0000,+0.0000,+0.0000,+0.0000,+0.0000,+0.0000,+0.0000,+0.0000
+0.0000,+0.0000,+0.0000,+0.0000,+0.0000,+0.0000,+0.0000,+0.0000,+0.0000,+0.0000
+0.0000,+0.0000,+0.0000,+0.0000,+0.0000,+0.0000,+0.0000,+0.0000,+0.0000,+0.0000
+0.0000,+0.0000,+0.0000,+0.0000,+0.0000,+0.0000,+0.0000,+0.0000,+0.0000,+0.0000
+0.0000,+0.0000,+0.0000,+0.0000,+0.0000,+0.0000,+0.0000,+0.0000,+0.0000,+0.0000

**** ROW 6 ****
+1.0000,+0.0000,+0.0000,+0.0000,+1.0000,-3.0000,+0.0000,+0.0000,+0.0000,+0.0000
+1.0000,+0.0000,+0.0000,+0.0000,+0.0000,+0.0000,+0.0000,+0.0000,+0.0000,+0.0000
+0.0000,+0.0000,+0.0000,+0.0000,+0.0000,+0.0000,+0.0000,+0.0000,+0.0000,+0.0000
+0.0000,+0.0000,+0.0000,+0.0000,+0.0000,+0.0000,+0.0000,+0.0000,+0.0000,+0.0000
+0.0000,+0.0000,+0.0000,+0.0000,+0.0000,+0.0000,+0.0000,+0.0000,+0.0000,+0.0000
+0.0000,+0.0000,+0.0000,+0.0000,+0.0000,+0.0000,+0.0000,+0.0000,+0.0000,+0.0000

**** ROW 7 ****
+0.0000,+1.0000,+0.0000,+0.0000,+0.0000,+0.0000,-3.0000,+0.0000,+0.0000,+0.0000
+0.0000,+0.0000,+0.0000,+0.0000,+0.0000,+0.0000,+1.0000,+0.0000,+0.0000,+0.0000
+0.0000,+0.0000,+0.0000,+0.0000,+0.0000,+1.0000,+0.0000,+0.0000,+0.0000,+0.0000
+0.0000,+0.0000,+0.0000,+0.0000,+0.0000,+0.0000,+0.0000,+0.0000,+0.0000,+0.0000
+0.0000,+0.0000,+0.0000,+0.0000,+0.0000,+0.0000,+0.0000,+0.0000,+0.0000,+0.0000
+0.0000,+0.0000,+0.0000,+0.0000,+0.0000,+0.0000,+0.0000,+0.0000,+0.0000,+0.0000

**** ROW 8 ****
+0.0000,+0.0000,+1.0000,+0.0000,+0.0000,+0.0000,+0.0000,-3.0000,+0.0000,+0.0000
+0.0000,+0.0000,+0.0000,+0.0000,+0.0000,+0.0000,+0.0000,+1.0000,+0.0000,+0.0000
+1.0000,+0.0000,+0.0000,+0.0000,+0.0000,+0.0000,+0.0000,+0.0000,+0.0000,+0.0000
+0.0000,+0.0000,+0.0000,+0.0000,+0.0000,+0.0000,+0.0000,+0.0000,+0.0000,+0.0000
+0.0000,+0.0000,+0.0000,+0.0000,+0.0000,+0.0000,+0.0000,+0.0000,+0.0000,+0.0000
+0.0000,+0.0000,+0.0000,+0.0000,+0.0000,+0.0000,+0.0000,+0.0000,+0.0000,+0.0000

**** ROW 9 ****
+0.0000,+0.0000,+0.0000,+1.0000,+0.0000,+0.0000,+0.0000,+0.0000,-3.0000,+0.0000
+0.0000,+0.0000,+0.0000,+1.0000,+0.0000,+0.0000,+0.0000,+1.0000,+0.0000,+0.0000
+0.0000,+0.0000,+0.0000,+0.0000,+0.0000,+0.0000,+0.0000,+0.0000,+0.0000,+0.0000
+0.0000,+0.0000,+0.0000,+0.0000,+0.0000,+0.0000,+0.0000,+0.0000,+0.0000,+0.0000
+0.0000,+0.0000,+0.0000,+0.0000,+0.0000,+0.0000,+0.0000,+0.0000,+0.0000,+0.0000
+0.0000,+0.0000,+0.0000,+0.0000,+0.0000,+0.0000,+0.0000,+0.0000,+0.0000,+0.0000

**** ROW 10 ****
+0.0000,+0.0000,+0.0000,+0.0000,+1.0000,+0.0000,+0.0000,+0.0000,+0.0000,-3.0000
+0.0000,+0.0000,+1.0000,+0.0000,+0.0000,+0.0000,+0.0000,+0.0000,+0.0000,+0.0000
+0.0000,+1.0000,+0.0000,+0.0000,+0.0000,+0.0000,+0.0000,+0.0000,+0.0000,+0.0000
+0.0000,+0.0000,+0.0000,+0.0000,+0.0000,+0.0000,+0.0000,+0.0000,+0.0000,+0.0000
+0.0000,+0.0000,+0.0000,+0.0000,+0.0000,+0.0000,+0.0000,+0.0000,+0.0000,+0.0000
+0.0000,+0.0000,+0.0000,+0.0000,+0.0000,+0.0000,+0.0000,+0.0000,+0.0000,+0.0000

**** ROW 11 ****
+0.0000,+0.0000,+0.0000,+0.0000,+0.0000,+1.0000,+0.0000,+0.0000,+0.0000,+0.0000
-3.0000,+0.0000,+0.0000,+0.0000,+0.0000,+0.0000,+0.0000,+0.0000,+0.0000,+0.0000
+0.0000,+1.0000,+1.0000,+0.0000,+0.0000,+0.0000,+0.0000,+0.0000,+0.0000,+0.0000
+0.0000,+0.0000,+0.0000,+0.0000,+0.0000,+0.0000,+0.0000,+0.0000,+0.0000,+0.0000
+0.0000,+0.0000,+0.0000,+0.0000,+0.0000,+0.0000,+0.0000,+0.0000,+0.0000,+0.0000
+0.0000,+0.0000,+0.0000,+0.0000,+0.0000,+0.0000,+0.0000,+0.0000,+0.0000,+0.0000

**** ROW 12 ****
+1.0000,+0.0000,+0.0000,+0.0000,+0.0000,+0.0000,+0.0000,+0.0000,+0.0000,+0.0000
+0.0000,-3.0000,+0.0000,+0.0000,+0.0000,+0.0000,+0.0000,+0.0000,+0.0000,+0.0000
+0.0000,+0.0000,+0.0000,+0.0000,+1.0000,+1.0000,+0.0000,+0.0000,+0.0000,+0.0000
+0.0000,+0.0000,+0.0000,+0.0000,+0.0000,+0.0000,+0.0000,+0.0000,+0.0000,+0.0000
+0.0000,+0.0000,+0.0000,+0.0000,+0.0000,+0.0000,+0.0000,+0.0000,+0.0000,+0.0000
+0.0000,+0.0000,+0.0000,+0.0000,+0.0000,+0.0000,+0.0000,+0.0000,+0.0000,+0.0000

**** ROW 13 ****
+0.0000,+0.0000,+0.0000,+0.0000,+0.0000,+0.0000,+0.0000,+0.0000,+0.0000,+1.0000
+0.0000,+0.0000,-3.0000,+1.0000,+1.0000,+0.0000,+0.0000,+0.0000,+0.0000,+0.0000
+0.0000,+0.0000,+0.0000,+0.0000,+0.0000,+0.0000,+0.0000,+0.0000,+0.0000,+0.0000
+0.0000,+0.0000,+0.0000,+0.0000,+0.0000,+0.0000,+0.0000,+0.0000,+0.0000,+0.0000
+0.0000,+0.0000,+0.0000,+0.0000,+0.0000,+0.0000,+0.0000,+0.0000,+0.0000,+0.0000
+0.0000,+0.0000,+0.0000,+0.0000,+0.0000,+0.0000,+0.0000,+0.0000,+0.0000,+0.0000

**** ROW 14 ****
+0.0000,+0.0000,+0.0000,+0.0000,+0.0000,+0.0000,+0.0000,+0.0000,+1.0000,+0.0000
+0.0000,+0.0000,+1.0000,-3.0000,+0.0000,+1.0000,+0.0000,+0.0000,+0.0000,+0.0000
+0.0000,+0.0000,+0.0000,+0.0000,+0.0000,+0.0000,+0.0000,+0.0000,+0.0000,+0.0000
+0.0000,+0.0000,+0.0000,+0.0000,+0.0000,+0.0000,+0.0000,+0.0000,+0.0000,+0.0000
+0.0000,+0.0000,+0.0000,+0.0000,+0.0000,+0.0000,+0.0000,+0.0000,+0.0000,+0.0000
+0.0000,+0.0000,+0.0000,+0.0000,+0.0000,+0.0000,+0.0000,+0.0000,+0.0000,+0.0000

**** ROW 15 ****
+0.0000,+0.0000,+0.0000,+0.0000,+0.0000,+0.0000,+0.0000,+0.0000,+0.0000,+0.0000
+0.0000,+0.0000,+1.0000,+0.0000,-3.0000,+0.0000,+0.0000,+0.0000,+1.0000,+0.0000
+0.0000,+0.0000,+0.0000,+0.0000,+0.0000,+0.0000,+0.0000,+0.0000,+0.0000,+0.0000
+0.0000,+0.0000,+0.0000,+0.0000,+0.0000,+0.0000,+0.0000,+0.0000,+0.0000,+0.0000
+0.0000,+0.0000,+0.0000,+1.0000,+0.0000,+0.0000,+0.0000,+0.0000,+0.0000,+0.0000
+0.0000,+0.0000,+0.0000,+0.0000,+0.0000,+0.0000,+0.0000,+0.0000,+0.0000,+0.0000

**** ROW 16 ****
+0.0000,+0.0000,+0.0000,+0.0000,+0.0000,+0.0000,+0.0000,+0.0000,+0.0000,+0.0000
+0.0000,+0.0000,+0.0000,+1.0000,+0.0000,-3.0000,+0.0000,+0.0000,+1.0000,+0.0000
+0.0000,+0.0000,+0.0000,+0.0000,+0.0000,+0.0000,+0.0000,+0.0000,+0.0000,+1.0000
+0.0000,+0.0000,+0.0000,+0.0000,+0.0000,+0.0000,+0.0000,+0.0000,+0.0000,+0.0000
+0.0000,+0.0000,+0.0000,+0.0000,+0.0000,+0.0000,+0.0000,+0.0000,+0.0000,+0.0000
+0.0000,+0.0000,+0.0000,+0.0000,+0.0000,+0.0000,+0.0000,+0.0000,+0.0000,+0.0000

**** ROW 17 ****
+0.0000,+0.0000,+0.0000,+0.0000,+0.0000,+0.0000,+1.0000,+0.0000,+0.0000,+0.0000
+0.0000,+0.0000,+0.0000,+0.0000,+0.0000,+0.0000,-3.0000,+0.0000,+0.0000,+0.0000
+1.0000,+0.0000,+0.0000,+1.0000,+0.0000,+0.0000,+0.0000,+0.0000,+0.0000,+0.0000
+0.0000,+0.0000,+0.0000,+0.0000,+0.0000,+0.0000,+0.0000,+0.0000,+0.0000,+0.0000
+0.0000,+0.0000,+0.0000,+0.0000,+0.0000,+0.0000,+0.0000,+0.0000,+0.0000,+0.0000
+0.0000,+0.0000,+0.0000,+0.0000,+0.0000,+0.0000,+0.0000,+0.0000,+0.0000,+0.0000

**** ROW 18 ****
+0.0000,+0.0000,+0.0000,+0.0000,+0.0000,+0.0000,+0.0000,+1.0000,+1.0000,+0.0000
+0.0000,+0.0000,+0.0000,+0.0000,+0.0000,+0.0000,+0.0000,-3.0000,+0.0000,+1.0000
+0.0000,+0.0000,+0.0000,+0.0000,+0.0000,+0.0000,+0.0000,+0.0000,+0.0000,+0.0000
+0.0000,+0.0000,+0.0000,+0.0000,+0.0000,+0.0000,+0.0000,+0.0000,+0.0000,+0.0000
+0.0000,+0.0000,+0.0000,+0.0000,+0.0000,+0.0000,+0.0000,+0.0000,+0.0000,+0.0000
+0.0000,+0.0000,+0.0000,+0.0000,+0.0000,+0.0000,+0.0000,+0.0000,+0.0000,+0.0000

**** ROW 19 ****
+0.0000,+0.0000,+0.0000,+0.0000,+0.0000,+0.0000,+0.0000,+0.0000,+0.0000,+0.0000
+0.0000,+0.0000,+0.0000,+0.0000,+1.0000,+1.0000,+0.0000,+0.0000,-3.0000,+0.0000
+0.0000,+0.0000,+0.0000,+0.0000,+0.0000,+0.0000,+0.0000,+0.0000,+0.0000,+0.0000
+0.0000,+0.0000,+0.0000,+0.0000,+0.0000,+0.0000,+0.0000,+0.0000,+0.0000,+0.0000
+0.0000,+0.0000,+0.0000,+0.0000,+0.0000,+0.0000,+0.0000,+0.0000,+0.0000,+0.0000
+0.0000,+0.0000,+0.0000,+0.0000,+0.0000,+0.0000,+1.0000,+0.0000,+0.0000,+0.0000

**** ROW 20 ****
+0.0000,+0.0000,+0.0000,+0.0000,+0.0000,+0.0000,+0.0000,+0.0000,+0.0000,+0.0000
+0.0000,+0.0000,+0.0000,+0.0000,+0.0000,+0.0000,+0.0000,+1.0000,+0.0000,-3.0000
+0.0000,+0.0000,+0.0000,+0.0000,+0.0000,+0.0000,+0.0000,+0.0000,+0.0000,+1.0000
+0.0000,+0.0000,+0.0000,+0.0000,+0.0000,+0.0000,+0.0000,+1.0000,+0.0000,+0.0000
+0.0000,+0.0000,+0.0000,+0.0000,+0.0000,+0.0000,+0.0000,+0.0000,+0.0000,+0.0000
+0.0000,+0.0000,+0.0000,+0.0000,+0.0000,+0.0000,+0.0000,+0.0000,+0.0000,+0.0000

**** ROW 21 ****
+0.0000,+0.0000,+0.0000,+0.0000,+0.0000,+0.0000,+0.0000,+1.0000,+0.0000,+0.0000
+0.0000,+0.0000,+0.0000,+0.0000,+0.0000,+0.0000,+1.0000,+0.0000,+0.0000,+0.0000
-3.0000,+0.0000,+0.0000,+0.0000,+0.0000,+0.0000,+0.0000,+0.0000,+0.0000,+0.0000
+0.0000,+1.0000,+0.0000,+0.0000,+0.0000,+0.0000,+0.0000,+0.0000,+0.0000,+0.0000
+0.0000,+0.0000,+0.0000,+0.0000,+0.0000,+0.0000,+0.0000,+0.0000,+0.0000,+0.0000
+0.0000,+0.0000,+0.0000,+0.0000,+0.0000,+0.0000,+0.0000,+0.0000,+0.0000,+0.0000

**** ROW 22 ****
+0.0000,+0.0000,+0.0000,+0.0000,+0.0000,+0.0000,+0.0000,+0.0000,+0.0000,+1.0000
+1.0000,+0.0000,+0.0000,+0.0000,+0.0000,+0.0000,+0.0000,+0.0000,+0.0000,+0.0000
+0.0000,-3.0000,+0.0000,+0.0000,+0.0000,+0.0000,+0.0000,+0.0000,+0.0000,+0.0000
+1.0000,+0.0000,+0.0000,+0.0000,+0.0000,+0.0000,+0.0000,+0.0000,+0.0000,+0.0000
+0.0000,+0.0000,+0.0000,+0.0000,+0.0000,+0.0000,+0.0000,+0.0000,+0.0000,+0.0000
+0.0000,+0.0000,+0.0000,+0.0000,+0.0000,+0.0000,+0.0000,+0.0000,+0.0000,+0.0000

**** ROW 23 ****
+0.0000,+0.0000,+0.0000,+0.0000,+0.0000,+0.0000,+0.0000,+0.0000,+0.0000,+0.0000
+1.0000,+0.0000,+0.0000,+0.0000,+0.0000,+0.0000,+0.0000,+0.0000,+0.0000,+0.0000
+0.0000,+0.0000,-3.0000,+0.0000,+1.0000,+0.0000,+1.0000,+0.0000,+0.0000,+0.0000
+0.0000,+0.0000,+0.0000,+0.0000,+0.0000,+0.0000,+0.0000,+0.0000,+0.0000,+0.0000
+0.0000,+0.0000,+0.0000,+0.0000,+0.0000,+0.0000,+0.0000,+0.0000,+0.0000,+0.0000
+0.0000,+0.0000,+0.0000,+0.0000,+0.0000,+0.0000,+0.0000,+0.0000,+0.0000,+0.0000

**** ROW 24 ****
+0.0000,+0.0000,+0.0000,+0.0000,+0.0000,+0.0000,+0.0000,+0.0000,+0.0000,+0.0000
+0.0000,+0.0000,+0.0000,+0.0000,+0.0000,+0.0000,+1.0000,+0.0000,+0.0000,+0.0000
+0.0000,+0.0000,+0.0000,-3.0000,+0.0000,+0.0000,+0.0000,+0.0000,+0.0000,+0.0000
+0.0000,+0.0000,+0.0000,+0.0000,+1.0000,+0.0000,+1.0000,+0.0000,+0.0000,+0.0000
+0.0000,+0.0000,+0.0000,+0.0000,+0.0000,+0.0000,+0.0000,+0.0000,+0.0000,+0.0000
+0.0000,+0.0000,+0.0000,+0.0000,+0.0000,+0.0000,+0.0000,+0.0000,+0.0000,+0.0000

**** ROW 25 ****
+0.0000,+0.0000,+0.0000,+0.0000,+0.0000,+0.0000,+0.0000,+0.0000,+0.0000,+0.0000
+0.0000,+1.0000,+0.0000,+0.0000,+0.0000,+0.0000,+0.0000,+0.0000,+0.0000,+0.0000
+0.0000,+0.0000,+1.0000,+0.0000,-3.0000,+0.0000,+0.0000,+1.0000,+0.0000,+0.0000
+0.0000,+0.0000,+0.0000,+0.0000,+0.0000,+0.0000,+0.0000,+0.0000,+0.0000,+0.0000
+0.0000,+0.0000,+0.0000,+0.0000,+0.0000,+0.0000,+0.0000,+0.0000,+0.0000,+0.0000
+0.0000,+0.0000,+0.0000,+0.0000,+0.0000,+0.0000,+0.0000,+0.0000,+0.0000,+0.0000

**** ROW 26 ****
+0.0000,+0.0000,+0.0000,+0.0000,+0.0000,+0.0000,+1.0000,+0.0000,+0.0000,+0.0000
+0.0000,+1.0000,+0.0000,+0.0000,+0.0000,+0.0000,+0.0000,+0.0000,+0.0000,+0.0000
+0.0000,+0.0000,+0.0000,+0.0000,+0.0000,-3.0000,+0.0000,+0.0000,+1.0000,+0.0000
+0.0000,+0.0000,+0.0000,+0.0000,+0.0000,+0.0000,+0.0000,+0.0000,+0.0000,+0.0000
+0.0000,+0.0000,+0.0000,+0.0000,+0.0000,+0.0000,+0.0000,+0.0000,+0.0000,+0.0000
+0.0000,+0.0000,+0.0000,+0.0000,+0.0000,+0.0000,+0.0000,+0.0000,+0.0000,+0.0000

**** ROW 27 ****
+0.0000,+0.0000,+0.0000,+0.0000,+0.0000,+0.0000,+0.0000,+0.0000,+0.0000,+0.0000
+0.0000,+0.0000,+0.0000,+0.0000,+0.0000,+0.0000,+0.0000,+0.0000,+0.0000,+0.0000
+0.0000,+0.0000,+1.0000,+0.0000,+0.0000,+0.0000,-3.0000,+0.0000,+0.0000,+0.0000
+0.0000,+0.0000,+1.0000,+0.0000,+0.0000,+0.0000,+0.0000,+0.0000,+0.0000,+0.0000
+0.0000,+0.0000,+0.0000,+0.0000,+0.0000,+1.0000,+0.0000,+0.0000,+0.0000,+0.0000
+0.0000,+0.0000,+0.0000,+0.0000,+0.0000,+0.0000,+0.0000,+0.0000,+0.0000,+0.0000

**** ROW 28 ****
+0.0000,+0.0000,+0.0000,+0.0000,+0.0000,+0.0000,+0.0000,+0.0000,+0.0000,+0.0000
+0.0000,+0.0000,+0.0000,+0.0000,+0.0000,+0.0000,+0.0000,+0.0000,+0.0000,+0.0000
+0.0000,+0.0000,+0.0000,+0.0000,+1.0000,+0.0000,+0.0000,-3.0000,+0.0000,+0.0000
+0.0000,+0.0000,+1.0000,+1.0000,+0.0000,+0.0000,+0.0000,+0.0000,+0.0000,+0.0000
+0.0000,+0.0000,+0.0000,+0.0000,+0.0000,+0.0000,+0.0000,+0.0000,+0.0000,+0.0000
+0.0000,+0.0000,+0.0000,+0.0000,+0.0000,+0.0000,+0.0000,+0.0000,+0.0000,+0.0000

**** ROW 29 ****
+0.0000,+0.0000,+0.0000,+0.0000,+0.0000,+0.0000,+0.0000,+0.0000,+0.0000,+0.0000
+0.0000,+0.0000,+0.0000,+0.0000,+0.0000,+0.0000,+0.0000,+0.0000,+0.0000,+0.0000
+0.0000,+0.0000,+0.0000,+0.0000,+0.0000,+1.0000,+0.0000,+0.0000,-3.0000,+0.0000
+0.0000,+0.0000,+0.0000,+1.0000,+1.0000,+0.0000,+0.0000,+0.0000,+0.0000,+0.0000
+0.0000,+0.0000,+0.0000,+0.0000,+0.0000,+0.0000,+0.0000,+0.0000,+0.0000,+0.0000
+0.0000,+0.0000,+0.0000,+0.0000,+0.0000,+0.0000,+0.0000,+0.0000,+0.0000,+0.0000

**** ROW 30 ****
+0.0000,+0.0000,+0.0000,+0.0000,+0.0000,+0.0000,+0.0000,+0.0000,+0.0000,+0.0000
+0.0000,+0.0000,+0.0000,+0.0000,+0.0000,+1.0000,+0.0000,+0.0000,+0.0000,+1.0000
+0.0000,+0.0000,+0.0000,+0.0000,+0.0000,+0.0000,+0.0000,+0.0000,+0.0000,-3.0000
+0.0000,+0.0000,+0.0000,+0.0000,+0.0000,+0.0000,+0.0000,+0.0000,+0.0000,+0.0000
+0.0000,+0.0000,+0.0000,+0.0000,+0.0000,+0.0000,+0.0000,+0.0000,+1.0000,+0.0000
+0.0000,+0.0000,+0.0000,+0.0000,+0.0000,+0.0000,+0.0000,+0.0000,+0.0000,+0.0000

**** ROW 31 ****
+0.0000,+0.0000,+0.0000,+0.0000,+0.0000,+0.0000,+0.0000,+0.0000,+0.0000,+0.0000
+0.0000,+0.0000,+0.0000,+0.0000,+0.0000,+0.0000,+0.0000,+0.0000,+0.0000,+0.0000
+0.0000,+1.0000,+0.0000,+0.0000,+0.0000,+0.0000,+0.0000,+0.0000,+0.0000,+0.0000
-3.0000,+0.0000,+0.0000,+0.0000,+0.0000,+0.0000,+0.0000,+0.0000,+0.0000,+0.0000
+0.0000,+0.0000,+0.0000,+1.0000,+0.0000,+1.0000,+0.0000,+0.0000,+0.0000,+0.0000
+0.0000,+0.0000,+0.0000,+0.0000,+0.0000,+0.0000,+0.0000,+0.0000,+0.0000,+0.0000

**** ROW 32 ****
+0.0000,+0.0000,+0.0000,+0.0000,+0.0000,+0.0000,+0.0000,+0.0000,+0.0000,+0.0000
+0.0000,+0.0000,+0.0000,+0.0000,+0.0000,+0.0000,+0.0000,+0.0000,+0.0000,+0.0000
+1.0000,+0.0000,+0.0000,+0.0000,+0.0000,+0.0000,+0.0000,+0.0000,+0.0000,+0.0000
+0.0000,-3.0000,+0.0000,+0.0000,+0.0000,+0.0000,+1.0000,+1.0000,+0.0000,+0.0000
+0.0000,+0.0000,+0.0000,+0.0000,+0.0000,+0.0000,+0.0000,+0.0000,+0.0000,+0.0000
+0.0000,+0.0000,+0.0000,+0.0000,+0.0000,+0.0000,+0.0000,+0.0000,+0.0000,+0.0000

**** ROW 33 ****
+0.0000,+0.0000,+0.0000,+0.0000,+0.0000,+0.0000,+0.0000,+0.0000,+0.0000,+0.0000
+0.0000,+0.0000,+0.0000,+0.0000,+0.0000,+0.0000,+0.0000,+0.0000,+0.0000,+0.0000
+0.0000,+0.0000,+0.0000,+0.0000,+0.0000,+0.0000,+1.0000,+1.0000,+0.0000,+0.0000
+0.0000,+0.0000,-3.0000,+0.0000,+0.0000,+0.0000,+0.0000,+0.0000,+0.0000,+0.0000
+0.0000,+0.0000,+1.0000,+0.0000,+0.0000,+0.0000,+0.0000,+0.0000,+0.0000,+0.0000
+0.0000,+0.0000,+0.0000,+0.0000,+0.0000,+0.0000,+0.0000,+0.0000,+0.0000,+0.0000

**** ROW 34 ****
+0.0000,+0.0000,+0.0000,+0.0000,+0.0000,+0.0000,+0.0000,+0.0000,+0.0000,+0.0000
+0.0000,+0.0000,+0.0000,+0.0000,+0.0000,+0.0000,+0.0000,+0.0000,+0.0000,+0.0000
+0.0000,+0.0000,+0.0000,+0.0000,+0.0000,+0.0000,+0.0000,+1.0000,+1.0000,+0.0000
+0.0000,+0.0000,+0.0000,-3.0000,+0.0000,+0.0000,+0.0000,+0.0000,+0.0000,+1.0000
+0.0000,+0.0000,+0.0000,+0.0000,+0.0000,+0.0000,+0.0000,+0.0000,+0.0000,+0.0000
+0.0000,+0.0000,+0.0000,+0.0000,+0.0000,+0.0000,+0.0000,+0.0000,+0.0000,+0.0000

**** ROW 35 ****
+0.0000,+0.0000,+0.0000,+0.0000,+0.0000,+0.0000,+0.0000,+0.0000,+0.0000,+0.0000
+0.0000,+0.0000,+0.0000,+0.0000,+0.0000,+0.0000,+0.0000,+0.0000,+0.0000,+0.0000
+0.0000,+0.0000,+0.0000,+1.0000,+0.0000,+0.0000,+0.0000,+0.0000,+1.0000,+0.0000
+0.0000,+0.0000,+0.0000,+0.0000,-3.0000,+1.0000,+0.0000,+0.0000,+0.0000,+0.0000
+0.0000,+0.0000,+0.0000,+0.0000,+0.0000,+0.0000,+0.0000,+0.0000,+0.0000,+0.0000
+0.0000,+0.0000,+0.0000,+0.0000,+0.0000,+0.0000,+0.0000,+0.0000,+0.0000,+0.0000

**** ROW 36 ****
+0.0000,+0.0000,+0.0000,+0.0000,+0.0000,+0.0000,+0.0000,+0.0000,+0.0000,+0.0000
+0.0000,+0.0000,+0.0000,+0.0000,+0.0000,+0.0000,+0.0000,+0.0000,+0.0000,+0.0000
+0.0000,+0.0000,+0.0000,+0.0000,+0.0000,+0.0000,+0.0000,+0.0000,+0.0000,+0.0000
+0.0000,+0.0000,+0.0000,+0.0000,+1.0000,-3.0000,+0.0000,+0.0000,+0.0000,+1.0000
+0.0000,+0.0000,+0.0000,+0.0000,+0.0000,+0.0000,+0.0000,+0.0000,+0.0000,+0.0000
+1.0000,+0.0000,+0.0000,+0.0000,+0.0000,+0.0000,+0.0000,+0.0000,+0.0000,+0.0000

**** ROW 37 ****
+0.0000,+0.0000,+0.0000,+0.0000,+0.0000,+0.0000,+0.0000,+0.0000,+0.0000,+0.0000
+0.0000,+0.0000,+0.0000,+0.0000,+0.0000,+0.0000,+0.0000,+0.0000,+0.0000,+0.0000
+0.0000,+0.0000,+0.0000,+1.0000,+0.0000,+0.0000,+0.0000,+0.0000,+0.0000,+0.0000
+0.0000,+1.0000,+0.0000,+0.0000,+0.0000,+0.0000,-3.0000,+0.0000,+0.0000,+0.0000
+0.0000,+0.0000,+0.0000,+0.0000,+0.0000,+0.0000,+0.0000,+1.0000,+0.0000,+0.0000
+0.0000,+0.0000,+0.0000,+0.0000,+0.0000,+0.0000,+0.0000,+0.0000,+0.0000,+0.0000

**** ROW 38 ****
+0.0000,+0.0000,+0.0000,+0.0000,+0.0000,+0.0000,+0.0000,+0.0000,+0.0000,+0.0000
+0.0000,+0.0000,+0.0000,+0.0000,+0.0000,+0.0000,+0.0000,+0.0000,+0.0000,+1.0000
+0.0000,+0.0000,+0.0000,+0.0000,+0.0000,+0.0000,+0.0000,+0.0000,+0.0000,+0.0000
+0.0000,+1.0000,+0.0000,+0.0000,+0.0000,+0.0000,+0.0000,-3.0000,+1.0000,+0.0000
+0.0000,+0.0000,+0.0000,+0.0000,+0.0000,+0.0000,+0.0000,+0.0000,+0.0000,+0.0000
+0.0000,+0.0000,+0.0000,+0.0000,+0.0000,+0.0000,+0.0000,+0.0000,+0.0000,+0.0000

**** ROW 39 ****
+0.0000,+0.0000,+0.0000,+0.0000,+0.0000,+0.0000,+0.0000,+0.0000,+0.0000,+0.0000
+0.0000,+0.0000,+0.0000,+0.0000,+0.0000,+0.0000,+0.0000,+0.0000,+0.0000,+0.0000
+0.0000,+0.0000,+0.0000,+0.0000,+0.0000,+0.0000,+0.0000,+0.0000,+0.0000,+0.0000
+0.0000,+0.0000,+0.0000,+0.0000,+0.0000,+0.0000,+0.0000,+1.0000,-3.0000,+0.0000
+0.0000,+0.0000,+0.0000,+0.0000,+1.0000,+0.0000,+0.0000,+0.0000,+1.0000,+0.0000
+0.0000,+0.0000,+0.0000,+0.0000,+0.0000,+0.0000,+0.0000,+0.0000,+0.0000,+0.0000

**** ROW 40 ****
+0.0000,+0.0000,+0.0000,+0.0000,+0.0000,+0.0000,+0.0000,+0.0000,+0.0000,+0.0000
+0.0000,+0.0000,+0.0000,+0.0000,+0.0000,+0.0000,+0.0000,+0.0000,+0.0000,+0.0000
+0.0000,+0.0000,+0.0000,+0.0000,+0.0000,+0.0000,+0.0000,+0.0000,+0.0000,+0.0000
+0.0000,+0.0000,+0.0000,+1.0000,+0.0000,+1.0000,+0.0000,+0.0000,+0.0000,-3.0000
+1.0000,+0.0000,+0.0000,+0.0000,+0.0000,+0.0000,+0.0000,+0.0000,+0.0000,+0.0000
+0.0000,+0.0000,+0.0000,+0.0000,+0.0000,+0.0000,+0.0000,+0.0000,+0.0000,+0.0000

**** ROW 41 ****
+0.0000,+0.0000,+0.0000,+0.0000,+0.0000,+0.0000,+0.0000,+0.0000,+0.0000,+0.0000
+0.0000,+0.0000,+0.0000,+0.0000,+0.0000,+0.0000,+0.0000,+0.0000,+0.0000,+0.0000
+0.0000,+0.0000,+0.0000,+0.0000,+0.0000,+0.0000,+0.0000,+0.0000,+0.0000,+0.0000
+0.0000,+0.0000,+0.0000,+0.0000,+0.0000,+0.0000,+0.0000,+0.0000,+0.0000,+1.0000
-3.0000,+1.0000,+1.0000,+0.0000,+0.0000,+0.0000,+0.0000,+0.0000,+0.0000,+0.0000
+0.0000,+0.0000,+0.0000,+0.0000,+0.0000,+0.0000,+0.0000,+0.0000,+0.0000,+0.0000

**** ROW 42 ****
+0.0000,+0.0000,+0.0000,+0.0000,+0.0000,+0.0000,+0.0000,+0.0000,+0.0000,+0.0000
+0.0000,+0.0000,+0.0000,+0.0000,+0.0000,+0.0000,+0.0000,+0.0000,+0.0000,+0.0000
+0.0000,+0.0000,+0.0000,+0.0000,+0.0000,+0.0000,+0.0000,+0.0000,+0.0000,+0.0000
+0.0000,+0.0000,+0.0000,+0.0000,+0.0000,+0.0000,+0.0000,+0.0000,+0.0000,+0.0000
+1.0000,-3.0000,+0.0000,+0.0000,+0.0000,+0.0000,+0.0000,+0.0000,+0.0000,+0.0000
+0.0000,+1.0000,+0.0000,+1.0000,+0.0000,+0.0000,+0.0000,+0.0000,+0.0000,+0.0000

**** ROW 43 ****
+0.0000,+0.0000,+0.0000,+0.0000,+0.0000,+0.0000,+0.0000,+0.0000,+0.0000,+0.0000
+0.0000,+0.0000,+0.0000,+0.0000,+0.0000,+0.0000,+0.0000,+0.0000,+0.0000,+0.0000
+0.0000,+0.0000,+0.0000,+0.0000,+0.0000,+0.0000,+0.0000,+0.0000,+0.0000,+0.0000
+0.0000,+0.0000,+1.0000,+0.0000,+0.0000,+0.0000,+0.0000,+0.0000,+0.0000,+0.0000
+1.0000,+0.0000,-3.0000,+0.0000,+0.0000,+0.0000,+0.0000,+0.0000,+0.0000,+0.0000
+0.0000,+0.0000,+1.0000,+0.0000,+0.0000,+0.0000,+0.0000,+0.0000,+0.0000,+0.0000

**** ROW 44 ****
+0.0000,+0.0000,+0.0000,+0.0000,+0.0000,+0.0000,+0.0000,+0.0000,+0.0000,+0.0000
+0.0000,+0.0000,+0.0000,+0.0000,+1.0000,+0.0000,+0.0000,+0.0000,+0.0000,+0.0000
+0.0000,+0.0000,+0.0000,+0.0000,+0.0000,+0.0000,+0.0000,+0.0000,+0.0000,+0.0000
+1.0000,+0.0000,+0.0000,+0.0000,+0.0000,+0.0000,+0.0000,+0.0000,+0.0000,+0.0000
+0.0000,+0.0000,+0.0000,-3.0000,+0.0000,+0.0000,+0.0000,+0.0000,+0.0000,+0.0000
+0.0000,+0.0000,+0.0000,+0.0000,+0.0000,+1.0000,+0.0000,+0.0000,+0.0000,+0.0000

**** ROW 45 ****
+0.0000,+0.0000,+0.0000,+0.0000,+0.0000,+0.0000,+0.0000,+0.0000,+0.0000,+0.0000
+0.0000,+0.0000,+0.0000,+0.0000,+0.0000,+0.0000,+0.0000,+0.0000,+0.0000,+0.0000
+0.0000,+0.0000,+0.0000,+0.0000,+0.0000,+0.0000,+0.0000,+0.0000,+0.0000,+0.0000
+0.0000,+0.0000,+0.0000,+0.0000,+0.0000,+0.0000,+0.0000,+0.0000,+1.0000,+0.0000
+0.0000,+0.0000,+0.0000,+0.0000,-3.0000,+0.0000,+0.0000,+1.0000,+0.0000,+0.0000
+0.0000,+0.0000,+0.0000,+0.0000,+1.0000,+0.0000,+0.0000,+0.0000,+0.0000,+0.0000

**** ROW 46 ****
+0.0000,+0.0000,+0.0000,+0.0000,+0.0000,+0.0000,+0.0000,+0.0000,+0.0000,+0.0000
+0.0000,+0.0000,+0.0000,+0.0000,+0.0000,+0.0000,+0.0000,+0.0000,+0.0000,+0.0000
+0.0000,+0.0000,+0.0000,+0.0000,+0.0000,+0.0000,+1.0000,+0.0000,+0.0000,+0.0000
+1.0000,+0.0000,+0.0000,+0.0000,+0.0000,+0.0000,+0.0000,+0.0000,+0.0000,+0.0000
+0.0000,+0.0000,+0.0000,+0.0000,+0.0000,-3.0000,+1.0000,+0.0000,+0.0000,+0.0000
+0.0000,+0.0000,+0.0000,+0.0000,+0.0000,+0.0000,+0.0000,+0.0000,+0.0000,+0.0000

**** ROW 47 ****
+0.0000,+0.0000,+0.0000,+0.0000,+0.0000,+0.0000,+0.0000,+0.0000,+0.0000,+0.0000
+0.0000,+0.0000,+0.0000,+0.0000,+0.0000,+0.0000,+0.0000,+0.0000,+0.0000,+0.0000
+0.0000,+0.0000,+0.0000,+0.0000,+0.0000,+0.0000,+0.0000,+0.0000,+0.0000,+0.0000
+0.0000,+0.0000,+0.0000,+0.0000,+0.0000,+0.0000,+0.0000,+0.0000,+0.0000,+0.0000
+0.0000,+0.0000,+0.0000,+0.0000,+0.0000,+1.0000,-3.0000,+0.0000,+0.0000,+0.0000
+0.0000,+0.0000,+1.0000,+0.0000,+0.0000,+1.0000,+0.0000,+0.0000,+0.0000,+0.0000

**** ROW 48 ****
+0.0000,+0.0000,+0.0000,+0.0000,+0.0000,+0.0000,+0.0000,+0.0000,+0.0000,+0.0000
+0.0000,+0.0000,+0.0000,+0.0000,+0.0000,+0.0000,+0.0000,+0.0000,+0.0000,+0.0000
+0.0000,+0.0000,+0.0000,+0.0000,+0.0000,+0.0000,+0.0000,+0.0000,+0.0000,+0.0000
+0.0000,+0.0000,+0.0000,+0.0000,+0.0000,+0.0000,+1.0000,+0.0000,+0.0000,+0.0000
+0.0000,+0.0000,+0.0000,+0.0000,+1.0000,+0.0000,+0.0000,-3.0000,+0.0000,+0.0000
+1.0000,+0.0000,+0.0000,+0.0000,+0.0000,+0.0000,+0.0000,+0.0000,+0.0000,+0.0000

**** ROW 49 ****
+0.0000,+0.0000,+0.0000,+0.0000,+0.0000,+0.0000,+0.0000,+0.0000,+0.0000,+0.0000
+0.0000,+0.0000,+0.0000,+0.0000,+0.0000,+0.0000,+0.0000,+0.0000,+0.0000,+0.0000
+0.0000,+0.0000,+0.0000,+0.0000,+0.0000,+0.0000,+0.0000,+0.0000,+0.0000,+1.0000
+0.0000,+0.0000,+0.0000,+0.0000,+0.0000,+0.0000,+0.0000,+0.0000,+1.0000,+0.0000
+0.0000,+0.0000,+0.0000,+0.0000,+0.0000,+0.0000,+0.0000,+0.0000,-3.0000,+1.0000
+0.0000,+0.0000,+0.0000,+0.0000,+0.0000,+0.0000,+0.0000,+0.0000,+0.0000,+0.0000

**** ROW 50 ****
+0.0000,+0.0000,+0.0000,+0.0000,+0.0000,+0.0000,+0.0000,+0.0000,+0.0000,+0.0000
+0.0000,+0.0000,+0.0000,+0.0000,+0.0000,+0.0000,+0.0000,+0.0000,+0.0000,+0.0000
+0.0000,+0.0000,+0.0000,+0.0000,+0.0000,+0.0000,+0.0000,+0.0000,+0.0000,+0.0000
+0.0000,+0.0000,+0.0000,+0.0000,+0.0000,+0.0000,+0.0000,+0.0000,+0.0000,+0.0000
+0.0000,+0.0000,+0.0000,+0.0000,+0.0000,+0.0000,+0.0000,+0.0000,+1.0000,-3.0000
+0.0000,+0.0000,+0.0000,+0.0000,+0.0000,+0.0000,+1.0000,+1.0000,+0.0000,+0.0000

**** ROW 51 ****
+0.0000,+0.0000,+0.0000,+0.0000,+0.0000,+0.0000,+0.0000,+0.0000,+0.0000,+0.0000
+0.0000,+0.0000,+0.0000,+0.0000,+0.0000,+0.0000,+0.0000,+0.0000,+0.0000,+0.0000
+0.0000,+0.0000,+0.0000,+0.0000,+0.0000,+0.0000,+0.0000,+0.0000,+0.0000,+0.0000
+0.0000,+0.0000,+0.0000,+0.0000,+0.0000,+1.0000,+0.0000,+0.0000,+0.0000,+0.0000
+0.0000,+0.0000,+0.0000,+0.0000,+0.0000,+0.0000,+0.0000,+1.0000,+0.0000,+0.0000
-3.0000,+1.0000,+0.0000,+0.0000,+0.0000,+0.0000,+0.0000,+0.0000,+0.0000,+0.0000

**** ROW 52 ****
+0.0000,+0.0000,+0.0000,+0.0000,+0.0000,+0.0000,+0.0000,+0.0000,+0.0000,+0.0000
+0.0000,+0.0000,+0.0000,+0.0000,+0.0000,+0.0000,+0.0000,+0.0000,+0.0000,+0.0000
+0.0000,+0.0000,+0.0000,+0.0000,+0.0000,+0.0000,+0.0000,+0.0000,+0.0000,+0.0000
+0.0000,+0.0000,+0.0000,+0.0000,+0.0000,+0.0000,+0.0000,+0.0000,+0.0000,+0.0000
+0.0000,+1.0000,+0.0000,+0.0000,+0.0000,+0.0000,+0.0000,+0.0000,+0.0000,+0.0000
+1.0000,-3.0000,+0.0000,+0.0000,+1.0000,+0.0000,+0.0000,+0.0000,+0.0000,+0.0000

**** ROW 53 ****
+0.0000,+0.0000,+0.0000,+0.0000,+0.0000,+0.0000,+0.0000,+0.0000,+0.0000,+0.0000
+0.0000,+0.0000,+0.0000,+0.0000,+0.0000,+0.0000,+0.0000,+0.0000,+0.0000,+0.0000
+0.0000,+0.0000,+0.0000,+0.0000,+0.0000,+0.0000,+0.0000,+0.0000,+0.0000,+0.0000
+0.0000,+0.0000,+0.0000,+0.0000,+0.0000,+0.0000,+0.0000,+0.0000,+0.0000,+0.0000
+0.0000,+0.0000,+1.0000,+0.0000,+0.0000,+0.0000,+1.0000,+0.0000,+0.0000,+0.0000
+0.0000,+0.0000,-3.0000,+1.0000,+0.0000,+0.0000,+0.0000,+0.0000,+0.0000,+0.0000

**** ROW 54 ****
+0.0000,+0.0000,+0.0000,+0.0000,+0.0000,+0.0000,+0.0000,+0.0000,+0.0000,+0.0000
+0.0000,+0.0000,+0.0000,+0.0000,+0.0000,+0.0000,+0.0000,+0.0000,+0.0000,+0.0000
+0.0000,+0.0000,+0.0000,+0.0000,+0.0000,+0.0000,+0.0000,+0.0000,+0.0000,+0.0000
+0.0000,+0.0000,+0.0000,+0.0000,+0.0000,+0.0000,+0.0000,+0.0000,+0.0000,+0.0000
+0.0000,+1.0000,+0.0000,+0.0000,+0.0000,+0.0000,+0.0000,+0.0000,+0.0000,+0.0000
+0.0000,+0.0000,+1.0000,-3.0000,+0.0000,+0.0000,+0.0000,+0.0000,+0.0000,+1.0000

**** ROW 55 ****
+0.0000,+0.0000,+0.0000,+0.0000,+0.0000,+0.0000,+0.0000,+0.0000,+0.0000,+0.0000
+0.0000,+0.0000,+0.0000,+0.0000,+0.0000,+0.0000,+0.0000,+0.0000,+0.0000,+0.0000
+0.0000,+0.0000,+0.0000,+0.0000,+0.0000,+0.0000,+0.0000,+0.0000,+0.0000,+0.0000
+0.0000,+0.0000,+0.0000,+0.0000,+0.0000,+0.0000,+0.0000,+0.0000,+0.0000,+0.0000
+0.0000,+0.0000,+0.0000,+0.0000,+1.0000,+0.0000,+0.0000,+0.0000,+0.0000,+0.0000
+0.0000,+1.0000,+0.0000,+0.0000,-3.0000,+0.0000,+0.0000,+1.0000,+0.0000,+0.0000

**** ROW 56 ****
+0.0000,+0.0000,+0.0000,+0.0000,+0.0000,+0.0000,+0.0000,+0.0000,+0.0000,+0.0000
+0.0000,+0.0000,+0.0000,+0.0000,+0.0000,+0.0000,+0.0000,+0.0000,+0.0000,+0.0000
+0.0000,+0.0000,+0.0000,+0.0000,+0.0000,+0.0000,+0.0000,+0.0000,+0.0000,+0.0000
+0.0000,+0.0000,+0.0000,+0.0000,+0.0000,+0.0000,+0.0000,+0.0000,+0.0000,+0.0000
+0.0000,+0.0000,+0.0000,+1.0000,+0.0000,+0.0000,+1.0000,+0.0000,+0.0000,+0.0000
+0.0000,+0.0000,+0.0000,+0.0000,+0.0000,-3.0000,+0.0000,+0.0000,+1.0000,+0.0000

**** ROW 57 ****
+0.0000,+0.0000,+0.0000,+0.0000,+0.0000,+0.0000,+0.0000,+0.0000,+0.0000,+0.0000
+0.0000,+0.0000,+0.0000,+0.0000,+0.0000,+0.0000,+0.0000,+0.0000,+1.0000,+0.0000
+0.0000,+0.0000,+0.0000,+0.0000,+0.0000,+0.0000,+0.0000,+0.0000,+0.0000,+0.0000
+0.0000,+0.0000,+0.0000,+0.0000,+0.0000,+0.0000,+0.0000,+0.0000,+0.0000,+0.0000
+0.0000,+0.0000,+0.0000,+0.0000,+0.0000,+0.0000,+0.0000,+0.0000,+0.0000,+1.0000
+0.0000,+0.0000,+0.0000,+0.0000,+0.0000,+0.0000,-3.0000,+0.0000,+1.0000,+0.0000

**** ROW 58 ****
+0.0000,+0.0000,+0.0000,+0.0000,+0.0000,+0.0000,+0.0000,+0.0000,+0.0000,+0.0000
+0.0000,+0.0000,+0.0000,+0.0000,+0.0000,+0.0000,+0.0000,+0.0000,+0.0000,+0.0000
+0.0000,+0.0000,+0.0000,+0.0000,+0.0000,+0.0000,+0.0000,+0.0000,+0.0000,+0.0000
+0.0000,+0.0000,+0.0000,+0.0000,+0.0000,+0.0000,+0.0000,+0.0000,+0.0000,+0.0000
+0.0000,+0.0000,+0.0000,+0.0000,+0.0000,+0.0000,+0.0000,+0.0000,+0.0000,+1.0000
+0.0000,+0.0000,+0.0000,+0.0000,+1.0000,+0.0000,+0.0000,-3.0000,+0.0000,+1.0000

**** ROW 59 ****
+0.0000,+0.0000,+0.0000,+0.0000,+0.0000,+0.0000,+0.0000,+0.0000,+0.0000,+0.0000
+0.0000,+0.0000,+0.0000,+0.0000,+0.0000,+0.0000,+0.0000,+0.0000,+0.0000,+0.0000
+0.0000,+0.0000,+0.0000,+0.0000,+0.0000,+0.0000,+0.0000,+0.0000,+0.0000,+0.0000
+0.0000,+0.0000,+0.0000,+0.0000,+0.0000,+0.0000,+0.0000,+0.0000,+0.0000,+0.0000
+0.0000,+0.0000,+0.0000,+0.0000,+0.0000,+0.0000,+0.0000,+0.0000,+0.0000,+0.0000
+0.0000,+0.0000,+0.0000,+0.0000,+0.0000,+1.0000,+1.0000,+0.0000,-3.0000,+1.0000

**** ROW 60 ****
+0.0000,+0.0000,+0.0000,+0.0000,+0.0000,+0.0000,+0.0000,+0.0000,+0.0000,+0.0000
+0.0000,+0.0000,+0.0000,+0.0000,+0.0000,+0.0000,+0.0000,+0.0000,+0.0000,+0.0000
+0.0000,+0.0000,+0.0000,+0.0000,+0.0000,+0.0000,+0.0000,+0.0000,+0.0000,+0.0000
+0.0000,+0.0000,+0.0000,+0.0000,+0.0000,+0.0000,+0.0000,+0.0000,+0.0000,+0.0000
+0.0000,+0.0000,+0.0000,+0.0000,+0.0000,+0.0000,+0.0000,+0.0000,+0.0000,+0.0000
+0.0000,+0.0000,+0.0000,+1.0000,+0.0000,+0.0000,+0.0000,+1.0000,+1.0000,-3.0000

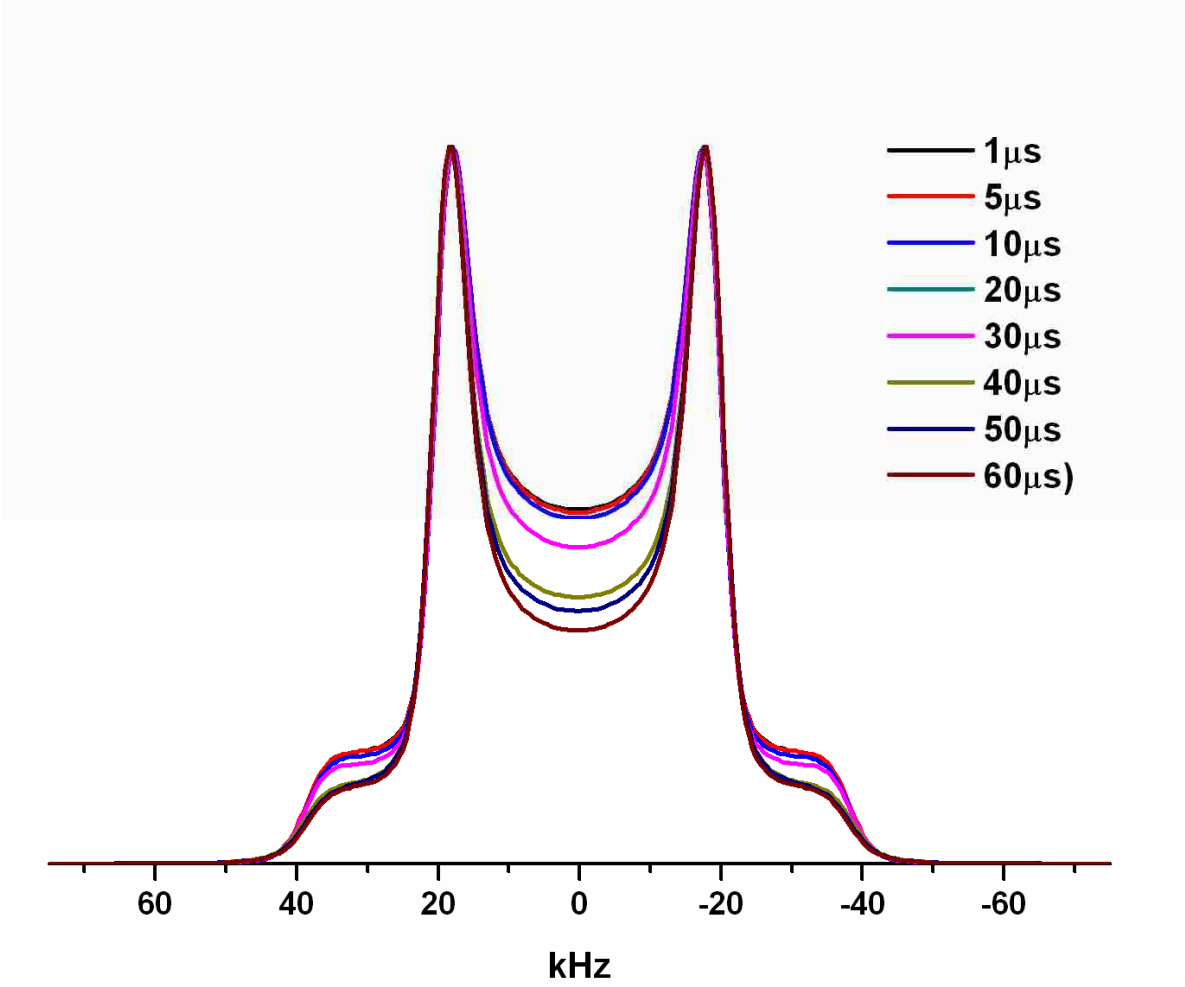

FigureB1. The simulated ^{2}H NMR lineshapes studied for the effect of pulse spacing.

Jump models = two-site jump + soccer ball model

Jump rate = 5×10^{3} Hz for both

The quadrupole coupling constant (QCC) = 52 kHz

90° pulse width = 2.8 μs

Spectral width = 250 kHz

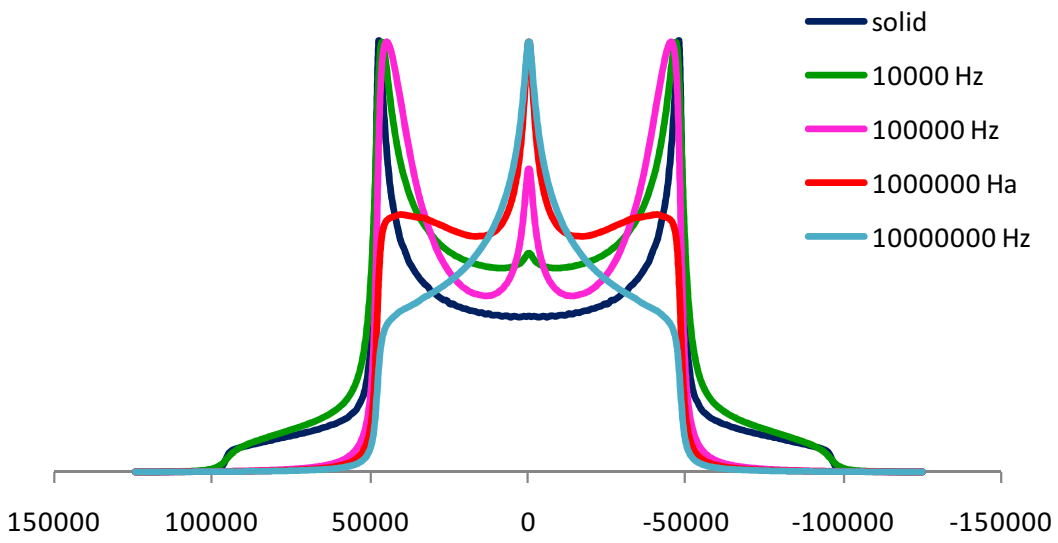

FigureB2. Simulation of ^{2}H NMR lineshape from a two-site hop with a 120^{o} jump angle with the QCC of 128 kHz as a function of jump rate.

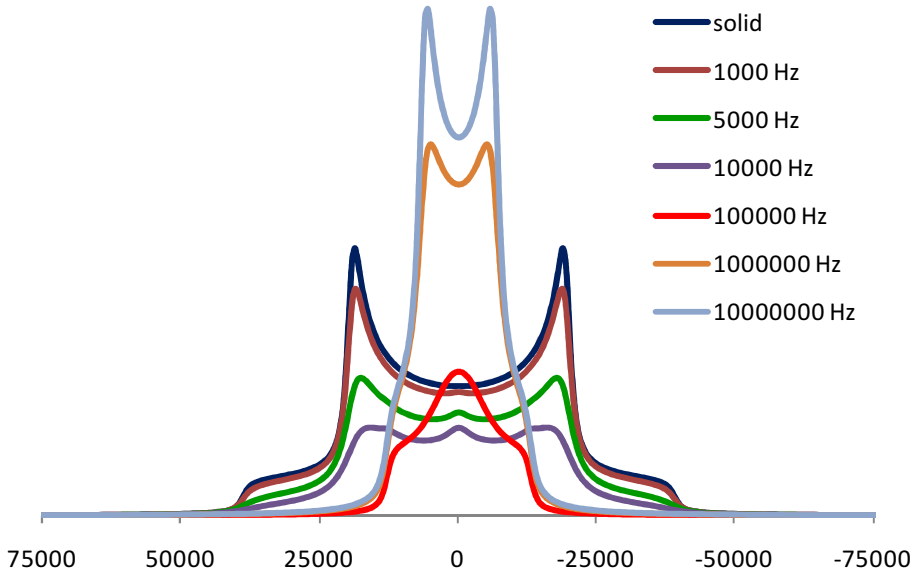

Figure B3. Simulation of ^{2}H NMR lineshape from a jump model of methyl rotation (3-site jump for the symmetry axis of methyl group) with the QCC of 52 kHz as a function of jump rate.

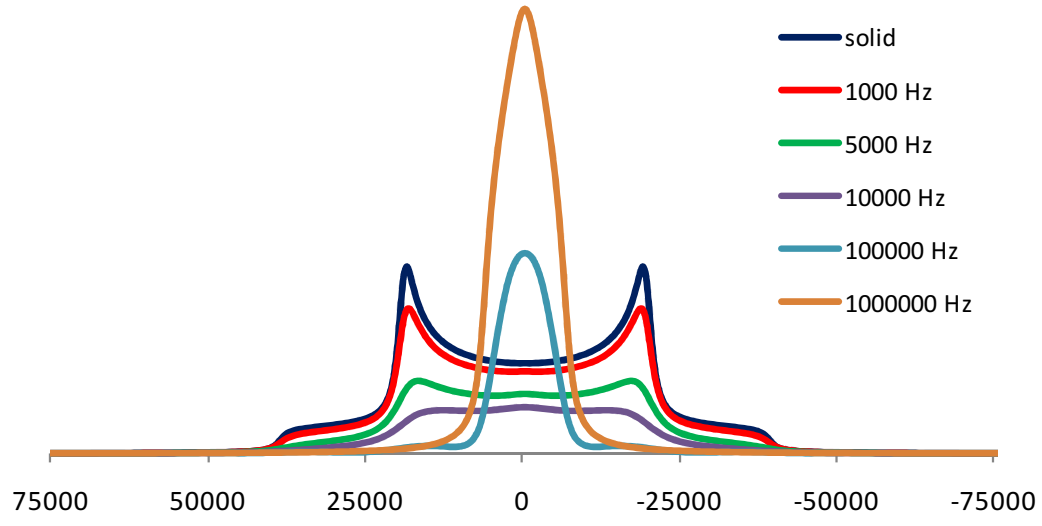

Figure B4. Simulation of ^{2}H NMR lineshape from the combination of two-site and three-site jump models with the symmetry axis of the methyl group with the QCC of 52 kHz as a function of jump rate.

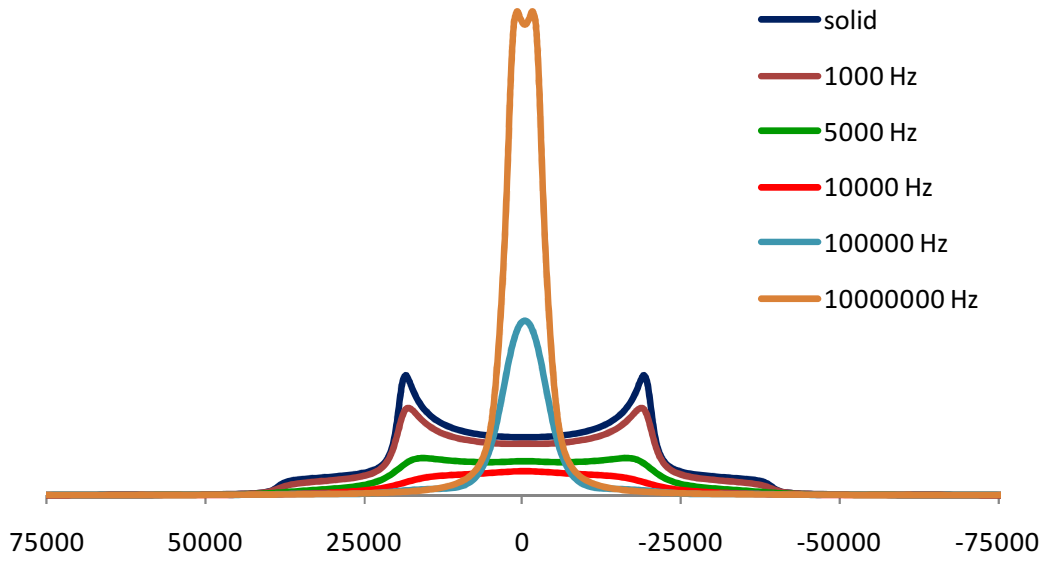

Figure B5. Simulation of ^{2}H NMR lineshape from the combination of two three-site jump models with the symmetry axis of methyl group with the QCC of 52 kHz as a function of jump rate.

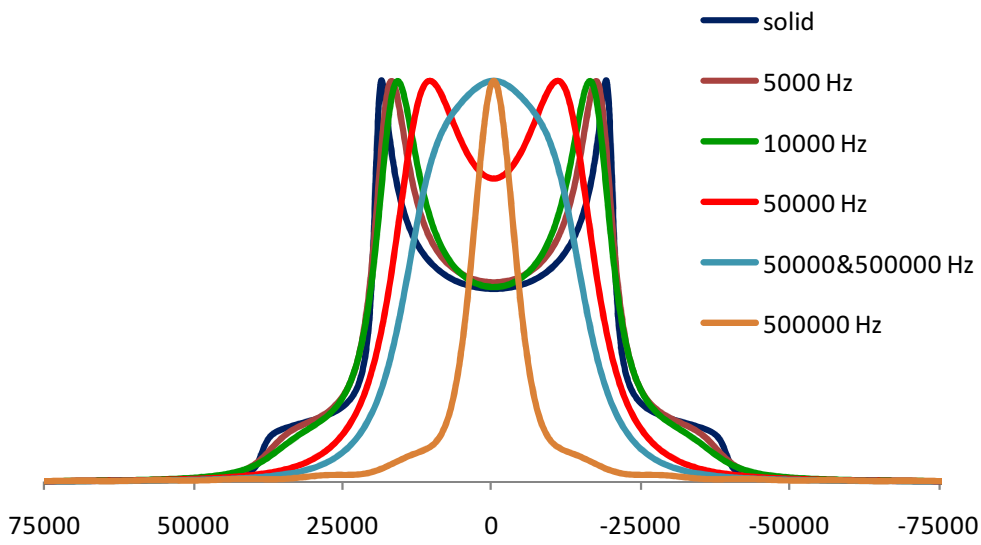

Figure B6. Simulation of ^{2}H NMR lineshape from the combination of two-site hop (with a jump angle of 120^{o}) and soccer ball models with the QCC of 52 kHz as a function of jump rate.

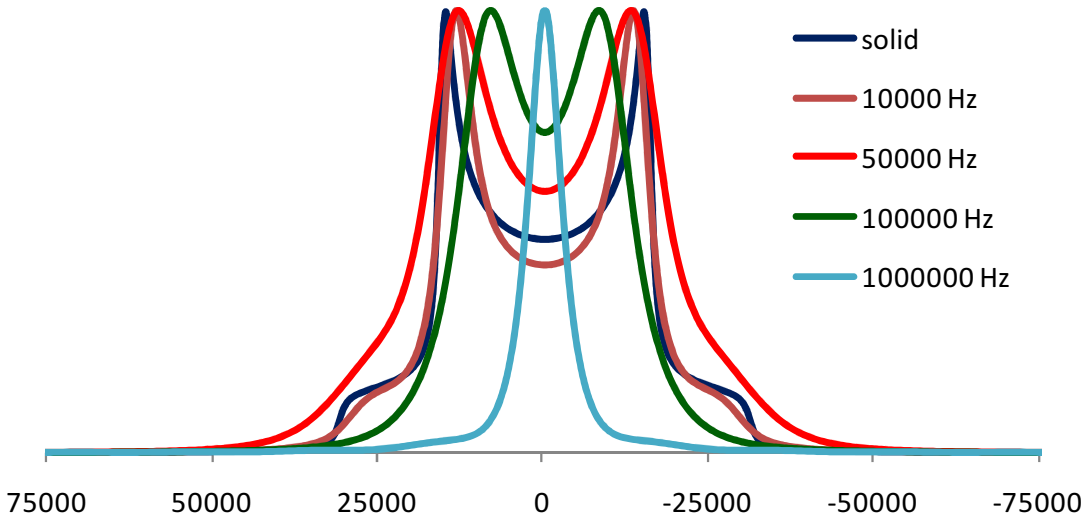

Figure B7. Simulation of ^{2}H NMR lineshape from the combination of three-site jump and soccer ball models with the QCC of 52 kHz as a function of jump rate.

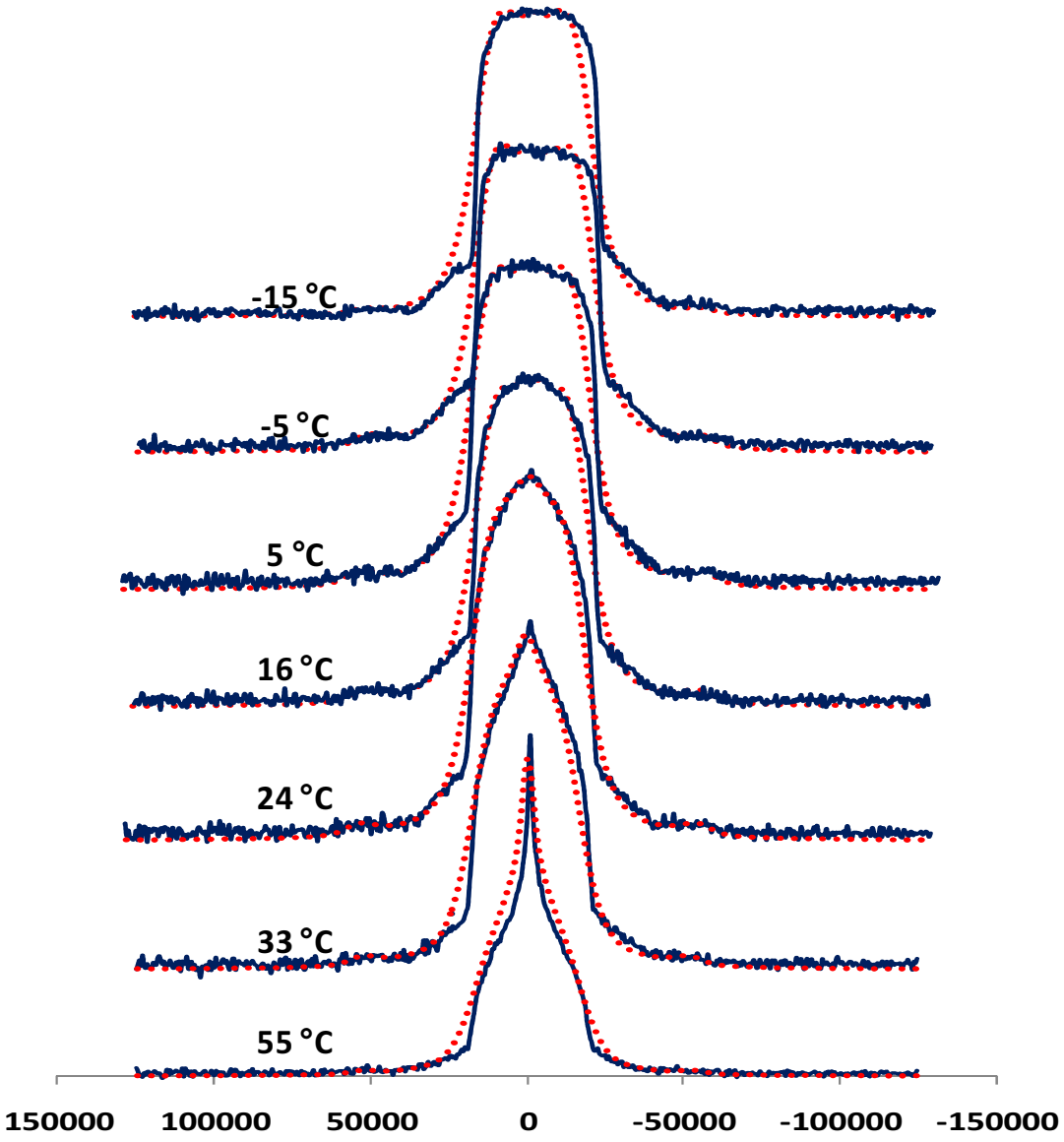

Figure B8. Experimental (——) and simulated (•••••) ^{2}H NMR spectra for 1.02 mg/m^{2} adsorbed PIPA-d_7.

APPENDIX C

FTIR FITTING OF SPECTRA FOR THE OTHER ADSORBED POLYMERS

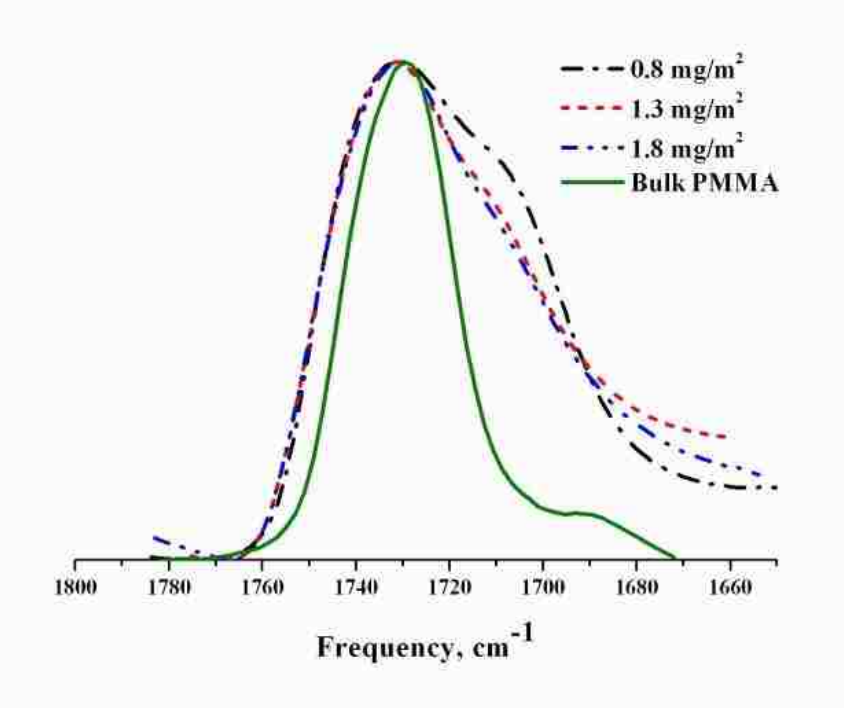

Figure C1. FTIR spectra of poly(methyl methacrylate) (PMMA) at carbonyl strectching as a function of the adsorbed amount and bulk polymer.

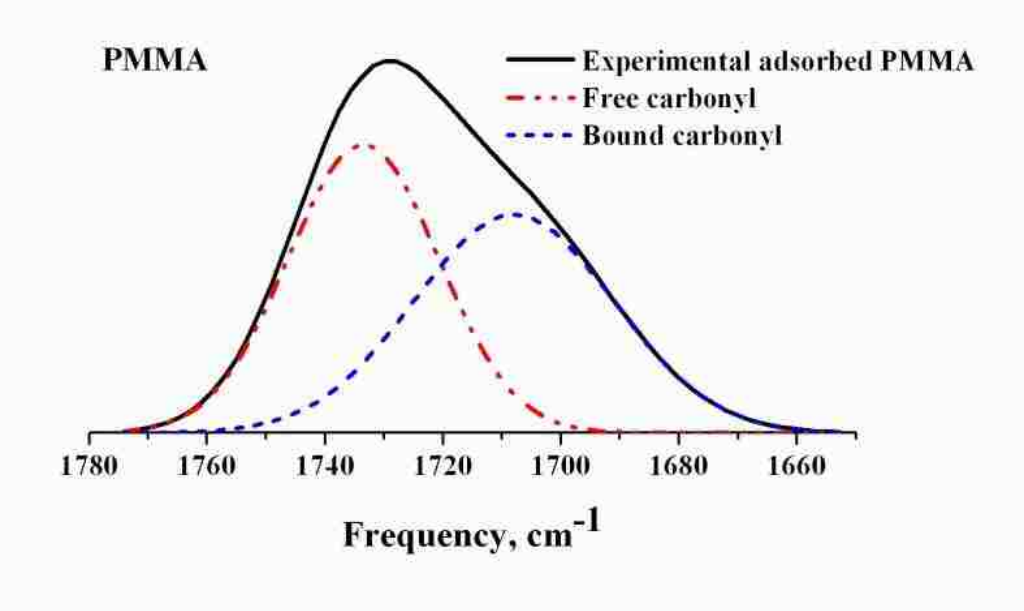

Figure C2. Gaussian lineshape fitted carbonyl peaks of 1.3 mg/m^2 adsorbed PMMA.

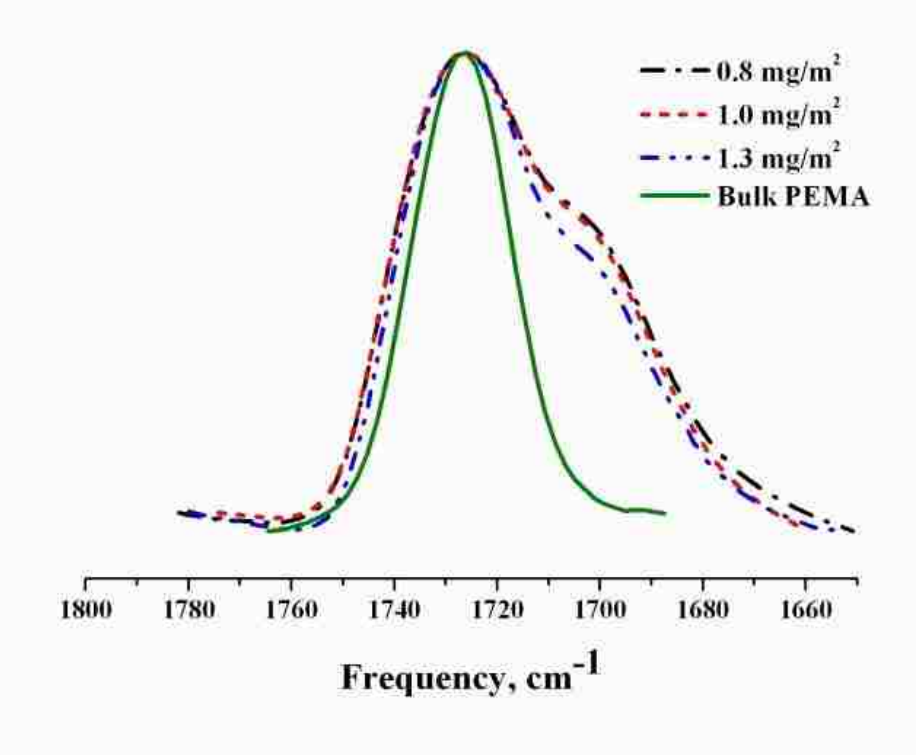

Figure C3. FTIR spectra of poly(ethyl methacrylate) (PEMA) at carbonyl stretching as a function of the adsorbed amount and bulk polymer.

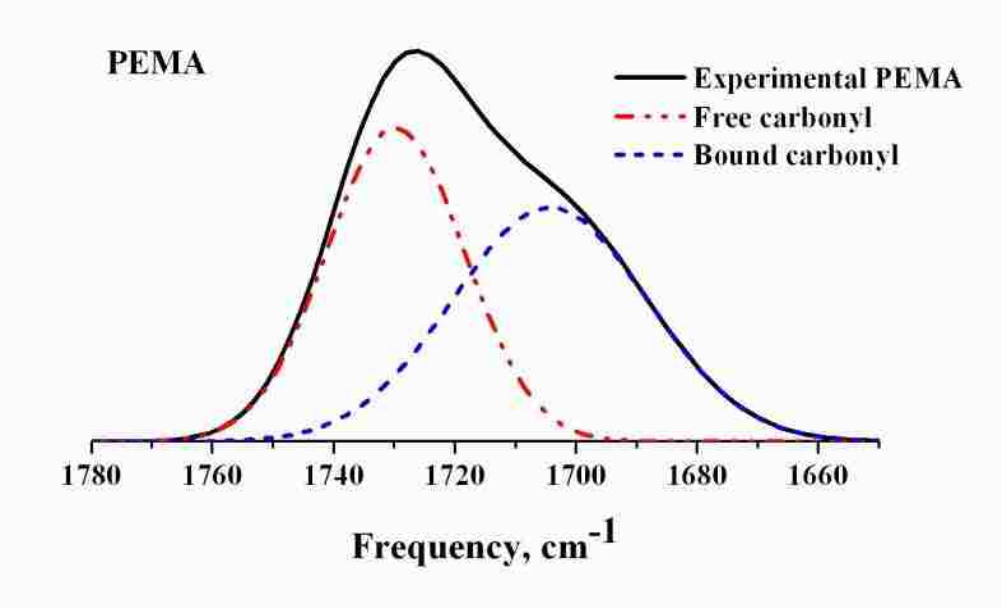

Figure C4. Gaussian lineshape fitted carbonyl peaks of 1.0 mg/m^2 adsorbed PEMA.

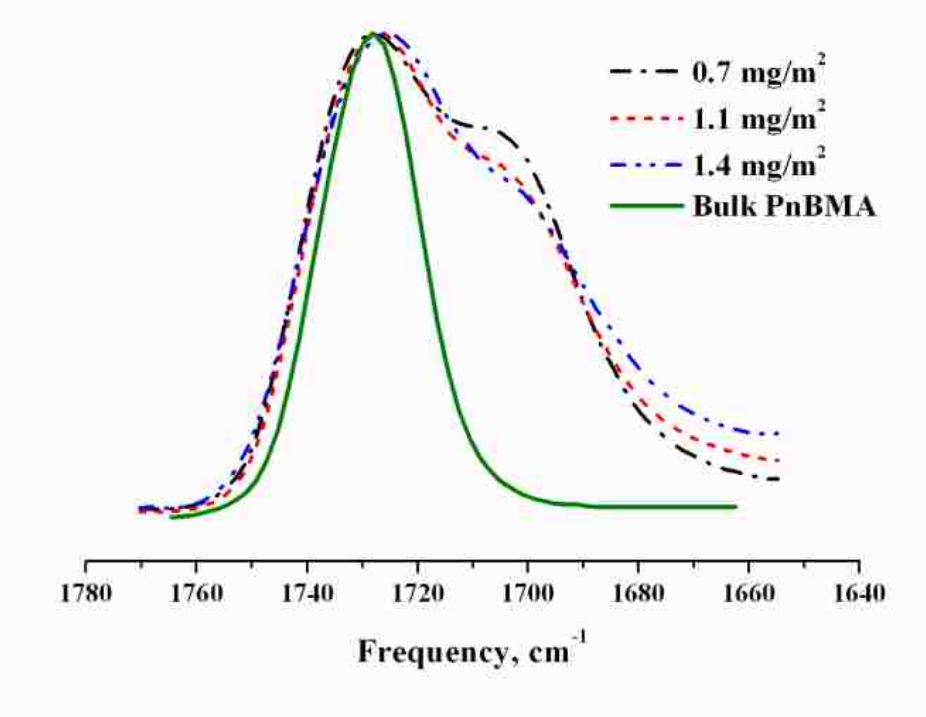

Figure C5. FTIR spectra of poly(n-butyl methacrylate) (PnBMA) at carbonyl stretching as a function of the adsorbed amount and bulk polymer.

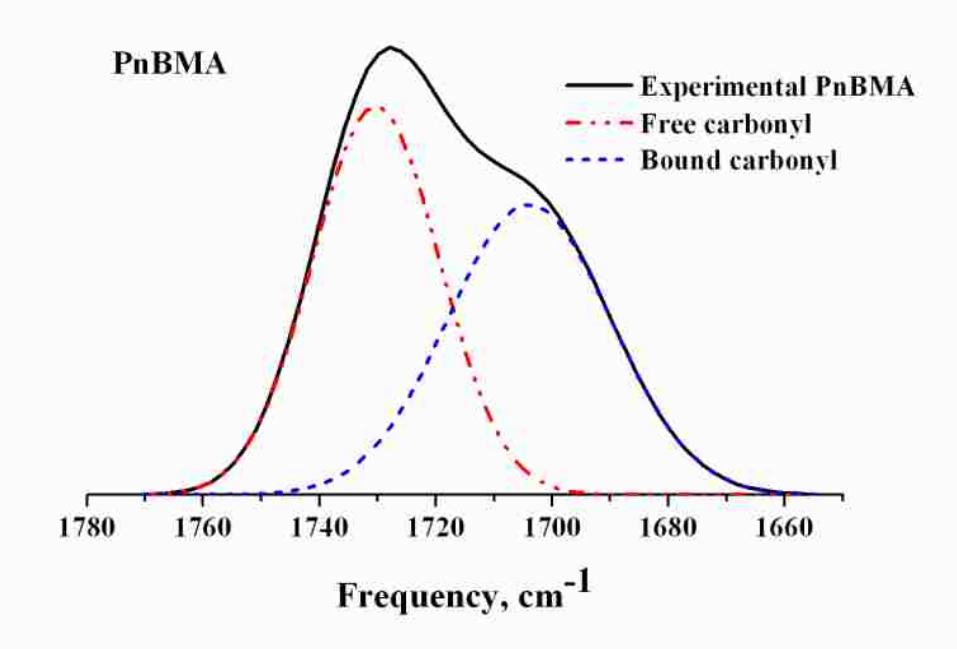

Figure C6. Gaussian lineshape fitted carbonyl peaks of 1.1 mg/m^2 adsorbed PnBMA.

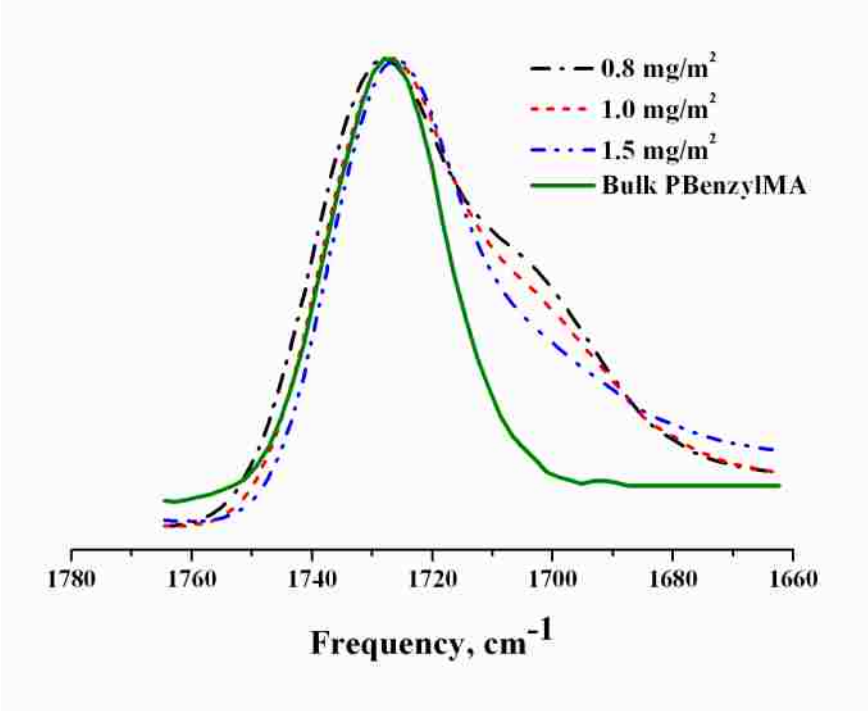

Figure C7. FTIR spectra of poly(benzyl methacrylate) (PBnzylMA) at carbonyl stretching as a function of the adsorbed amount and bulk polymer.

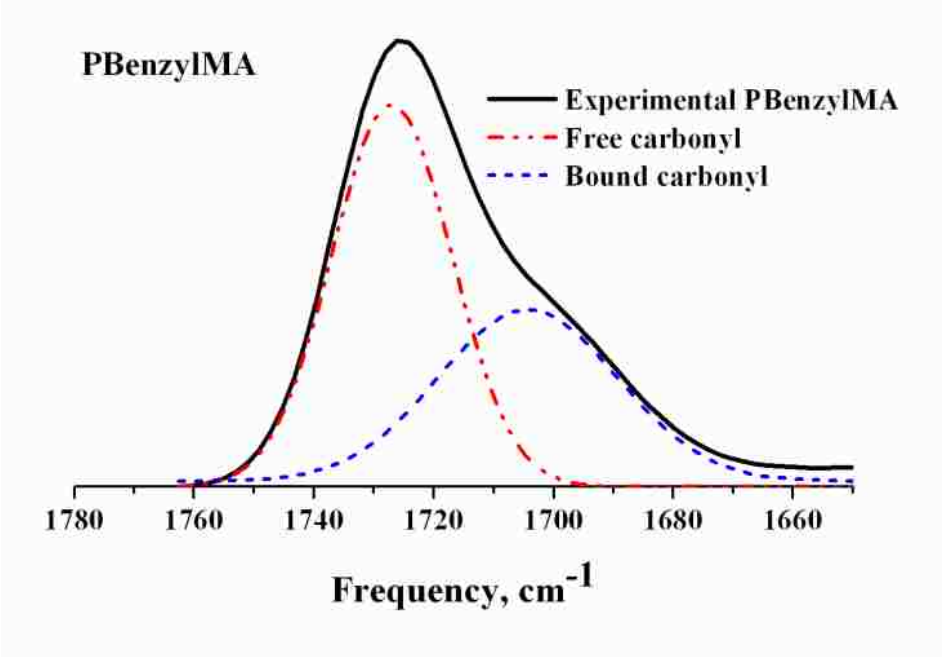

Figure C8. Gaussian lineshape fitted carbonyl peaks of 1.0 mg/m^2 adsorbed PBenzylMA.

BIBLIOGRAPHY

1) Krisanangkura, Piyawan; Blum, Frank D., **Segmental dynamics of poly(isopropyl acrylate)-d_7 on silica.** *Polymer Preprints*, **2006**, *47(1)*, 254.

2) Kabomo, Moses T.; Blum, Frank D.; Kulkeratiyut, Suntree; Kulkeratiyut, Suriyaphongse; Krisanangkura, Piyawan., **Effects of molecular mass and surface treatment on adsorbed poly(methyl methacrylate) on silica.** *J. Polym. Sci., Part B: Polymer Physics*, **2008**, *46(6)*, 649.

3) Krisanangkura, Piyawan; Blum, Frank D., **Dynamics of PIPA-d_7 on silica.** *Polymer Preprints*, **2008**, *49(1)*, 668.

4) Blum, Frank D.; Krisanangkura, Piyawan, **Comparison of differential scanning calorimetry, FTIR, and NMR to measurements of adsorbed polymers.** *Thermochimica Acta*, 2009, *492(1-2)*, 55.

5) Blum, Frank D.; Krisanangkura, Piyawan, **Bound fractions of methacrylate polymers adsorbed on silica using FTIR.** *(To be submitted).*

VITA

Piyawan Krisanangkura was born on November 7th 1976, in Songkhla, Thailand. She earned a Bachelor of Science (BS) degree in Chemical Technology (2000), from Chulalongkorn University in Bangkok, Thailand. She joined Office of Atomic Energy for Peace (OAEP), Ministry of Science and Technology in Thailand as a Nuclear Chemist. She got a scholarship from Ministry of Science and Technology to pursue her Ph.D. degree, and joined Chemistry Department, Missouri University of Science and Technology in August 2002. She studied adsorption and segmental dynamics of acrylate and methacrylate polymers adsorbed on a silica surface using ^{2}H solid-state NMR, FTIR, and other characterization techniques.